ABSTRACT

Title of Dissertation: RAPID HARVEST OF ALGAE FOR BIOFUEL PRODUCTION WITH THE AGGREGATING BACTERIUM *BACILLUS* SP. STRAIN RP1137

Ryan J. Powell, Doctor of Philosophy, 2014

Directed By: Dr. Russell T. Hill, Professor, University of Maryland Center for Environmental Science

Algal biofuels represent one of the most promising means of sustainably replacing liquid fuels. However significant challenges remain before algal based fuels become competitive with fossil fuels. One of the largest challenges is the ability to harvest the algae in an economic and low energy manner. In this dissertation I describe the isolation of the bacterium, *Bacillus* sp. strain RP1137, which can rapidly aggregate several algae that are candidates for biofuel production. This bacterium aggregates algae in a pH dependent and reversible manner and retains its aggregation ability after paraformaldehyde fixation. The optimal ratio of bacteria to algae is described as well as

the robustness of aggregation at different salinities and temperatures. Aggregation is dependent on the presence of calcium or magnesium ions and likely occurs via charge neutralization through binding of calcium ions to the cell surface of both algae and bacteria. I show charge neutralization occurs at least in part through binding of calcium to negatively charged teichoic acid residues. A comparison of the aggregation efficiency of RP1137, *Bacillus megaterium* QM B1551 and *Bacillus subtilis* SMY showed that RP1137 and B1551 are equally efficient at aggregating algae while SMY does not aggregate algae. The genome of RP1137 was sequenced to understand the molecular underpinning of the mechanism of aggregation. The difference in aggregation phenotypes between the three bacilli was used to inform a genomic comparison which revealed two putative proteins that are predicted to be bound to the cell wall and are found only in RP1137 and B1551 but not SMY. This work characterizes the conditions under which *Bacillus* sp. RP1137 aggregates algae and the mechanism by which that aggregation occurs.

RAPID HARVEST OF ALGAE FOR BIOFUEL PRODUCTION WITH THE AGGREGATING BACTERIUM *BACILLUS* SP. STRAIN RP1137

By

Ryan Joseph Powell

Dissertation submitted to the Faculty of the Graduate School of the
University of Maryland, College Park, in partial fulfillment
of the requirements for the degree of
Doctor of Philosophy
2014

Advisory Committee:
Professor Russell T. Hill, Chair
Professor Allen Place
Professor Feng Chen
Professor Harold Schreier
Professor Paul Behrens

Dedication

I dedicate this work to my wife Kerry for her love and support and to my parents John and Connie Powell who taught me how to work hard and persevere through the most difficult of times.

Acknowledgments

I am forever in debt to my parents who taught me how to work hard and to strive to do good for those around me. These lessons prepared me for life better than anything else they could have done. Focusing on the good I can do for others is the prime motivating force behind the work within this dissertation and the work that I will continue after my Ph.D. For this motivation and for their love and support I thank my parents.

I thank my advisor Dr. Russell Hill for bringing me into his lab after a rocky initial three years starting my Ph.D. in another lab and for finding ways to support me. Working with Russell has been a pleasure; he has allowed me the freedom to investigate what interests me and the guidance to turn those interests into papers and patents. Russell has been a staunch ally who has fought to help me get to my goals and has provided excellent guidance on the path to achieving these ambitions.

There are many great people in the Hill lab and within IMET that have helped me complete this dissertation. I thank Leah Blasiak for many scientific discussions, expert editing of manuscripts and the reminder to check the literature. I thank Jan Vicente for accompanying me on over 500 runs in the rain, snow and heat of Baltimore. Jan has been a constant source of support and great friend. Jeanette Davis has also been a great friend and confidant in the toughest of times for me. I thank Jindong Zan for many great scientific discussions and for being a great friend. Within IMET I thank Joel Graham for great scientific advice. I thank the Place lab, particularly Ernest and Grant for always being very helpful and somehow always knowing where to find that one key chemical or piece of equipment that I needed. Finally, I thank Matt Moore for always finding a way to

get things done, whether that was helping me find parts for my next prototype or wading through the paperwork needed to hold my wedding at the institute.

Statement of contribution

Taylor Carter helped gather data for the bioinformatics analyses presented in Chapter 4. Diane Sumutka, Donald Belle and Li Zheng helped with the isolation of the bacteria from the HTB1 culture, testing those bacteria for their effect on the growth of HTB1 and testing the isolates for AHL production respectively.

Table of contents

List of Figures

List of Tables

Chapter 1 Introduction

1.1 Motivation for studying biofuels

Why study biofuels? The answer to this question can be found by understanding our need for energy and how we currently obtain that energy. Energy is required for almost everything we do. As you read these words take a moment to look around you and think about what requires energy and where that energy came from. If you are reading from a computer screen in the US then on average 70% of the energy needed to run your computer came from a combination of coal and natural gas (1). This percentage is the average for electricity generation in in the US. Energy from these sources is being used directly or indirectly for heating or cooling to make the room you are sitting in comfortable. Look around and note anything that you did not make yourself, a pen, a piece of paper or the food you may be eating. All of these items had to be transported to you at some point from where they were produced. Transportation is overwhelmingly powered by energy derived from oil, with 93% of the energy used to move goods and people coming from this source of energy (1). Most of that energy for food production also comes from fossil fuels, including the oil needed to transport the food, the electricity needed to refrigerate or process it or the natural gas used to make fertilizer to grow food though the Haber-Bosch process. This means even our own metabolism is reliant on fossil fuels. These examples of the energy used in daily life demonstrate our current need for energy to survive. This critical need for energy is the first part of the answer as to why we should study biofuels.

If we were only concerned about generating energy and not about how that energy was generated then biofuels would not make a very interesting or important research topic. However, it is becoming increasingly clear that how we generate the energy that

powers our society does matter. Currently, the vast majority of energy used in the US comes from non-renewable or finite sources of energy with 80% of energy used coming from oil, natural gas or coal. The major energy sources used in the US in quadrillion British thermal units (BTUs) and in order of abundance are oil (34.7), natural gas (26), coal (17.4), nuclear (8), biomass (4.3), hydroelectric (2.7), wind (1.4), solar (0.24) and geothermal (0.23) (1). To give some meaning to these numbers, one quadrillion BTUs equals the entire energy requirements for a city the size of Chicago for a year. Therefore when we talk about replacing 35 quads of energy from oil we can accurately say we are replacing the yearly energy needs of 35 large cities. Heavy reliance on high carbon fossil fuels has led to many problems. Perhaps the most notable and widespread problem is increased concentrations of CO_2 in the atmosphere which has been linked to climate change and is predicted to have several major and long lasting impacts. The most well-known changes to global climate are increases in mean surface temperature and rising sea levels (2). However, climate change is also predicted to cause widespread extinctions and increases in the severity and incidence of climate events such as droughts and floods (2). This last impact on the incidence and severity of climatic events is perhaps the most damaging as it will cause widespread crop failures. The increasing concentration of CO_2 concentrations in the atmosphere is also predicted to increase CO_2 concentrations in the oceans, resulting in ocean acidification (2). It is worth remembering that these effects are predicted to reverberate for several hundred to a thousand years after the initial climatic forcing occurs (2). The need for access to energy has driven major international conflicts and shapes global politics. This effect is broadly known as energy security and is the reason the US Navy is one of the biggest supporters of locally produced biofuels (3).

Considering the mixture of energy sources listed above is apparent is that oil makes up the largest share of energy used, with more than 36% of the energy used in the US coming from oil (1). One problem with using any finite resource to supply our energy is that when consumption becomes large enough the resource will be depleted. We have partially depleted conventional oil reserves and we are currently using more oil from nonconventional sources such as from oil reservoirs found in deep water, from hydraulic fracturing and from extraction of oil from tar sands. Each of these methods is more expensive than traditional drilling and carries with it more associated risks due to the increased difficulty of recovering the oil. Hydraulic fracturing has been linked to contamination of ground water (4). Similarly, extraction of oil from tar sand has been linked to contamination of local waterways due to the large amounts of water that is contaminated in these processes (5). These oil sources are also high-carbon sources of oil due to the increased energy needed to extract them. Therefore using these sources of oil accelerates the increase of CO_2 concentration in the atmosphere even faster than use of traditional sources of oil. As problematic as this is, our great demand for liquid fuels drives the extraction of oil from these non-traditional sources. This demand comes primarily from the transportation sector where 71% of oil is currently used (1). Within the transportation sector it is possible that passenger cars and other short range vehicles could be converted to electric-based systems, however other parts of the transportation infrastructure such as jets, long haul trucks and cargo ships are likely to require liquid fuels well into the future due to the high energy densities required for these modes of transportation. These requirements mean liquid fuels from oil are not easy to replace for key parts of the economy. This convergence of the critical need for liquid fuels and the

damage currently caused by how those fuels are obtained answers the question I originally posed about why we should study biofuels. If we wish to replace the energy used by these sectors with energy from renewable and low carbon sources, we need a fungible liquid fuel that can replace the fuel that is currently derived from petroleum.

1.2 Introduction to biofuels

Biofuels are currently filling about 1% of our transportation needs (6) and with more development could make up a larger fraction of the liquid fuels that are used. Biofuels can address many of the challenges posed by traditional fossil fuels. Foremost among them is the production of a potentially carbon neutral fuel. The widespread adoption of carbon neutral biofuels would slow the increase of atmospheric CO_2 concentrations. One key advantage of biofuels is that they can provide liquid fuels that can be used in within the current transportation infrastructure. Thus, adoption of biofuels rests on developing production and not retooling the downstream energy infrastructure. Biofuels can also eliminate many of the environmental problems that are being caused by extraction of oil from non-conventional sources. The widespread adoption of biofuels could revitalize rural communities by providing a source of income, employment and economic development. This has been observed with the advent of widespread production of corn ethanol which, while controversial, has increased the income flowing into rural communities due to the increased demand for agricultural products. A final advantage of biofuels is that they can be locally produced meaning that global politics and conflicts over access to oil reserves can be reduced. Due to these advantages over traditional fossil fuels the federal Renewable Fuel Standard (RFS) was enacted to spur

the production of liquid biofuels. The original RFS was enacted in 2005 under the Energy Policy Act and was expanded in 2007 under the Energy Independence and Security Act. The current RFS requires 136 billion liters of renewable fuel to be produced by 2022 and it requires that the fuel have a lower carbon footprint than conventional petroleum-based fuels (7). Within the RFS three generations of biofuels are recognized. In the following section these different types of biofuels will be examined.

1.3 First generation biofuels

First generation biofuels are primarily derived from food crops by converting corn and sugar cane into ethanol. The main advantage of first generation biofuels is that the technology has been well established and much of the infrastructure was already in place at the time the RFS was enacted. Conversion of sugars into ethanol has been practiced at an industrial scale for over a hundred years. The cultivation of corn and sugar cane are also well established with large existing supply chains for these commodities. In Brazil the sugarcane to ethanol program has been running for 30 years (8). Ethanol from sugarcane is projected to fill 30% of Brazil's energy needs by 2020 (8). Other first generation biofuels include biodiesel from vegetable oils such as soybean oil and rapeseed. First generation biofuels have driven a recovery of the agricultural sector of the economy by boosting commodity prices to record levels. While this has brought relief to many small farmers, it has also been the cause of the contentious food versus fuel debate. The key issue of this debate is that using food crops for fuel causes increased food prices. In the US, the increase in food price attributable to biofuel production is about 20% (9). On average American families spend 13% of their budget on food. A 20% increase changes this to 16% of their total budget, which while noticeable amounts to a relatively

minor inconvenience (10). However, in developing countries such as Egypt food accounts for 40% of the budget of an average family, thus an increase in price of 20% percent has a much more dramatic effect (11).

Another disadvantage of biofuel production from corn is that it has been shown to be a net negative energy process, meaning more energy is consumed in the process of making a given quantity of ethanol than is contained in the fuel itself (12). Ethanol derived from sugar cane fairs better in a life cycle analysis and has been shown to be a net positive energy process (13). However, the low areal productivity of first generation biofuels crops is what truly limits their use. First generation biofuels currently provide about 1% the world transportation fuel and occupy about 1% of the total arable land (6). The use of all 100% of the arable land to supply the world's transportation energy needs is clearly not an option. Despite these limitations biofuel production from corn and sugar cane is the largest source of biofuel in the world.

1.4 Second generation biofuels

To overcome the limitations of first generation biofuels, second generation biofuels were devised to generate fuel from non-food crops. Second generation biofuels are made by converting cellulosic plant matter to sugars and then fermenting those sugars into ethanol. A key advantage of these fuels is that crops do not need to be grown on prime arable land and the biofuels can be derived from waste biomass. Second generation biofuels are commonly made from woody material such as tree biomass, switchgrass, corn stover, miscanthus and jatropha (14). These crops are in general less energy and labor intensive to cultivate than corn. They can also have longer growing seasons which

means more solar energy per year can be harvested. One of the disadvantages of most second generation biofuels is the requirement for pre-processing the biomass before conversion to fuel. For woody biomass the material must first be chopped into small fragments. These fragments are then typically treated with acid to further break down the biomass. Finally it is treated with enzymes known as cellulases to break down the cellulose into its component sugar monomers. The sugar is then fermented into ethanol by yeast. Another disadvantage is that ethanol cannot be used for some applications such as jet planes and large cargo ships because it is insufficiently energy-dense for these applications. Second generation biofuels are just beginning to reach industrial scale with large processing plants in the planning or construction phase.

1.5 Third generation biofuels

Fuels from algae are often listed as the third and perhaps most promising iteration of biofuels due to several advantages over other biofuels. Chief among the advantages of algae is the productivity that is possible per unit area, with some algae being able to double their biomass in a few hours. Biofuels are based on converting biomass to fuel, so greater biomass productivity results in greater fuel productivity. Other advantages of algae are their ability to grow in salt water or waste water and to grow on land not suited for agriculture (15, 16). Algae can also be harvested multiple times per season unlike many land-based crops (17). Despite these advantages the current scale of algal biofuel production is small. The largest production facility to date is Sapphire energy with a production rate of 1-5 barrels of oil per day with plans to produce a 100 barrel-a-day facility. To date no company has made money producing fuel from algae. Production of fuel from algae is technically feasible but not yet economically viable. This point is a

major focus of this dissertation. To understand why algal biofuels have not achieved economic viability we need to understand how fuel from algae is produced and where research is needed to bridge the gap to economic viability.

1.6 Algal biofuel production systems

There are three key steps to making fuel from algae: growth, harvesting and conversion of the biomass to fuel. There are two primary ways in which algae are cultivated for large-scale production. Algae can be grown in photobioreactors (PBRs) and in open ponds. Each design comes in many variations and each have advantages and disadvantages. In general, PBRs are closed systems that are designed to minimize contamination and maximize control of environmental conditions such as light, mixing, CO_2, temperature and pH to obtain maximal algal productivity. Due to tight control of growth conditions algal productivity can be 3-5 times higher in a PBR compared to an open pond (18). Several common PBR designs include tubular, flat plate and column. Evaporation is minimized and thus water usage is less in a PBR compared to an open pond. However, since evaporation passively cools water, the absence of evaporative cooling requires additional engineering in a closed PBR to ensure that the reactor does not overheat. While PBRs are capable of higher productivity their major disadvantage is the high capital costs needed to construct the reactors. Open ponds can be constructed more cheaply and require less maintenance than PBRs. The tradeoff is that open ponds have lower productivity and thus require a larger area to produce the same amount of algal biomass. However, open ponds are likely the only viable option for producing low cost commodities such as fuels (19).

The next step in the production of algal biofuels is harvesting the algal biomass from the water. This step is one of the major challenges in the production of algal biofuels. At the laboratory scale algae cultures can be harvested by centrifugation or filtration, but these methods are too energy and capital intensive for harvesting algae from the immense volumes of water needed for commercial scale production of algal biofuels (20). For most biomass conversion technologies the algae must be concentrated, with most of the water removed before the biomass can be converted to fuel. Mature technologies for algal harvest include filtration, centrifugation, sedimentation, electrocoagulation, dissolved air floatation, chemical flocculation and bio-aggregation (21). These methods have differing harvesting efficiencies. Some of the physical means of harvest have the following efficiencies: tangential flow filtration (70-89%), dissolved air floatation (80-90%), electrocoagulation (95%) and centrifugation (>95%) (21). While many physical means are efficient at concentrating algal biomass they tend to be expensive, energy intensive and difficult to scale to large volumes. Chemical flocculants such as aluminum sulfate and polyacrylamide have harvest efficiencies of 72% and 78% respectively (22) and can be scaled easily. However, these methods require post treatment of the effluent water before it is released into the environment or is reused in algal culture. Bioaggregation can be achieved using biopolymers such as chitosan (23-25) and extracellular polymeric substances such as polysaccharides (26, 27). Bacterial bioaggregation is a natural process and is often observed in laboratory grown algal cultures. Several bacteria have been identified as bio-aggregation agents that can be used to aggregate algae (22, 28-31).

Once the algal biomass is harvested the next and final step is to recover the energy stored in the biomass by converting it to fuel. The most commonly researched method of deriving fuel from algae is production of biodiesel from algal lipids. Biodiesel can also be generated from oils extracted from canola, soy and palm oil (17). The technology for converting lipids to biodiesel has been well studied. It involves base-catalyzed transesterification of triacylglycerol in the presence of alcohol. While most research has focused on this pathway, it is limited to algae that accumulate high concentrations of lipids. Another limitation is that the biomass requires drying before it can be processed and this drying process is energy intensive. Anaerobic digestion is another major pathway for conversion of algal biomass to fuel. In this case the biomass is converted to biogas which is composed mostly of methane and CO_2. Anaerobic digestion can be coupled with biodiesel production from lipids to take advantage of the remaining proteins and starches that are not converted to fuel in the transesterification process. The starches found in some algae can also be converted to ethanol via traditional fermentation pathways. Fermentation can also be linked with biodiesel production to increase the amount of energy recovered from the algal biomass. Hydrothermal liquefaction of biomass is recently gaining more attention from the biofuel community due to several distinct advantages over the previously mentioned methods. One key advantage is that the biomass does not need be dried as it can be processed with a 95% moisture content. Perhaps the largest advantage of hydrothermal liquefaction that it produces a biocrude that is equivalent to traditional crude oil. This biocrude can be refined to diesel fuel, jet fuel, gasoline and many of the other products traditionally made from oil without retooling the entire energy infrastructure. Hydrothermal liquefaction extracts up to 95%

of the energy stored in the algal biomass in the form of solid, liquid and gaseous fuel products (32), with about 80% of the energy residing in the liquid biocrude fraction (33). Finally the process allows for the recovery of up to 80% of the nitrogen and phosphorous in the algal biomass for reuse as fertilizer (33).

While there are many conversion technologies and many investigators working on building algal biofuel systems, to our knowledge no one has yet devised a system that is able to produce fuel from algae in a cost-effective manner. Cost is at the heart of the problem of developing a new energy production system. Richardson et al. reviewed available public data and determined that current production systems had a 0% chance of being economically viable over a 10 year period (34). Figure 1.1 is derived from the data of Richardson et al. and shows the major costs involved in preparing biodiesel from algae. The major problems listed in this and other analyses are the cost of production systems versus the return from those systems. This is predicted to be true both for low cost open pond systems and for closed photobioreactors. While closed photobioreactors benefit from increased algal productivity they are crippled by the massive capital required to build production scale facilities. The solution is to create technology that lowers the cost of production and increases algal yield per unit area. Harvesting microalgae efficiently and cheaply is one of the biggest challenges for algal biofuels. Even in dense algal cultures, the biomass represents only a few grams per liter of water. This water must be removed before the biomass can be converted into fuel. Harvesting the algae is the number one operating expense and number two capital expense for open pond systems (34). Therefore research into new, low cost methods of harvesting algae is critical to the development of algal biofuels.

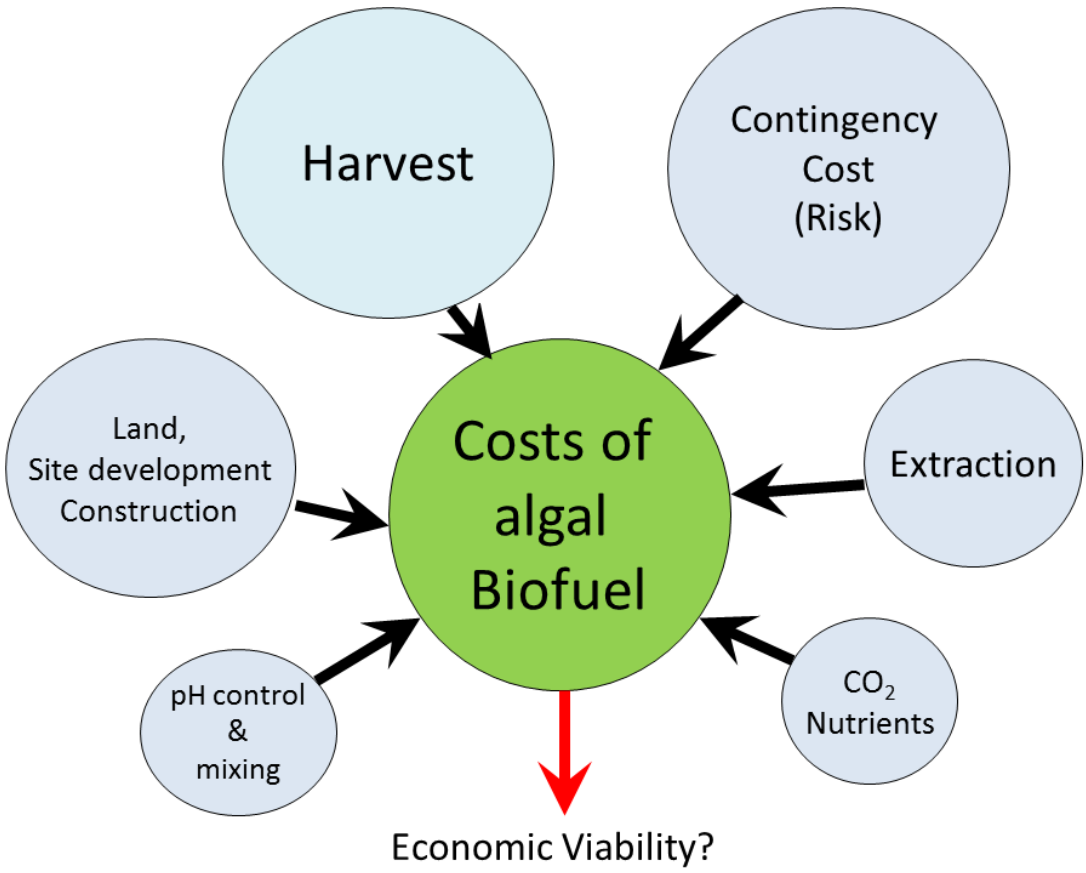

Figure 1. 1 Costs of algal biofuels

Costs involved in producing algal biodiesel from algae from Richardson et al. (34). The size of the blue circles is scaled with the amount of cost for that particular part of the production process. The two largest costs identified by Richardson were harvest and contingency costs.

1.7 Focus and Objectives

Algal biofuels represent a promising means of generating a renewable source of liquid fuels. To fulfill that promise several technical hurdles must be overcome. Perhaps the most important hurdle is developing a cost effective means of harvesting algae from large volumes of water. My research focuses on isolation, identification and characterization of an algal aggregating bacterium designated *Bacillus* sp. strain RP1137. The research presented here characterizes the conditions under which aggregation is most effective and elucidates the mechanism of aggregation by using both a chemical and bioinformatic based approach. To fulfill these research goals my objectives are:

a. **Characterize the aggregation ability of RP1137 under different environmental conditions and with different algae.**
b. **Define the mechanism of aggregation of RP1137.**
c. **Sequence and identify the potential genomic loci important for aggregation.**

The results of this research provide the information needed to use this bacterium to harvest algae and to potentially increase the efficiency of harvest. The information presented here will be useful to those interested in evaluating the strain for harvesting algae. On a broader scale the data provide mechanistic details of how RP1137 aggregates algae and provides a model of how aggregation processes between Gram-positive bacteria and algae may occur outside of the laboratory, where interactions between algae and bacteria are common.

Chapter 2: Rapid Aggregation of Biofuel Producing Algae by the Bacterium *Bacillus* sp. RP1137.

2.1 Abstract

Algal biofuels represent one of the most promising means of sustainably replacing liquid fuels. However significant challenges remain before algal based fuels become competitive with fossil fuels. One of the largest challenges is the ability to harvest the algae in an economic and low energy manner. In this chapter I describe the isolation of a bacterial strain, *Bacillus* sp. RP1137, which can rapidly aggregate several algae that are candidates for biofuel production, including *Nannochloropsis* sp. This bacterium aggregates algae in a pH dependent and reversible manner and retains its aggregation ability after paraformaldehyde fixation, opening the possibility for reuse of the cells. The optimal ratio of bacteria to algae is described as well as the robustness of aggregation at different salinities and temperatures. Aggregation is dependent on the presence of calcium or magnesium ions. The efficiency of aggregation of *Nannochloropsis oceanica* IMET1 is between 70-95%, and is comparable to other means of harvest, however the rate of harvest is fast with aggregates forming in 30 seconds.

2.2 Introduction

Microalgae are promising candidates for producing renewable liquid fuels, however, several barriers must be reduced before large-scale production can be economically viable. It is important to note that these challenges are technical and economic in nature as the process of creating biofuels from algae is proven. These barriers include supplying sufficient nutrients and CO_2 to the algae as well as mixing and controlling the pH in the large facilities needed to produce significant amounts of biofuel (34). Other challenges come from a systems perspective where the reliability of production must be improved (34). The risk associated with inconsistent production stems from the presence of algal grazers as well as infections by bacteria or viruses which can lower productivity or even result in rapid decline of algal cultures.

We focused on the harvest step of algal biofuel production because this step must be improved for algal biofuels to become economically viable. In an analysis done by Richardson et al., harvesting was the number one operating expense and number two capital expense in an outdoor production system (34). Harvesting microalgae efficiently and cheaply is one of the biggest challenges for algal biofuels. Even in dense algal cultures, the biomass represents only a few grams per liter of water. This water must be removed before the biomass can be converted into fuel. Several strategies have been developed to concentrate algae including filtration, centrifugation, sedimentation, dissolved air flotation, electrocoagulation, chemical flocculation and bio-aggregation (21). Each method has advantages and disadvantages with respect to cost, throughput and post treatment effects on both water and biomass, reviewed in detail by Uduman et al. (21).

Bioaggregation can be achieved using biopolymers such as chitosan (23-25) and extracellular polymeric substances such as polysaccharides (26, 27). Bacterial bioaggregation is a natural process and is often observed in laboratory grown algal cultures. Several bacteria have been identified as bio-aggregation agents that can be used to aggregate algae (22, 28-31). In this study I isolate and identify a bacterium designated *Bacillus* sp. RP1137 that is capable of rapidly aggregating microalgae that are candidates for biofuel production. I characterize the conditions under which aggregation is effective and the range of algae which the bacterium can aggregate.

2.3 Experimental procedures

2.3.1 Strains and culture conditions.

The bacterial strain, *Bacillus* sp. RP1137, was grown in marine broth 2216 (BD, Franklin Lakes, NJ) at 30°C in 125 ml Erlenmeyer flasks with shaking at 180 rpm. Solid media was prepared from marine broth 2216 by addition of 15 g/l Difco Technical Agar (BD).

Nannochloropsis oceanica IMET1 was grown in f/2 medium (35) with a salinity of 20 ppt. This alga has been maintained for ten years at the Institute of Marine and Environmental Technology by the Aquaculture Research Center in Baltimore Maryland. The algae were grown in photobioreactors which consisted of 500 ml borosilicate glass bottles (Pyrex no. 1395; 13.6 cm diameter, 26.2 cm height) with three ports in the cap. Two ports were connected to tubes leading to the bottom of the bottle. Air was pumped into these two ports through 0.22 µm syringe filters at a rate of 5 l/min to provide constant mixing and to provide the carbon dioxide present in the air. The third port was

used as a vent. The bottles were positioned 25 cm from 215 watt Phillips white fluorescent lights with a light intensity of 275 µmol/m^2/s at the front of the bottle and were grown on a light/dark photoperiod of 14/10 at 25°C. Algae were subcultured weekly using an inoculating volume of 10% and were used for experiments at an OD_{600} of 1.0 and a pH of 10.2.

Tetraselmis chuii, *Tetraselmis sucia* and *Phaeodactylum* sp. were grown using the same set-up as described above and were also grown in f/2 medium and were obtained from the Institute of Marine and Environmental Technology Aquaculture Research Center culture collection. Cells were grown in 250 ml Erlenmeyer flasks at 180 rpm shaking at 20°C with a light/dark photoperiod of 14/10.

Neochloris oleoabundans MK8520 was grown in *Neochloris* medium and was a gift from Dr. Paul Behrens. This medium was composed of 5.82 g/l NaCl, 2.47 g/l $MgSO_4.7H_2O$, 1 g/l KNO_3, 0.75 g/l KCl, 66 mg/l $CaCl_2$, 1.24 g/l H_3BO_3, 4.2 g/l $NaHCO_3$, 0.109 g/l KH_2PO_4, 10 µg/l thiamine-HCl, 50 µg/l biotin, 50 µg/l vitamin B12, 0.24 mg/l Na2$MoO_4 \cdot 2H_2O$, 6.6 mg/l $FeCl_3$, 0.1 mg/l $CuSO_4 \cdot 5H_2O$, 0.08 mg/l $CoCl_2 \cdot 6H_2O$, 3.2 mg/l $MnCl_2 \cdot 4H_2O$, 0.22 mg/l $ZnCl_2$, and 40 mg/l Na_2EDTA. Cells were grown in 250 ml Erlenmeyer flasks at 180 rpm shaking at 20°C with a light/dark photoperiod of 14/10.

Nitzschia angularis MK8708 was grown in 100% Instant Ocean medium and was a gift from Dr. Paul Behrens. This medium was composed of 35 g/l Instant Ocean, 0.75 g/l $NaNO_3$, 0.3 g/l $Na_2SiO_3 \cdot 9H_2O$, 15 mg/l NaH_2PO_4, 20 mg/l $Fe_2SO_4 \cdot 7H_2O$, 17 mg/l Na_2EDTA, 34.2 mg/l H_3BO_3, 4.3 mg/l $MnCl_2 \cdot 4H_2O$, 0.3 mg/l $ZnCl_2$, 0.13 mg/l $CoCl_2 \cdot 6H_2O$, 0.025 mg/l $NaMoO_4 \cdot 2H_2O$, 0.01 mg/l $CuSO_4 \cdot 5H_2O$, 0.26 mg/l

$NiSO_4 \cdot 6H_2O$, 0.3 mg/l vitamin B12, 6 mg/l thiamine and 0.3 mg/l biotin. Cells were grown in 250 ml Erlenmeyer flasks at 180 rpm shaking at 20°C with a light/dark photoperiod of 14/10.

Cyclotella cryptica MK89172 was grown in 50% Instant Ocean medium and was a gift from Dr. Paul Behrens. This medium is the same as the 100% Instant Ocean medium listed above except 17.5 g/l of Instant Ocean was used instead of 35 g/l and the medium is supplemented with 8 g/l glucose. Cells were grown in 250 ml Erlenmeyer flasks at 180 rpm shaking at 20°C with a light/dark photoperiod of 14/10.

2.3.2 16S rRNA gene based strain identification.

To identify the aggregating strain, 16S rRNA gene PCR was performed using primers 27f and 1492r (36) and RP1137 cells added directly in the PCR reaction as the DNA template. Cycling conditions were one cycle at 95°C for 3 minutes, then 30 cycles of 95°C for 30 seconds, 46°C for 30 seconds, and 72°C for 90 seconds, with one cycle of 72°C for five minutes. The ca. 1465 bp product was purified using Qiagen's Qiaquick PCR purification kit. The purified PCR product was sequenced using primers 27f, 1492r, 700f (GTGKAGCRGTGAAA) and 700r (CTACGCATTTCACY) to obtain full-length double stranded sequence. The closest match for RP1137's 16S rRNA gene sequence was identified using NCBI's BLASTn algorithm. The GenBank accession number for the 16S rRNA gene sequence from *Bacillus* sp. RP1137 is KF015297.

2.3.3 Filtration aggregation assay.

Aggregation data was collected using a filtration aggregation 96 well assay. This assay was developed to allow testing of multiple parameters with replicates in a 96 well plate.

Filtration rigs were built by sandwiching a 50-µm mesh between two pipette tip racks (Tip One, USA Scientific) and sealing this mesh in place with silicon. The resultant apparatus was designated a "filtration rig", and fit neatly in a 96 well plate and retained aggregates on the mesh while non-aggregated algal cells (2-3 µm diameter) passed through into the wells of the microtiter plate. In a typical aggregation experiment 150 µl of algae at 1 x 10^7 cells/ml were pipetted into a round bottom 96 well plate. 1.5 µl of 100 fold concentrated bacterial suspension (original density of 1 x 10^7 cells/ml) was added to to the algae in the designated wells to give a 1:1 alga to bacterium ratio. Wells not receiving bacteria served as negative controls for aggregation induced by the addition of bacteria. The plate was sealed with parafilm and mixed by vortexing for 1 minute. A filtration rig was placed on a round bottom 96 well plate and the 150 µl containing the aggregates was pipeted from the first microtiter plate into the top of the filtration rig using wide bore pipet tips. The plate and rig were centrifuged at 100 x *g* for 10 seconds to ensure that the entire volume in the rig passed through the mesh into the second lower 96 well plate. At this point the aggregates are retained on the mesh and the non-aggregated cells have passed into the second plate. The algae in the second plate were suspended and diluted into the linear range for chlorophyll fluorescence measurement in a Spectromax M5 microplate reader. Chlorophyll fluorescence was measured with an excitation wavelength of 488 nm, a 515 nm cutoff filter and an emission wavelength of 685 nm. From these data the percentage of algae that had aggregated and remained on the mesh were calculated from the fluorescence of the algae that were not aggregated using the formula $P = (1-(A/N))\cdot 100$, where P = percent algae aggregated, A =

fluorescence of the filtrate from the aggregated sample and N = fluorescence of the filtrate from the nonaggregated sample.

2.3.4 Fluorescence microscopy.

Microscopy was used to visualize the structure of the bacterial/algal aggregates. A 1 ml aliquot of *Bacillus* sp. RP1137 was stained with 2.5 µl of SYBR green I nucleic acid stain for 10 minutes in the dark. The bacteria were concentrated by centrifugation at 13,000 x *g* for 2 minutes and the cell pellet was suspended in 10 µl of fresh medium giving a 100-fold concentration of the bacteria. An 8 µl portion of this suspension was added to 800 µl of *Nannochloropsis* cells in f/2 medium at an OD_{600} of 1.0 and mixed. Aggregates were pipetted onto a slide and visualized using laser scanning confocal microscopy using a Zeiss Axioskop with a BioRad Radiance 2100 laser light source. Both algal chlorophyll and SYBR green I stained bacteria were excited with a 488 nm argon laser. The SYBR green signal was visualized using a 415/30 nm band pass filter and the chlorophyll autofluorescence was visualized with a 600 nm long pass filter. Controls comprising bacteria only and algae only were used to ensure there was no cross bleeding of signals between the two channels.

2.3.5 Temperature dependence.

To determine the effect of temperature on aggregation 150 µl of algae was transferred into PCR tubes. The PCR tubes were placed in a thermocyler to hold the algal suspensions at 10, 20, 30 or 40°C. These temperatures were chosen because they represent the range of temperatures likely to occur in an outdoor algal production pond. The algae at 1 x 10^7 cells/ml were incubated for 10 minutes to ensure they reached the set temperatures. To half of the tubes at a given temperature 1.5 µl of 100-fold concentrated

RP1137 cells (original density of 1 x 10^7 cells/ml) were added and mixed by votexing. The other half of the tubes served as "no aggregation" controls. All samples were transferred to the top of the filtration aggregation rig and the assay was continued as described above.

2.3.6 Salinity dependence.

Salinity dependence of aggregation was determined by harvesting a 5 ml aliquot of algae at 5580 x *g* for each salinity tested. Half of the supernatant was removed (2.5 ml). *Nannochloropsis* was grown in 20 ppt salinity. To get 10 ppt salinity, 2.5 ml of dH_2O was added; for 20 ppt salinity, 2.5 ml of 20 ppt NaCl was added; for 30 ppt salinity 2.5 ml of 40 ppt NaCl was added; for 40 ppt salinity, 2.5 ml of 60 ppt NaCl was added; and for 156 ppt salinity, 2.5 ml of 292 ppt NaCl was added. For the 0 ppt salinity sample, the cell pellet was suspended in dH_2O and the pH was adjusted to match the other samples (pH 10.2). This last sample had an effective salinity of 0.005 ppt due to the NaOH used to adjust the pH. After salinity adjustment the filtration aggregation assay was carried out to quantify the effect of salinity on aggregation.

2.3.7 pH dependence.

The pH dependence of aggregation was determined by adjusting the pH of a 200 ml aliquot of *Nannochloropsis* at 1 x 10^7 cells/ml in a beaker with constant stirring. pH was adjusted with either 5M NaOH or 5M HCl, concentrated base or acid was used to limit changes in algal cell concentration. When pH stabilized at a desired value, 150 µl of algal suspension was quickly pipetted into a 96 well plate. An overnight culture of *Bacillus* sp. RP1137 with a density 1 x 10^7 cells/ml was 100-fold concentrated and 1.5 µl of the concentrate was added to half of the wells. The other half of the wells served as

0% “aggregation negative” controls. The filtration aggregation assay was carried out and a final pH measurement was taken to ensure the pH had not shifted significantly during the assay. This process was repeated for each pH tested.

2.3.8 Viability dependence.

Two 5 ml portions of algae and two 5 ml portions of bacteria were used. To one algal sample and one bacteria sample, 5 ml of 8% paraformaldehyde (pH 7) was added and mixed. To the other algal and bacterial samples 5 ml of dH_2O was added. All samples were then incubated at RT for 1 hour with mixing every 15 minutes. All samples were then harvested by centrifugation at 5580 x *g* for 5 minutes. The supernatants were aspirated and the algal samples were suspended in 5 ml of cell free spent algal media from the original algal culture. Bacterial samples were suspended in 5 ml of 2216 marine broth. All samples were again concentrated by centrifugation, aspirated and suspended. The algae were suspended in 5 ml to keep their original concentration while the bacteria were suspended in 50 µl to give a 100 fold concentration. 150 µl aliquots of the algae at 1×10^7 cells/ml were transferred to a 96 well plate and 1.5 µl of the concentrated bacteria per well (original density of 1×10^7 cells/ml) were used for aggregation experiments. The filtration aggregation assay was followed to complete quantitation of aggregation with the live and dead cells.

2.3.9 Cell ratio.

For cell ratio experiments, the concentration of bacteria and algae were determined using an Accuri C6 flow cytometer. Media that had been filtered through a 0.22-µm filter was used to grow both the algae and bacteria. The same media was used as the blank for determining the correct parameters for detecting cells. Chlorophyll fluorescence was

used as the cutoff for gating algal cells. A forward scatter area cutoff of greater than 5000 was used for gating RP1137 cells, which excluded non-cellular debris found in both 0.22 µm sterile filtered 2216 medium and the RP1137 cultures. The algal cell concentration and volume (150 µl) was held constant in all wells in the 96 well-plate, while the concentration of the bacteria added was adjusted. Bacterial volume added was held constant. The bacterial culture was either concentrated by centrifugation or diluted to achieve the bacteria:algae ratios tested of 25:1, 5:1, 1:1, 1:5, 1:25, and 1:125. As before, 1.5 µl of concentrated bacteria were added to each well and the filtration aggregation assay was used to quantify the percent of algae that were aggregated.

2.3.10 Aggregation of other algae.

T. chuii, *T. sucia*, *Phaeodactylum* sp., *N. oleoabundans* MK8520, *C. cryptica* MK89172 and *N. angularis* MK8708 were grown until the pH of cultures was between 9.5 - 10. The strains were tested using the filtration aggregation assay as described above.

2.3.11 Filament shearing assay.

RP1137 cells were split into two portions. One portion serves as the control and the other portion was sheared by passing the cells through a 28.5 gauge needle 80 times. These conditions were determined empirically. The cells were then tested using the filtration aggregation assay as described above.

2.3.12 Proteinase K digestion assay.

RP1137 cells were digested with 100 µg/ml proteinase K in 1x PBS buffer at pH 7.4 following the manufacturer's directions. Non-digested samples were incubated in 1x PBS. Samples were incubated for two hours at room temperature or 50°C. Bacteria were

then washed twice with 1x PBS to remove the proteinase K and then tested using the filtration aggregation assay.

2.3.13 Carbohydrate inhibition assay.

Glucose, galactose, mannose and lactose were individually added to aliquots of *Nannochloropsis* cells at concentrations from 200-800 mM. RP1137 cells were added to these algal aliquots to assay the effectiveness of each carbohydrate at inhibiting aggregation.

2.3.14 Ca^{2+} & Mg^{2+} dependence assay.

Nannochloropsis and RP1137 cells were washed three times in pH 10.3 deionized water. The washing procedure involved concentrating the cells via centrifugation followed by aspiration of the supernatant and resuspension of the cells in pH 10.3 deionized water. A 0.5 M stock of $CaCl_2$ or $MgSO_4$ was added to the algae obtain the final Ca^{2+} or Mg^{2+} concentrations of 0.125, 0.25, 0.5, 1, 2, 4, 8, and 16 mM. The algae solution containing the metal ions was then tested using the filtration aggregation assay with RP1137 cells.

2.4 Results

2.4.1 Isolation of an algae-aggregating bacterium.

An environmental bacterium that was able to rapidly aggregate algae was isolated from a *Nannochloropsis oceanica* IMET1 aggregation experiment. When this bacterium was added to *Tetraselmis sp.* cultures and mixed, it quickly aggregated the algae, with most of the algae settling out of solution in large aggregates in 30 seconds (Fig. 2.1). This new strain was found serendipitously as a contaminant in a broth culture of HW001, a

bacterium previously reported to have the ability to aggregate algae (30). The contaminant was isolated into pure culture and was shown to have a superior ability to aggregate algae compared to HW001. The 16S rRNA gene of this new isolate was PCR amplified and sequenced. The sequence was identified using BLASTn and was found to have a 99% sequence identity to *Bacillus megaterium* strain PPB7. This aggregating strain was designated as *Bacillus* sp. RP1137. Previous work by Wang et al. showed bacteria that match the 16S sequence of *Bacillus* sp. RP1137 are not present in *Nannochloropsis* cultures and indeed no bacteria within the phylum *Firmicutes* were found (30), indicating it is unlikely that RP1137 is a major component of the natural algal bacterial community.

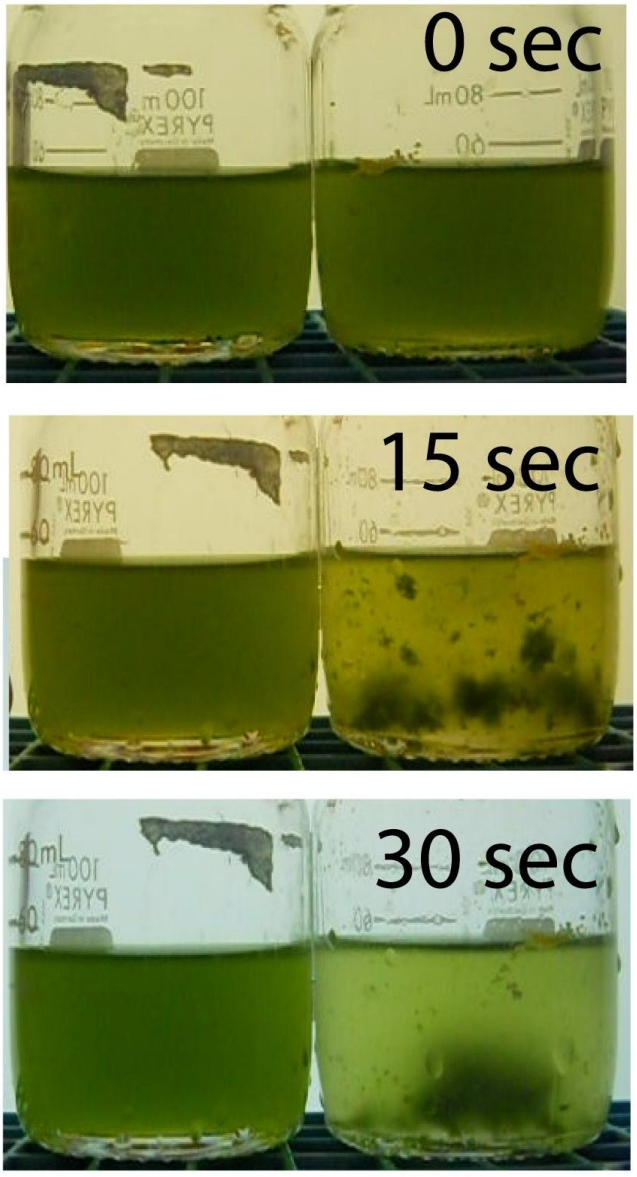

Figure 2.1 Rapid aggregation of algae by RP1137

Aggregation of algae is rapid upon addition of the bacterium *Bacillus* sp. RP1137. Aggregates form within 15 seconds and by 30 seconds the aggregates have settled out of solution. RP1137 cells were added to the bottle of *Tetraselmis* sp. on the right at a 1:1 ratio of algae to bacteria. The bottle on the left serves as a control.

The original cryo-preserved stock of HW001 was examined and found to be pure. Comparison of the 16S rRNA gene sequences to all sequences derived from culture based and culture independent analyses in the laboratory revealed no matches. *B. megaterium* species can be found in seawater, freshwater and soil (37), suggesting the environment where the strain originated from will likely remain unknown.

To investigate the nature of the aggregates formed when *Bacillus* sp. RP1137 is added to *Nannochloropis* cultures the aggregates were visualized by laser scanning confocal microscopy. Visualization of the microstructure of the aggregates was done to help elucidate the mechanism of aggregation. Bacteria in these images are filamentous and are intercalated between algal cells (Fig. 2.2). In general, the bacteria are mostly in contact with algae, with little bacterium to bacterium contact along the length of the cell, as opposed to the bacteria packing tightly along the cell length. The algae are in contact with both the bacterial cells and other algal cells. Packing of the cells in the aggregates is tight, with apparent cell-to-cell contact, which suggests the mechanism of aggregation involves interactions at the cell surface.

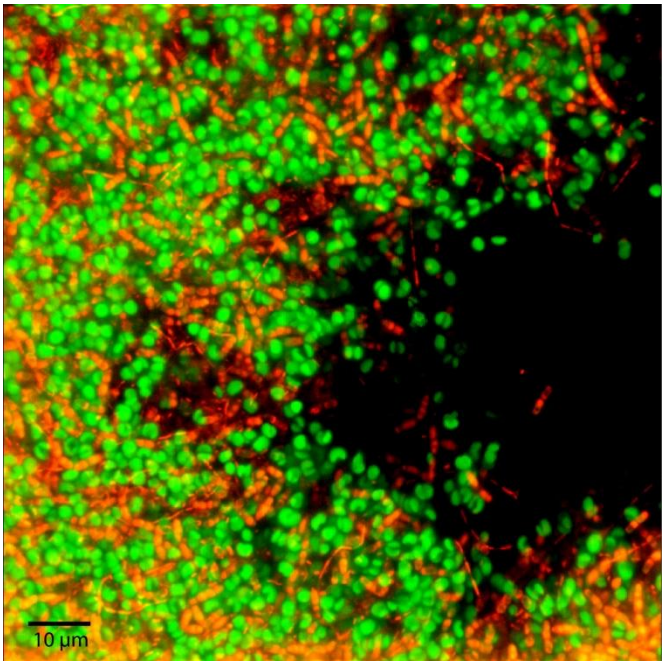

Figure 2.2 Laser scanning confocal micrograph of a *N. oceanica* IMET1-*Bacillus* sp. RP1137 aggregate.

Algae (green) were visulized by chlorophyll autofluorescence and the bacteria (orange) were visulized using SYBR green I staining.

2.4.2 Determination of the optimal bacterium:alga ratio.

Microscopy showed that the bacterial filaments within an aggregate are intertwined throughout the structure and interact with multiple algal cells. This raised the question of how many bacteria are needed per algal cell to efficiently form these aggregates. The optimal bacteria to algae ratio is also important for practical use of this strain in harvesting algae, to maximize aggregation efficiency with a minimum of bacteria. To test multiple ratios of bacteria to algae and get statistically meaningful data, a 96-well plate aggregation assay was developed and is discussed in detail in the materials and methods section. Briefly, the bacteria and algae are combined in a 96-well plate and mixed to form aggregates. The entire volume of each well (aggregated and nonaggregated cells) is passed through a mesh with 50 μm openings. *Nannochloropsis* cells in culture are mostly found as single, spherical cells with a diameter of 2-3 μm. The few natural aggregates are small and have an average cross sectional area of 71.6 μm^2 (30) which easily pass through the mesh which has 2500 μm^2 openings. The algal/bacterial aggregates are retained on this mesh while nonaggregated cells pass through into a second 96 well plate. The algal cells that pass through into the second plate are then quantitated using chlorophyll fluorescence and compared to a control where only algae (no bacteria added to induce aggregation) were passed through the mesh. From these data the percentage of algae that have been aggregated by the bacteria can be calculated. This process is referred to here as the filtration aggregation assay.

To determine the optimal bacteria to algae ratio, the volume and concentration of algae were held constant in each well and different concentrations of bacteria were added. Ratios between 25 bacteria to one algal cell and one bacterium to 125 algal cells were

tested. The ratio of bacteria to algae for optimal aggregation was 1:1, with 1:5 bacteria to algae being only slightly less efficient than 1:1 bacteria to algae at aggregating *Nannochloropsis* (Fig. 2.3). These data are consistent with the visual results seen in fluorescence micrographs, where one bacterial cell interacts with several algal cells. At less than one bacterium per five algal cells the efficiency of aggregation decreases. The efficiency of aggregation also decreases when the number of bacteria used becomes higher than the number of algae. This is likely due to increased self-aggregation between bacterial cells, leaving fewer bacteria to aggregate algal cells. Self-aggregation does occur when the bacteria are present in pure culture if the pH of the culture is increased to pH > 10, which is similar to the pH in dense *Nannochloropsis* cultures. The data presented above indicate there is an optimal ratio of bacteria to algae cell for bioaggregation and at higher or lower ratios, the efficiency of aggregation decreases.

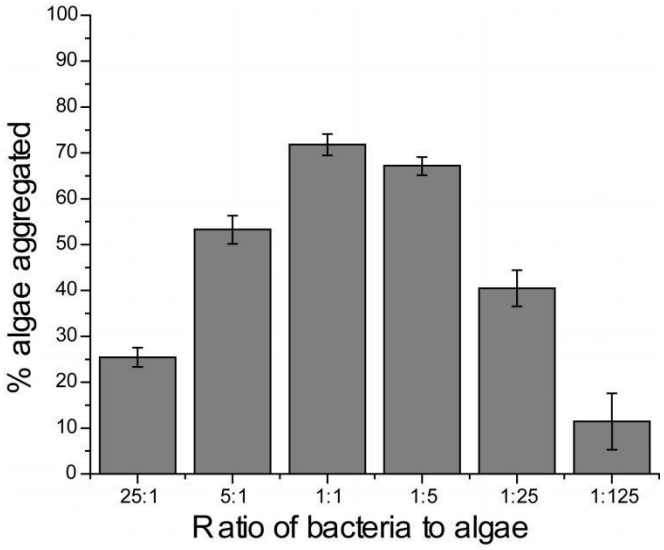

Figure 2.3 Optimal ratio of bacteria to algae

Aggregation efficency is highest when one bacterium is added for every one to five algal cells present. At ratios above and below this aggreagtion efficency is reduced. The ratio of 5:1 is statistically different than the ratio of 1:1 ($p = 8.0E\text{-}5$). The ratio of 1:1 is statistically different than the ratio of 1:5 ($p = 0.009$). Bar and error bars represent the mean and standard error respectively of five independent aggregation reactions. A value of 100% is aggregation of all algal cells.

2.4.3 Characterization of the physical conditions that affect algal aggregation.

Next I was interested in determining which physical factors affect aggregation of the algae. From the microscopy data it appears the mechanism of aggregation likely involves cell to cell contact, as opposed to aggregation of the algae by unassociated cellular exudates. To begin unraveling the nature of this cell-to-cell adhesion I decided to test if aggregation is pH dependent. Solution pH dictates the surface charge of exposed proteins and will affect both specific and non-specific protein driven interactions. From a practical stand point the effect of pH on aggregation is also important because dense algal cultures can quickly increase pH through carbon fixation and also rapidly decrease pH through respiration. The effect of pH on aggregation was tested by adjusting the pH of the aliquots of algal cultures with either NaOH or HCl. The pH values tested ranged from pH 6-10. In this experiment the pH of the algae was set, then the filtration aggregation assay was run and a final pH reading was taken to ensure the pH did not change significantly during the experiment. The pH value does have a significant effect on aggregation as shown in Fig. 2.4 A. At pH 8 and below there is no significant aggregation and at pH 9 and above aggregation is highest. These data show aggregation of *Nannochloropsis oceanica* IMET1 by *Bacillus* sp. RP1137 is pH dependent with aggregation occurring only when pH is above 9. When the pH of the solution was decreased, disaggregation was observed showing that aggregation was also reversible (Fig. 2.4 B).

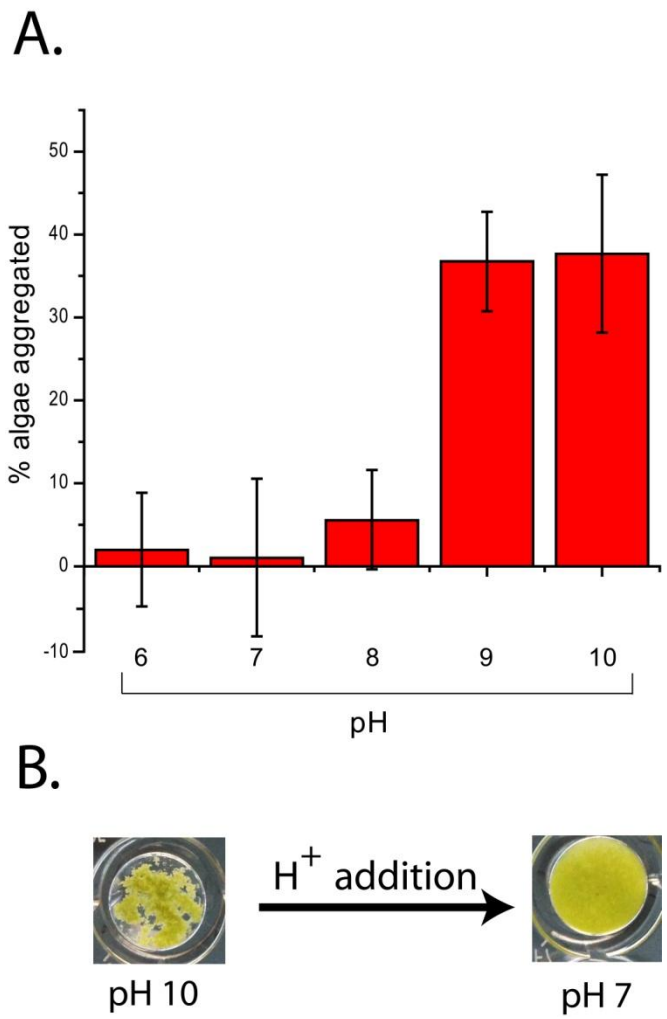

Figure 2.4 pH dependence of aggregation

Aggregation efficiency is pH dependent and reversible. (A) Optimal aggregation occurs at pH 9 and above. Aggregation at pH 9 is significantly higher than pH 8 ($p=5.9E-8$). Aggregation above pH 9 is not significantly increased ($p>0.05$). There is no significant change in aggregation below pH 8 ($p>0.05$). Bar and error bars represent the mean and standard error respectively of eight independent aggregation reactions. A value of 100% is aggregation of all algal cells. (B) Aggregates formed at pH 10 disperse when pH is lowered to 7. pH was lowered with HCl.

In addition to pH, the salinity and temperature of algal production ponds can vary. The effect of salinity on aggregation was determined by adjusting the salinity of aliquots of *Nannochloropsis* cultures from 0-156 ppt. Optimal aggregation occurred at 20 ppt salinity with minor, but significant decreases in aggregation between 20 ppt and 156 ppt (Fig. 2.5). Aggregation was also significantly decreased at 0 ppt salinity compared to 20 ppt salinity.

Outdoor algal production ponds can experience changes in temperature, which could result in different potential harvesting conditions. I tested the effect of temperature by performing the aggregation process between 10-40°C. Large differences that would be significant in practical applications at different temperatures were not observed, however minor statistically significant changes were observed (Fig. 2.6). Optimal aggregation occurred at 20°C.

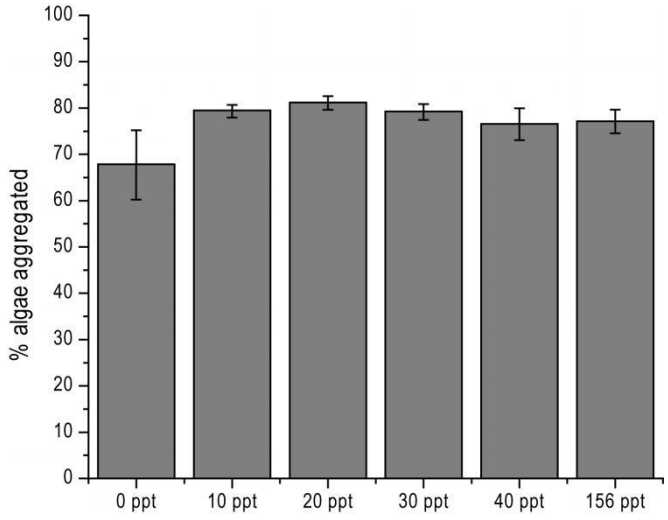

Figure 2.5 Salinity dependence of aggregation

Aggregation is inhibited at low salinity and high salinity relative to the 20 ppt salinity used in the algal medium. Aggregation is significantly reduced at 0 ppt compared to 10 ppt salinity ($p=0.002$) and 20 ppt ($p=0.001$). Samples at 20, 30 and 40 ppt salinity are not significantly different ($p>0.05$). A small but significant decrease in aggregation is observed between samples at 20 and 156 ppt salinity ($p=0.002$). Bar and error bars represent the mean and standard error respectively of eight independent aggregation reactions. A value of 100% is aggregation of all algal cells.

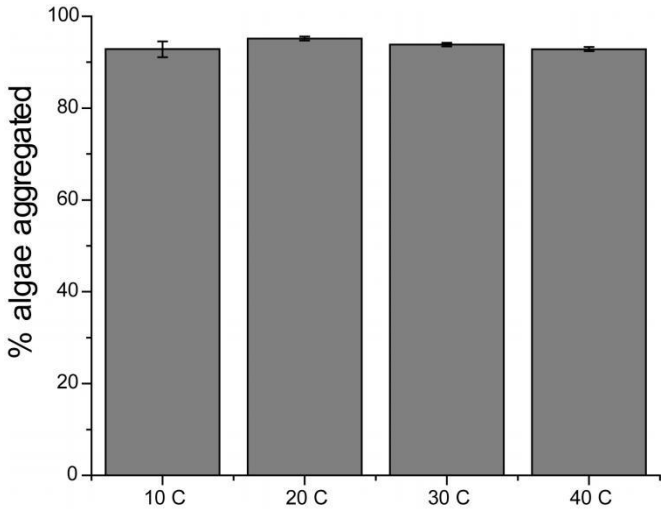

Figure 2.6 Temperature dependence of aggregation

Temperature has minor but significant effects on aggregation. Aggregation is optimal at 20°C and is significantly higher at 20°C than 10°C (p=0.006), 30°C (p=3.9E-5) and 40°C (p=3.1E-7). Bar and error bars represent the mean and standard error respectively of eight independent aggregation reactions. A value of 100% is aggregation of all algal cells.

One concern in using bacterial bioaggregation as a means of harvesting microalgae is that the production of the bacteria must be scaled with the production of the microalgae. One way to dramatically reduce the number of bacteria needed is to recycle the bacterial cells, effectively using the bacteria as aggregating microparticles. This would be made easier if dead cells retained their aggregation phenotype. To test if dead cells still aggregate algae, *Bacillus* sp. RP1137 cells were killed with 4% paraformaldehyde and the aggregation potential of these dead cells was compared to the same number of live cells. Plating of PFA-treated cells revealed no viable colonies versus $2.6 \times 10^8 \pm 6.3 \times 10^7$ cells in the untreated controls. The efficiency of aggregation by the PFA killed cells had a minor but significant increase relative to live cells (Fig. 2.7A). These data show that the aggregation phenotype of RP1137 is not due to a response by the cell and is instead a passive characteristic that is likely part of the cell surface. As a further step, aggregation of live and PFA-killed *Nannochloropsis* was attempted with both live and dead *Bacillus* sp. RP1137 cells. Aggregation efficiency with PFA killed algal cells had a minor but significant increase relative to live algal cells ($p=0.009$). As with the live algae the dead bacteria had a minor but significant increase in aggregation efficiency relative to the live RP1137 cells (Fig. 2.7B).

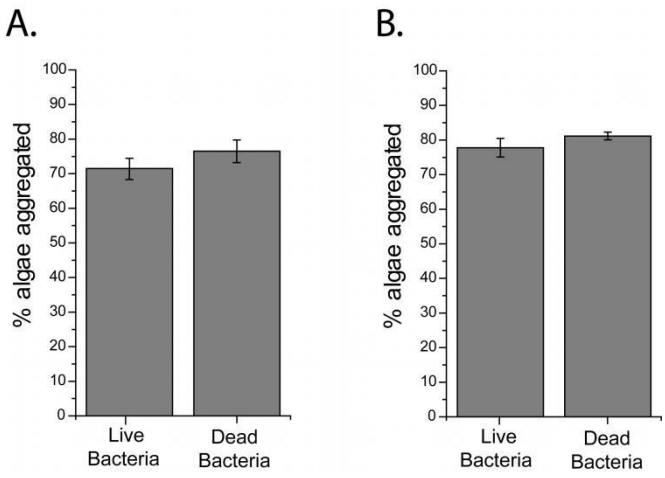

Figure 2.7 Aggregation with live and dead RP1137 cells

The mechanism of aggregation does not depend on live bacteria or live algae. (A) Live algae were aggregated with both live and dead bacteria. Dead bacteria have a minor but significant increase in aggregation relative to live ($p=0.06$). (B) Dead algae were aggregated with both live and dead bacteria, with dead bacteria aggregating the dead bacteria significantly better ($p=0.01$). Bar and error bars represent the mean and standard error respectively of eight independent aggregation reactions. A value of 100% is aggregation of all algal cells.

2.4.4 Aggregation of candidate biofuel producing algae.

Bacillus sp. RP1137 effectively aggregates *N. oceanica* IMET1 in a pH dependent and reversible manner. The *Bacillus* sp. RP1137 cells can also be used effectively after the cells have been killed by fixation. Next I was interested in seeing if this bacterium can aggregate algae other than *Nannochloropsis*. A panel of algal strains was tested that are of interest for their potential as biofuel production strains. The strains tested were *T. chuii* , *T. sucia, Phaeodactylum* sp., *N. oleoabundans* MK8520, *C. cryptica* MK89172 and *N. angularis* MK8708. The bacterium *Bacillus* sp. RP1137 was able to aggregate both of the *Tetraselmis* species with a measured aggregation efficiency of 78.3 % ± 4.3% for *T. sucia* and an efficiency of 13.1 % ± 3.1 % for *T. chuii*. The bacterium was also able to aggregate the *Phaeodactylum* sp. with a 17.3 % ± 3% efficiency. *N. oleoabundans*, *C. cryptica* and *N. angularis* had little or no aggregation with efficiencies of 6 % ± 4.4 %, 1.3 % ± 9 % and 0.02 % ± 5.7 % respectively. The reason the diatom *Phaeodactylum* aggregated but the other diatoms did not is unknown, however it is likely dependent on differences in the cell wall of these organisms.

2.4.5 Characterization of the mechanism of aggregation.

Next I was interested in exploring the mechanism of algal aggregation by the bacterium RP1137. *N. oceanica* IMET1 was used as the model alga for these investigations. From the confocal microscopy images I hypothesized that RP1137's filamentous morphology was important for aggregation of algae. To test this I sheared the filaments by passing the cells through a 28.5 gauge needle repeatedly. Shearing reduced the RP1137 population to single cells and doublets (Fig. 2.8A). Sheared and unsheared cells were used for aggregation assays. The results showed that the morphology of the cells does have a

significant effect on aggregation ($p = 2.71E-7$), with sheared cells having a 2.6% decrease in aggregation efficiency compared to the unsheared cells (Fig. 2.8B). While statistically significant this minor difference between filaments and single cells or doublets indicates that the filamentous form of RP1137 is not a major factor in the process of aggregation.

Fixed RP1137 cells are still able to aggregate algae, suggesting that the cell surface rather than active metabolic processes are important. To determine if the aggregation potential of the cells is dependent on exposed surface proteins I digested RP1137 cells with proteinase K. This approach has been used with *Helicobacter pylori* to digest off and identify surface proteins (38). When cells were incubated at room temperature with proteinase K there was no significant difference in aggregation efficiency between digested and non-digested RP1137 cells (Fig. 2.9). Cells incubated with proteinase K at 50°C displayed a significant ($p = 0.002$) yet small decrease in aggregation efficiency of 4% when compared to non-digested controls, indicating that proteinase K cleavable surface proteins are not a major factor in the aggregation process.

Adhesion between different cells is often mediated by lectin-carbohydrate type interactions. These interactions can be disrupted by blocking the lectin with the addition of other carbohydrates. To determine whether lectin-carbohydrate interactions are important in aggregation, glucose, galactose, lactose and mannose were added at concentrations ranging from 200 mM to 800 mM in aggregation reactions. No significant inhibition of aggregation was observed during any of these experiments.

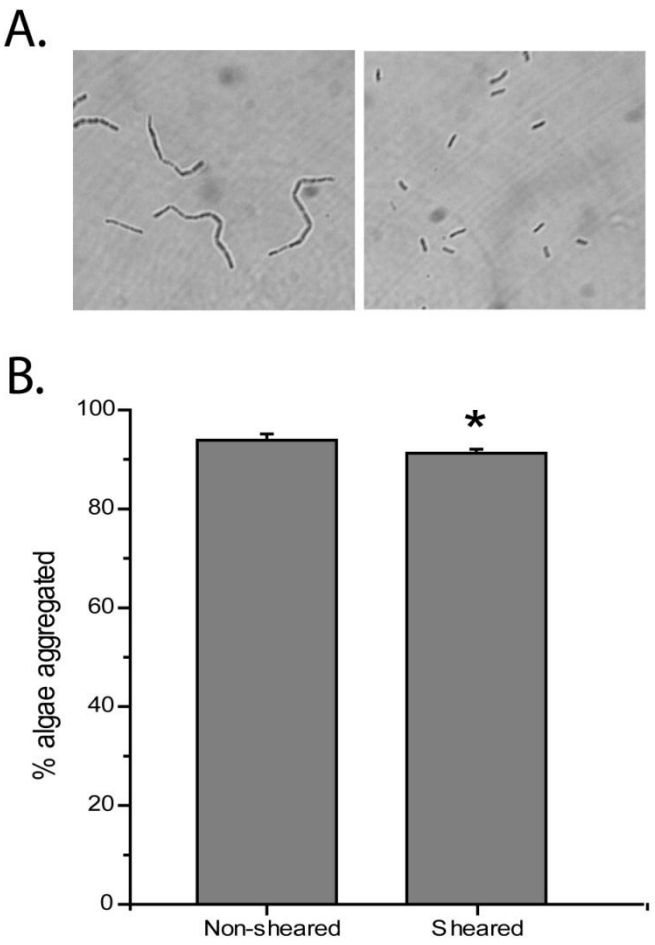

Figure 2.8 Filament dependence of aggregation

Bacterial filament length has minor effect on aggregation efficiency. (A) Phase contrast image of RP1137 before shearing (left) and the same population of cells after shearing (right). (B) Aggregation of *Nannochloropsis* with non-sheared cells and sheared cells, showing a statistically significant ($p = 2.71E-7$) but minor effect due to filament length. Bar and error bars represent the mean and standard error respectively of 16 independent aggregation reactions. A value of 100% is aggregation of all algal cells.

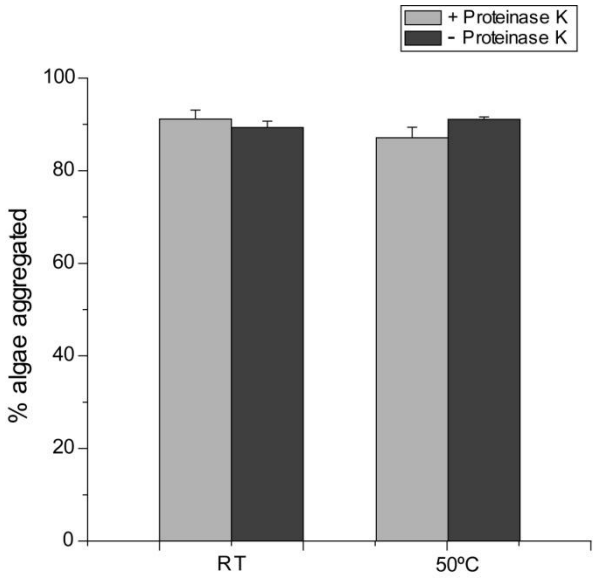

Figure 2.9 Proteinase K treatment of RP1137 cells and its effect of aggregation

Aggregation with RP1137 cells who were treated with proteinase K to digest surface associated proteins. Cells incubated at room temperature (RT) with proteinase K do not have a statistically significant difference in aggregation efficiency compared to untreated control($p>0.05$), while cells treated at 50°C show a minor but statistically significant decrease in aggregation efficiency ($p=0.002$) relative to the untreated control. Bar and error bars represent the mean and standard error respectively of eight independent aggregation reactions. A value of 100% is aggregation of all algal cells.

I next hypothesized that divalent cations are required for aggregation. As an initial test of this hypothesis I added 50 mM ethylenediaminetetraacetic acid (EDTA) and 50 mM ethylene glycol tetraacetic acid (EGTA) to *Nannochloropsis* in f/2 medium while maintaining pH at 10.3. Both EDTA and EGTA chelate divalent cations with EDTA having a higher affinity for magnesium and EGTA having a higher affinity for calcium. EDTA and EGTA at 50 mM were sufficient to inhibit aggregation by RP1137 cells (Fig. 2.10A). To confirm the importance of divalent cations I next performed dose-dependent aggregation assays in deionized water with different concentrations of magnesium or calcium ions. The cells were washed several times with deionized water (pH 10.3) to remove trace ions. Fixed algae and fixed bacterial cells were used. Aggregation was found to be highly dependent on the concentration of magnesium and calcium present in solution with the algae (Fig. 2.10B). At micromolar concentrations of either ion, little or no aggregation was observed. At 8 mM of calcium maximum aggregation efficiency is observed, while maximum aggregation efficiency with magnesium occurs at 16 mM. Addition of calcium or magnesium to *Nannochloropsis* alone does not precipitate aggregation in the absence of RP1137 cells. These data show that aggregation of *Nannochloropsis* by RP1137 is highly dependent on magnesium and calcium concentration.

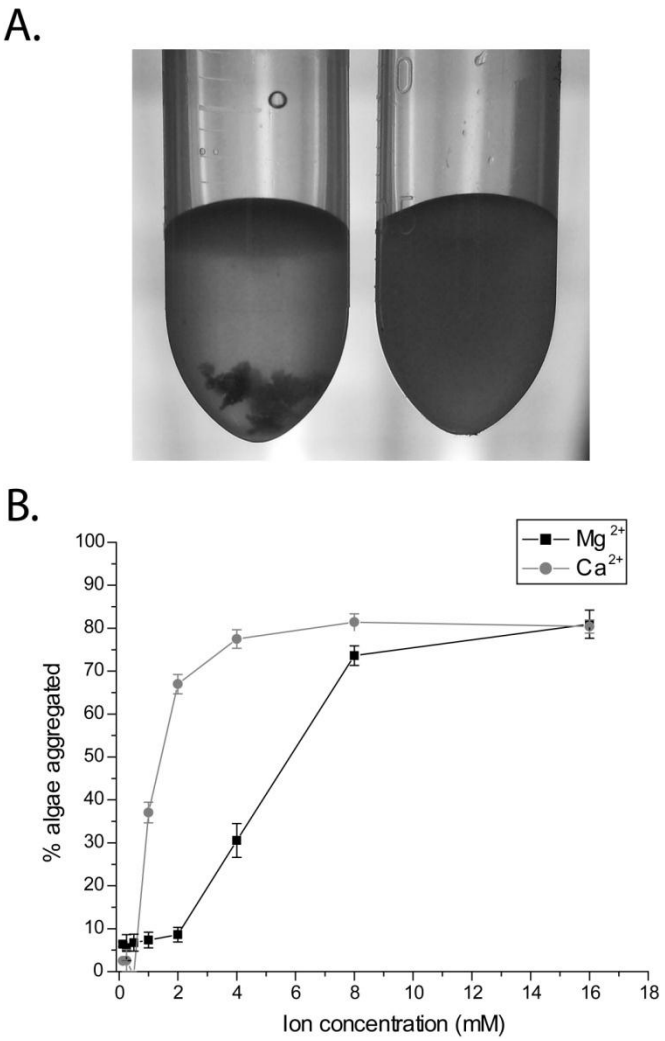

Figure 2.10 Calcium and magnesium dependence of aggregation

FIG 7 Aggregation is dependent on divalent cations. (A) Aggregation in artificial seawater is inhibited by the addition of EDTA and EGTA at 50 mM each (right) compared to the untreated control (left) when pH is held constant. (B) Dose dependent effect of calcium and magnesium on aggregation, showing increasing aggregation with increasing concentrations of calcium or magnesium. Points and error bars represent the mean and standard error respectively of four independent aggregation reactions. A value of 100% is aggregation of all algal cells.

2.5 Discussion

I show live and dead *Bacillus* sp. RP1137 cells can rapidly aggregate *N. oceanica* IMET1 in a pH dependent manner. I previously reported a novel bacterial isolate from Permian groundwater that can aggregate *N. oceanica* IMET1 but this process occurred over hours to days (30). By contrast, aggregation of *N. oceanica* IMET1 by *Bacillus* sp. RP1137 occurs extremely rapidly, in seconds. I also show that *Bacillus* sp. RP1137 can aggregate other biofuel producing algae. The purpose of this study is the identification and evaluation of the aggregation ability of this bacterial isolate and specifically to test the robustness of its aggregation phenotype under different conditions. Due to the practical implications of the work experiments were generally carried out in algal growth media so the results can be directly interpreted. It is also worth noting that a simple assay was developed to quantify aggregation potential, to avoid some pitfalls that befall other methods when trying to measure algae aggregated upon addition of bacteria. For example, using dry weight of the aggregated algae is complicated by the unknown biomass that is contributed by bacteria to the aggregates. The other common method to quantitate aggregation is to measure sedimentation rates, usually via absorbance of the supernatant (22). The bacteria added during aggregation assays contribute to absorbance, occluding the removal of algae from the water column. To deal with these complications, the filtration aggregation assay measures chlorophyll autofluorescence to exclude any signal from the bacteria. Additionally, our method measures the uniform, non-aggregated algae fraction to get an accurate signal of the amount of algae remaining after aggregation. By comparing the remaining fluorescence after aggregation to the

fluorescence of same algal stock that received no treatment the percent of algae aggregated can be calculated.

One of the most important questions for the practicality of using bacteria as a means to harvest algae is how many bacteria are need to harvest a given number of algae. Here the data show a ratio of one bacterium to five algal cells is sufficient to efficiently harvest the algae Below this ratio efficiency of aggregation decreases; this decrease is likely due to individual bacterial cells being coated by algae and preventing the formation of larger flocs. When the number of bacteria increases above one-to-one the efficiency of aggregation also decreases. This may be due to increased bacterium to bacterium interactions which again occlude the formation of larger aggregates. The bacteria can grow to densities ten times higher than the algae meaning if the bacteria are used once then one unit volume of bacteria are needed to aggregate 50 volumes of algae. This represents a substantial amount of bacteria to be cultured for a large scale algal production facility. As a means to gain information about the mechanism of aggregation I tested if bacteria that had been killed with paraformaldehyde could still effectively aggregate the algae. These killed cells exhibit an equivalent aggregation potential compared to their live counterparts. Mechanistically, this rules out any response by the cell to initiate aggregation and suggests that the mechanism of aggregation is associated with factors located at the cell surface. When cells are fixed by paraformaldehyde their structure is preserved which opens the possibility of incorporating the fixed cells onto a solid surface that would allow them to be reused after the algae have been removed from the water. This type of reuse of the bacterial cells could be facilitated by the finding that the aggregation process can be reversible by lowering the pH. An additional advantage of

using killed cells is that there is no concern of contamination of the main algal culture or the environment because the cells will not propagate.

The physical conditions under which harvesting of algae by *Bacillus* sp. RP1137 is most effective were investigated. Of the conditions tested, pH was the most critical with aggregation occurring when the pH was at or above 9. In general, in experiments testing effects of pH on aggregation, a lower percent of algae were aggregated than in other experiments. This may be due to these earlier pH experiments being done with RP1137 cells at a different phase of growth than later experiments. Preliminary data suggests that aggregation potential of RP1137 changes over the growth period of the culture. Detailed experiments supporting these preliminary results are presented in chapter 3. Obtaining pH values in this range does not require addition of base to the media because algal cultures naturally increase pH via the consumption of CO_2 during photosynthesis. Maximum values of pH 10.2 to 10.4 were routinely observed in the *Nannochloropsis* cultures used in this study, with pH varying from 7.5 in newly inoculated cultures to nearly 10.3 – 10.4 in dense cultures In naturally occurring systems and algal production ponds pH varies throughout the day (39). Water temperature will also vary during a day and throughout different times of year. I tested the effect of temperature and found only minor differences among the temperatures tested. There was also no large effect of salinity effect on aggregation except at 0 ppt salinity where aggregation was 15% lower than the 20 ppt samples. It should be noted that in the pH, temperature and salinity experiments data were collected on aliquots of algae that were grown under standard conditions and then after harvesting a sample the condition being tested was varied so the direct effect of these conditions on the aggregation ability of

these cells could be measured. These measurements are likely dependent on how the particular condition tested impacts the surface chemistry of the cells. However cells grown for extended periods of time under differing conditions of salinity, temperature or pH may have different surface characteristics than the cells tested in these experiments.

The aggregation of several different algae by RP1137 was tested to determine if this bacterium could be used for harvesting other algae besides *Nannochloropsis.* The results showed that this bacterium could aggregate two strains of *Tetraselmis* and a *Phaeodactylum* species but was not able to aggregate *N. oleoabundans, C. cryptica* and *N. angularis* effectively without increasing pH first by the addition of base. These data show that *Bacillus* sp. RP1137 has the potential to aggregate other algae and may be useful for the harvest of other algae besides the potential biofuel producer *N. oceanica* IMET1, although optimization would be needed to achieve the efficiencies that I achieved with *Nannochloropsis* aggregation.

RP1137 forms long filaments which were hypothesized to aid aggregation by increasing bridging between separate algal cells. I tested this hypothesis by shearing the filaments to break them into single cells or doublets and then using the sheared cells in aggregation assays. I found a significant, though minor, decrease in the percent of algae aggregated in the sheared population. This suggests the filaments are not the major phenotype responsible for aggregation. The minor effect of filament length and the fact that killed cells retain the ability to aggregate microalgae suggests that the cell surface characteristics may be important in aggregation. There are different types of potential cell surface interactions that could lead to aggregation, including specific and non-specific protein interactions. To look for an effect due to surface proteins, I digested RP1137 cells

with proteinase K to digest exposed and cleavable proteins. Digestion at room temperature yielded no significant differences in the aggregation potential of digested cells relative to a non-digested control A significant, though minor, decrease in the percent of algae aggregated was observed when the cells were digested at 50°C at which proteinase K has a higher activity. The lack of a large effect upon digestion with proteinase K does not exclude the possibility that surface localized proteins play a role in aggregation since there may be surface proteins that are recalcitrant to digestion by proteinase K. Proteinase K was shown to exert an activity on the cells through the dispersal of filaments into single cells in only the treated cells and not the controls. The strong effect on aggregation of higher pH values when the bacterial cell surface would likely become increasingly negatively charged suggested that the aggregation mechanism may be charge-related. The finding that aggregation was completely abolished by washing the algae and bacteria several times in deionized water indicated that ionic species may be important for aggregation Addition of EDTA and EGTA completely abolished aggregation in f/2 medium, suggesting that divalent cations are important for aggregation. The calculated concentrations of the major divalent cations in the f/2 medium used are 5.9 mM and 30.5 mM for calcium and magnesium ions respectively. To confirm dependence of aggregation on these divalent cations, experiments in which magnesium or calcium concentrations were varied were performed. In these experiments, a strong dose-dependent increase in aggregation was observed with the addition of calcium or magnesium. Our preliminary investigation of the mechanism of aggregation therefore points to a charge-based mechanism that is dependent on divalent cations. In gram positives, like RP1137, it is known that negatively charged teichoic acids and

peptidoglycan can bind magnesium and calcium ions (38). Therefore I hypothesize that these divalent cations bind to these components in the cell wall of RP1137 and reduce negative surface charge. Calcium ions may also neutralize surface charge on *Nannochloropsis* cells, allowing both cell types to overcome electrostatic repulsion and form aggregates. Little is known about the cell wall of *Nannochloropsis*, though it is likely decorated with polysaccharides. Aggregation via charge neutralization with divalent cations has been hypothesized in other studies to where bacteria were found to be involved in aggregation (37) and where algal autofloculation in response to calcium was studied (40). The underlying mechanism of aggregation by RP1137 is likely similar to another bacillus, *Paenibacillus kribbensis*, the aggregation potential of which was also correlated with higher pH and the presence of calcium (22, 31). Investigations into the detailed mechanism of aggregation of algae by RP1137 are discussed in chapter 3 in which the mechanism of action is investigated in detail.

Choosing the best method of harvesting algae will differ based on the species used and the culturing system, however, some common measures can be used to compare differing methods of harvest. In particular efficiency of harvest, harvest rate, and energy input are important parameters. Efficiency of harvest refers to the percentage of algae that are removed from the water. In this study the bacterium *Bacillus* sp. RP1137 has a typical harvest efficiency with *Nannochloropsis* where 70-95% of chlorophyll is removed from the water. Preliminary work suggests the difference in efficiency is due to changes in bacterial growth stage and warrants further investigation. These values are similar to the harvest efficiency of 83% reported for the aggregation of *Chlorella vulgaris* by the bacterium *Paenibacillus kribbensis* (22, 31), however *Bacillus* sp. RP1137 is capable of

aggregating multiple algae. Other flocculating agents such as aluminum sulfate and polyacrylamide resulted in harvest efficiencies of 72% and 78% respectively (22). Harvest can also be done using other physical means with the following harvest efficiencies tangential flow filtration (70-89%), dissolved air floatation (80-90%), electrocoagulation (95%) and centrifugation, which has greater the 95% harvest efficiency (21). It should be pointed out that these methods were tested with different algal strains, but they do provide a baseline of what can typically be achieved by the different harvest methods available. *Bacillus* sp. RP1137-based harvest efficiencies compares favorably with these known methods of algal harvest. Another important measure of a harvesting system is the rate at which the algae can be removed from the water, sometimes known as harvest productivity. The rate of aggregation by *Bacillus* sp. RP1137 is fast with large aggregates forming in seconds, which is similar to other flocculation type harvest methods**.** By comparison centrifuges, while having excellent harvesting efficiencies, have low harvesting rates.

Aggregation is typically a low energy method to remove algae from water (21) I do not have data on the energy associated with harvesting using *Bacillus* sp. RP1137, however it could be estimated that the energy needed would involve the energy needed to grow the bacterium and the energy needed to apply the bacteria to the algal culture. Other systems of harvest are often energy intensive with centrifugation requiring 8 kWh/m^3 of water which contributes to operating cost (21). Energy efficiency must be considered because the final product of algal biofuels is energy. Any system that costs more energy than is recovered from the algae is not sustainable.

Creating the next generation of liquid fuel infrastructure based on the sustainable conversion of algal biomass to fuels will require the development of new technologies to reduce the barriers of large scale production. One of the largest barriers to economically viable scale-up remains the harvesting step. Here I presented a new bacterial isolate that rapidly aggregates algae in a reversible manner. After fixation, the aggregation phenotype remains which effectively renders the cells specialized aggregating microparticles that may permit reuse of the cells with further research. Our results indicate that *Bacillus* sp. RP1137 may be useful in reducing one of the barriers to large-scale algal biofuel production.

Chapter 3 Mechanism of algal aggregation by *Bacillus* sp. strain RP1137

3.1 Abstract

I identified *Bacillus* sp. strain RP1137 chapter 2 and showed this strain can rapidly aggregate several biofuel producing algae in a pH and divalent cation dependent manner. In this chapter, I further characterize the mechanism of algal aggregation by RP1137. I show aggregation of both algae and bacteria is optimal in the exponential phase of growth and that the density of ionizable residues on the RP1137 cell surface changes with growth stage. Aggregation is likely via charge neutralization through binding of calcium ions to the cell surface of both algae and bacteria. I show charge neutralization occurs at least in part through binding of calcium to negatively charged teichoic acid residues. The addition of calcium also renders both algae and bacteria more able to bind to hydrophobic beads, suggesting aggregation may be occurring through hydrophobic type interactions. Knowledge of the aggregation mechanism may enable engineering of RP1137 to obtain more efficient algal harvesting.

3.2 Introduction

In chapter 2 I described the algae aggregating bacterium *Bacillus* sp. RP1137 (41). This bacterium can rapidly aggregate multiple algae that are candidates for biofuel production. Aggregation is pH and divalent cation dependent (41). Fixed cells were also shown to be as effective as live cells at aggregating algae. However, the detailed mechanism of aggregation of algae by RP1137 was unknown. Knowledge of the mechanism may be useful for understanding why it is able to aggregate some algae but not others and for applying the strain to large scale algal harvest.

In this chapter I define the mechanism of algal aggregation by *Bacillus* sp. RP1137. I determine that aggregation is growth stage dependent and that calcium is involved in charge neutralization at the cell surface. Calcium binding to negatively charged teichoic acids is responsible, at least in part, for charge neutralization at the RP1137 cell surface. Finally, charge neutralization dispels electrostatic repulsion and likely allows the bacterial and algal cells to bind via hydrophobic type interactions. The purpose of this research is to understand the aggregation mechanism of *Bacillus* sp. RP1137 to determine its suitability for harvest of algae and to understand how harvest might be improved.

3.3 Experimental Procedures

3.3.1 Strains and culture conditions.

Liquid cultures of *Bacillus* sp. strain RP1137 were grown in marine broth 2216 (BD, Franklin Lakes, NJ) at 30°C in 125 ml Erlenmeyer flasks with shaking at 180 rpm. Marine broth 2216 plus 15 g/l Difco technical agar (BD) was used for solid medium.

Nannochloropsis oceanica IMET1 was grown as described in chapter 2. Briefly, *N. oceanica* was grown in 20 ppt salinity f/2 medium (35) in 500 ml ported photo-bioreactors at 25°C with a light/dark photoperiod of 14/10.

3.3.2 Filtration aggregation assay.

A filtration aggregation assay was used to quantitate the amount of algae that were aggregated under a given condition. This assay has been described in detail in chapter 2. Briefly, the assay involves carrying out aggregation reactions with *N. oceanica* IMET1 and *Bacillus* sp. strain RP1137 in a 96 well plate. The entire volume of the reaction is then passed through a 50 µm mesh, aggregates that are larger than the mesh are retained and smaller particles pass through. Chlorophyll fluorescence is measured in the flow-through and compared to control samples without bacteria added to determine the percent of algae that are aggregated upon addition of the bacteria. Unless noted otherwise, aggregation assays were carried out in deionized water where pH was adjusted to 10.5 with NaOH and 10 mM $CaCl_2$ had been added.

3.3.3 Bacterial aggregation efficiency time course.

RP1137 cells were streaked from cryo-stocks and a single colony was used to start a 10 ml culture in marine broth medium. The culture was incubated at 30°C in a 125 ml flask with 180 rpm shaking. From the initial culture three subcultures were started at a calculated optical density (OD) of 0.01 in 200 ml of marine broth. Cultures were grown in 1 L flasks at 30°C with 180 rpm shaking. Time points were taken every one to two hours for 24 hours. At each time point cells were collected, concentrated by centrifugation at 5580 x *g* for 5 minutes, supernatant was aspirated, the cell pellet was suspended in 4% PFA in 1x PBS pH 7.4 and incubated for one hour at room temperature.

Cells were then concentrated by centrifugation, the supernatant was aspirated and cells were suspended in 1x PBS to wash the cells. The cells were then again concentrated by centrifugation and suspended in a fresh aliquot of 1x PBS. Fixed cells were used to preserve the surface chemistry of the cell and ensure that chemistry was not altered due to stress responses by the cell. Filtration aggregation assays were carried out using bacteria from each time point with algae from +2 days after subculturing. The samples were normalized by cell surface area to 3×10^8 μm^2/ml (described below) so each sample had the same surface area available for interacting with algal cells.

3.3.4 Algal aggregation efficiency time course.

N. oceanica IMET1 cultures were grown as described above. Samples of algae were taken at two, five and 17 days after being subcultured, which represents early exponential, exponential and stationary phases of growth respectively. Cells were fixed following the protocol used for the bacterial cells. Samples were normalized by cell surface area per ml (described below) so each sample had the same available surface area for interacting with bacterial cells. Aggregation assays were carried out using bacterial cells from exponential phase (OD = 0.7)

3.3.5 Determining cell size and surface area.

Cells from the time course were stained in 1X SYBR green I nucleic acid stain for 10 minutes in the dark. SYBR green staining was used to illuminate the cell body and provide crisp cell margins that were amenable to automated image analysis. Cells were then visualized on a Zeiss Axioplan microscope with excitation from a Zeiss X-Cite 120Q Iris FL light source using a filter cube with a 470/40 BP excitation filter, a FT 495 dichroic mirror and a 525/50 BP emission filter. Cells were diluted or concentrated as

needed to obtain well separated cells. The volume of each field of view was determined using the known depth of the bacterial hemacytometer and the height and width of the field of view. For each time point 20-30 fields of view were captured and saved as TIFF files. Image processing was done in Cell Profiler (42) with the following series of commands in a custom pipeline: LoadImage, ColorToGrey, IdentifyPrimaryObjects, ReassignObjectNumbers, MeasureObjectSizeShape and ExportToSpreadsheet. LoadImage imports the images. ColorToGrey converts the image to greyscale to reduce processor time. IdentifyPrimaryObjects was used to find and identify objects using the Otsu global algorithm, a 4-40 pixel cutoff and a 0.02 – 1 threshold cutoff. ReassignObjectNumbers was used to join cells within a filament into one object using a six pixel cutoff. MeasureObjectSizeShape was used to measure the perimeter and area of the identified objects. ExportToSpreadsheet was used to export the data as a .cvs file for import into Microsoft Excel for further analysis. Data were converted from pixels to micrometers using data gathered from a stage micrometer. Cell length was approximated by dividing cell perimeter by two; this provides a good estimate of cell length for filamentous bacilli though it does introduce a slight overestimate of the absolute size of the cells. To obtain cell surface area for normalization both perimeter and area data are used. The key parameter needed, but unavailable directly in Cell Profiler, for calculating surface area of a cell is the radius of the cell. To derive the radius of individual cells the 2D images of cells were used and the bacilli were modeled as a rectangle with half circles on each end. The resulting equation for area is then sum of the area of a circle and the area of a rectangle or $A = \pi r^2 + 2r((P/2) - 2r)$ where A is the area of the cell, r is the radius of the cell and P is the perimeter of the cell. Since A and P are measured values the

equation can be solved for r using the quadratic equation which yields two solutions, one of which is the real radius of the cell. Derived radius values were checked against the manually measured average radius along the length of individual cells. Calculated values are very close to measured values indicating the method can be used to accurately calculate cell radius in an automated format. Cell radius was used to calculate surface area of a three dimensional cell by modeling the cell as two halves of a sphere plus the surface area of a cylinder minus the ends. Surface area of individual cells was calculated for 900-1600 cells per time point. Cell numbers per ml were then used to calculate available surface area per unit volume. Surface area per ml of individual sample were used to normalize available surface area for interaction with algal cells between samples at different time points. The available surface area of *N. oceanica* IMET1 time points was determined using a similar pipeline to that used for RP1137 cells with the following modifications. Images were captured using chlorophyll autofluorescence. *Nannochloropsis* cells are spherical so the measured area of the 2D images could be used to directly derive radius using the equation for the area of a circle ($A = \pi r^2$). Radius could then be used to calculate 3D surface area of a sphere ($A = 4\pi r^2$). Surface area per unit volume was determined by combining surface area data with cell concentration data. All experiments were normalized by surface area using the cells prepared above. The OD of the culture is referred to below to orient the reader to which growth phase is being used in each experiment.

3.3.6 Base titration of whole bacterial cells.

Live RP1137 cells were used for base titration experiments. Cells were taken in exponential phase (OD = 0.7, 3.4 x 10^6cells/ml) and stationary phase (OD = 1.6, 7.2 x

10^6cells/ml). Culture volumes were normalized by surface area to ensure the same amount of bacterial cell surface was being titrated in each sample. Cells were concentrated by centrifugation at 15,000 *g* for 5 minutes and the cell pellet was suspended in pH 5 deionized water. This washing step was repeated twice more to ensure salts had been removed and the cells were equilibrated to pH 5. Base in the form of 0.25 M NaOH was added to the cell suspension and pH was recorded after each addition when the value stabilized.

3.3.7 Calcium binding assay.

Calcium binding was evaluated by measuring the concentration of calcium remaining after 1 ml of cells had been added. Calcium binding assays were performed with fixed RP1137 cells from the exponential phase (OD = 0.7, 3.4 x 10^6cells/ml) of growth. Known concentrations of $CaCl_2$ were added to cells in pH 10 deionized water. Cells were then removed by centrifugation at 20,000 *g* for 3 minutes. The calcium concentration in the supernatant was measured using the LaMotte Calcium Hardness colormetric kit (Chestertown, MD). The kit was adapted for use in a 96 well format and measurement in a Spectro Max M5 plate reader. The readout for the assay was absorbance at 635 nm. Absorbance at this wavelength is linear for calcium concentrations between 0-160 µM. Samples were diluted to ensure they were within the linear range of the assay. Absorbance values were compared to a $CaCl_2$ standard curve to determine the concentration of calcium remaining.

3.3.8 Calcium coordination experiment.

RP1137 and *Nannochloropsis* cells were separately suspended in pH 10.5 water with 10 mM $CaCl_2$. To ensure the cells were pre-loaded with calcium both bacteria and algae

were concentrated by centrifugation at 20,000 *g* and the cell pellets were suspended in the same solution. This pre-loading step was repeated once. The cells were then used in filtration aggregation assays compared to controls where only the algal cells were pre-loaded with calcium.

3.3.9 C18 binding assay.

Binding of cells to C18 resin was performed with fixed RP1137 cells from the exponential phase of growth (OD = 0.7) and with fixed *Nannochloropsis* cells from +5 days post inoculation. Dry C18 beads with a 10 µm diameter were purchased from Hamilton (Reno, Nevada). Beads were reconstituted in methanol overnight. The beads were concentrated by centrifugation at 20,000 *g* for 1 minute. The beads were then suspended in pH 10.5 deionized water with 10 mM $CaCl_2$. This process of concentration and suspension in pH 10.5 deionized water with 10 mM $CaCl_2$ was repeated twice more to ensure methanol was removed and the beads were equilibrated in the test solution. The equilibration process was repeated without $CaCl_2$ for a separate aliquot of beads to obtain beads for the "no calcium" samples. For each experiment 200 beads were used per cell as this was found to give maximal binding with the minimum number of beads. Equal numbers of algal or bacterial cells were incubated with C18 beads (200:1 bead to cell ratio) in the presence or absence of 10 mM $CaCl_2$. The mixtures were analyzed with an Accuri C6 flow cytometer to count the number of unbound algal or bacterial cells. The beads were distinguished from cells by their larger forward scatter area with an upper forward scatter area cutoff of 1,270,000. A lower cutoff of 44,000 was used to remove background particles found within the medium. RP1137 cells fell between these two cutoffs. Algal chlorophyll autofluorescence was used to distinguish *Nannochloropsis*

cells from their associated bacterial cells using the FL3 channel (excitation 488 nm, emission 670 LP filter) on the flow cytometer. Only particles that were between the two forward scatter cutoffs and had a chlorophyll autofluorescence of greater than 10,000 were counted as algal cells. These settings counted the unbound bacterial or algal cells which allowed comparison of the number of bound cells in the presence or absence of calcium.

3.3.10 Zeta potential.

Measurement of cell surface charge or zeta potential was done on a dynamic light scattering instrument (Malvern Instruments Ltd, Worcestershire, UK). Measurements were done on fixed algal cells from two, five and 17 days after being subcultured and on fixed RP1137 cells that were taken in exponential phase (OD = 0.7) and stationary phase (OD = 1.6). Cells were concentrated by centrifugation at 20,000 *g* for 1 min. The supernatant was aspirated and the cells were suspended in pH 10.5 deionized water. To ensure removal of trace salts the cells were again concentrated by centrifugation, supernatant was aspirated and the cells were suspended in pH 10.5 deionized water. For each sample zeta potential was measured at 0, 0.156, 0.313, 0.625, 1.25, 2.5, 5, 10, 20 and 40 mM $CaCl_2$.

3.3.11 SDS inhibition of aggregation.

Inhibition of aggregation by sodium dodecyl sulfate (SDS) was tested using the filtration aggregation assay. Fixed algae from two days after subculture were used. Fixed RP1137 cells from exponential phase (OD = 0.7) were used. Both algae and bacteria were concentrated by centrifugation at 20,000 *g* for 1 min and normalized as mentioned in section 3.3.3 of the Experimental Procedures. The supernatant was aspirated and the cells

were suspended in pH 10.5 deionized water with 10 mM $CaCl_2$. This washing step was repeated once. In the treatment samples SDS was added to algae to a final concentration of 1 %. Filtration aggregation assays were carried out as described for quantitation of the percentage of algae aggregated in the SDS treated cells compared to the untreated controls.

3.3.12 Calcium displacement of pinacyanol.

To determine if calcium displaces pinacyanol bound to the bacterial cell surface, fixed RP1137 cells from exponential phase were concentrated by centrifugation at 20,000 *g* for 1 min, supernatant was aspirated and the cells were suspended in pH 10.5 deionized water. This washing step was repeated once. RP1137 cells were then stained with 20 µM pinacyanol chloride (Sigma). The stained cells were added to an equal volume of water or water with $CaCl_2$ resulting in a final pinacyanol concentration of 10 µM. The final concentration of $CaCl_2$ solutions tested were 0, 0.15, 0.6, 2.5 and 10 mM. The samples were mixed by vortexing and then centrifuged at 20,000 *g* for 3 minutes. The supernatant was aspirated to remove unbound dye and the cells were suspended in a fresh aliquot of water with the same calcium concentration. Absorbance of the dyed cell solutions were measured at 485 nm in an M5 Spectromax plate reader. Absorbance spectra from 450-650 nm were gathered at 5 nm increments for unstained RP1137 cells, stained cells, water + pinacyanol and water + pinacyanol + 10 mM $CaCl_2$.

3.3.13 Effect of higher pH and calcium concentrations on algal self-aggregation.

To determine if *Nannochloropsis* cells will self-aggregate under the conditions tested and at higher pH value and calcium concentration I perform filtration aggregation assays with only the algae, no bacteria added. The pH of the algae culture was adjusted with NaOH.

Calcium concentrations were adjusted with $CaCl_2$. Once the algal culture was at the desired condition the filtration aggregation assay was performed to quantitate the amount of algae that was found in aggregates.

3.4 Results and discussion

3.4.1 Characterization of cell length over a growth period.

In this chapter I characterize the mechanism by which *Bacillus* sp. strain RP1137 aggregates algae. A better understanding of the mechanism may help to improve the efficiency of the system. In the previous chapter I showed that divalent cations are important for aggregation and that fixed cells were just as effective at aggregating algae as live cells, pointing to the cell surface as the important cell structure for investigation of the aggregation mechanism. Our previous work also ruled out filament length as an important factor for aggregation but, initial observations suggested aggregation ability changed over the growth cycle of a culture. Since the cell morphology changes over the growth period I cannot accurately normalize by optical density or cell counts. To accurately normalize between time points I first needed to characterize this change in morphology. Single cells and filaments of cells are present in RP1137 cultures. In this chapter I define cell length as the total length of either a lone single cell or the length of a chain of cells in a filament. Changes in cell length are shown in Fig. 3.1 where I measured cell length over time through a combination of fluorescent microscopy and automated image analysis of thousands of cells. The results show cell length does change over a growth period.

3.4.2 Change in aggregation ability of RP1137 over a growth period.

With the cell length data I was able to calculate cell surface area data which were used to normalize the cell surface area between different time points. Normalization of cell surface area allowed us to isolate changes in the cell surface composition from changes in the amount of cells or amount of cell surface area in a sample. Using normalization, I then asked whether aggregation potential changes over a growth cycle. In Fig. 3.2, the percent algae aggregated is plotted with the growth curve of the bacterium. Aggregation is most effective in the exponential phase of bacterial growth where 80% of the algae are found in the aggregates. As the cells enter stationary phase the aggregation potential per normalized cell surface area decreases and reaches a minimum value of 40% aggregated algae at 20 hours. These data show the aggregation potential of the bacterial cell surface decreases when the cells enter stationary phase, indicating the surface chemistry of the cell was likely changing. From the perspective of applying RP1137 for algal harvest these results show it is important use bacteria from exponential phase to obtain the best aggregation ability.

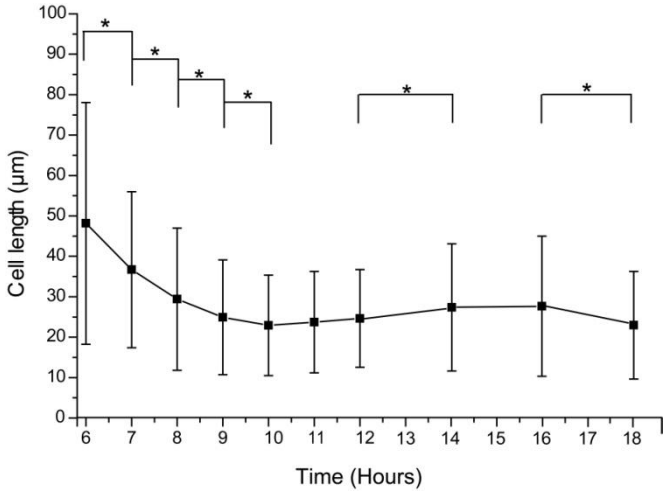

Figure 3. 1 Change in RP1137 cell length over time

Bacillus sp. RP1137 cell length changes over a growth period. Time points match the growth curve shown in Fig. 2. Bar and error bars represent the mean and standard error respectively of cell length measurements of between 900 – 1600 individual cells per time point. (*) indicates statistically significant difference where $p < 0.0005$.

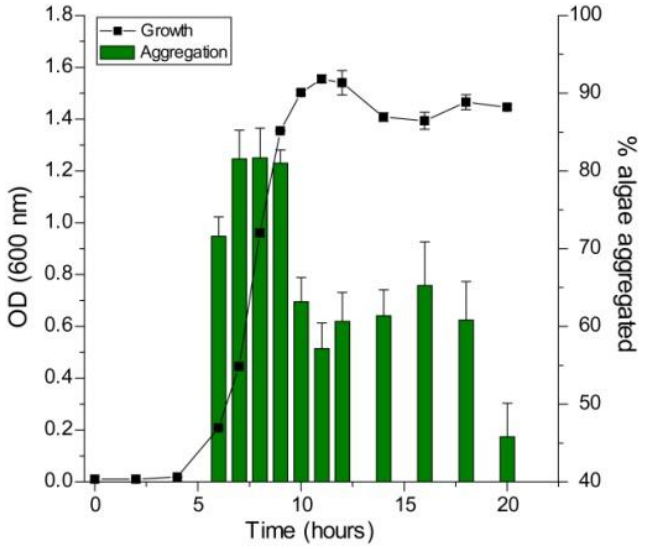

Figure 3. 2 Change in aggregation efficiency over a growth period

Normalized aggregation efficiency of RP1137 cells is highest in exponential phase. Samples are normalized by cell surface area so the same surface area (3×10^8 μm^2/ml) is available for aggregating algae at each time point. Bar and error bars represent the mean and standard error respectively of eight independent aggregation reactions. A value of 100% is aggregation of all algal cells.

3.4.3 Change in aggregation ability of *N. oceanica* IMET1 over time.

Next I measured the aggregation potential of *N. oceanica* IMET1 algal cultures at different growth stages. The same bacterial sample was used for the experiments and the algal cells were normalized between samples using the cell surface area. Unlike the bacteria, algal cell morphology does not change significantly over a growth cycle (data not shown). Algal aggregation was tested at two, five and 17 days after subculturing. Cells in the +2 days samples are just beginning to grow while the algae are fully into exponential phase by day five. At +17 days the algae are in stationary phase. Aggregation is most efficient with cells at the +5 day time point (93.4 ± 0.7 %) and is significantly more efficient than cells at +2 days (88.4 ± 2.3 %, $p = 0.0005$) and +17 days (68.3 ± 10.2 %, $p = 0.0003$). The data show the algae are most effectively aggregated during exponential phase and have decreased aggregation ability when they enter stationary phase. Little is known about the cell surface of *Nannochloropsis*; however these results suggest the surface chemistry of the cell is changing with the growth phase of the alga. Changes in surface chemistry will be investigated further in subsequent sections. The change in aggregation efficiency indicates that when harvesting algae with RP1137 cells it is best to harvest the algae when the algae are in exponential growth phase. However the harvest time must be balanced production system that is being used. For example if high lipid algae are desired then it may not be advantageous to harvest in exponential phase. However if total maximizing total biomass productivity is the goal then continuously harvesting in exponential phase may be the best option.

3.4.4 Base titration of the RP1137 cell surface.

The data I have collected show that specific or non-specific protein-protein interactions at the cell surface are inconsistent with available data. I next hypothesized that perhaps a more general property of the cell surface is involved in the aggregation phenotype of RP1137. Since the bacterial cells show a significant difference in aggregation ability between exponential and stationary phase I decided to test if the surface chemistry of the cells at these growth stages is different, specifically if the density of deprotonatable residues at the cell surface was different. To test this I used base titration of whole live cells. The results of base titration of RP1137 cells, in Fig. 3.3, show that cells in exponential phase have a lower number of deprotonatable residues compared to the cells in stationary phase because pH increases more quickly as base is added relative to stationary phase cells. Since these experiments were normalized by cell surface area this translates to more positive or neutral residues per unit area of cell surface. The data show there is a measurable difference in surface chemistry between these two populations of cells.

3.4.5 Binding of calcium to the cell surface.

Cell surface chemistry can also be affected by the ions that are present. In chapter 2 I showed that aggregation is dependent on divalent cations, and I hypothesized these ions reduce or neutralize negative charge at the cell surface. To determine if calcium ions bind to the surface of the bacterium I measured the amount of calcium removed by the cells at increasing calcium concentrations. Fig. 3.4 shows that calcium binds to the bacteria and that bound calcium increases with increasing calcium concentration up to a concentration of 0.625 mM. A saturating concentration of surface bound calcium ions could allow cells

to aggregate in at least two ways. Charge neutralization eliminates electrostatic repulsion between cells and is commonly cited as a method in which cells can get close enough to adhere via other attractive forces such as hydrophobic or Van der Waals type interactions (43).

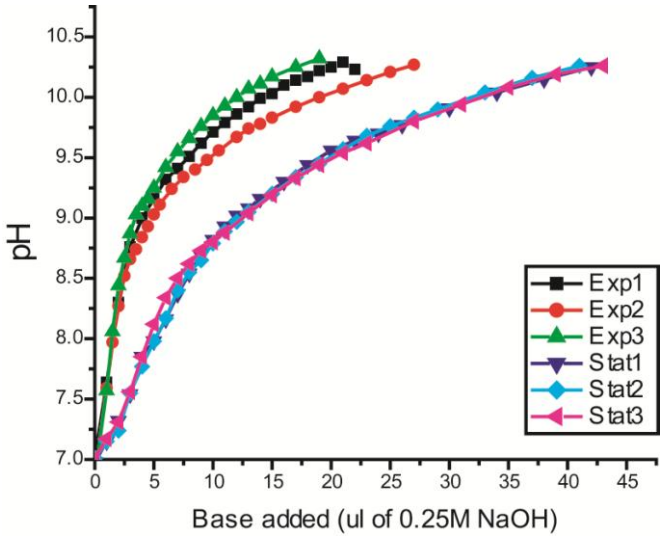

Figure 3. 3 Base titration of RP1137 cells

Base titration curves of live RP1137 cells. Cells were titrated with 0.25 M NaOH. Curves represent individual trials from RP1137 cells from either exponential phase (Exp) or stationary phase (Stat).

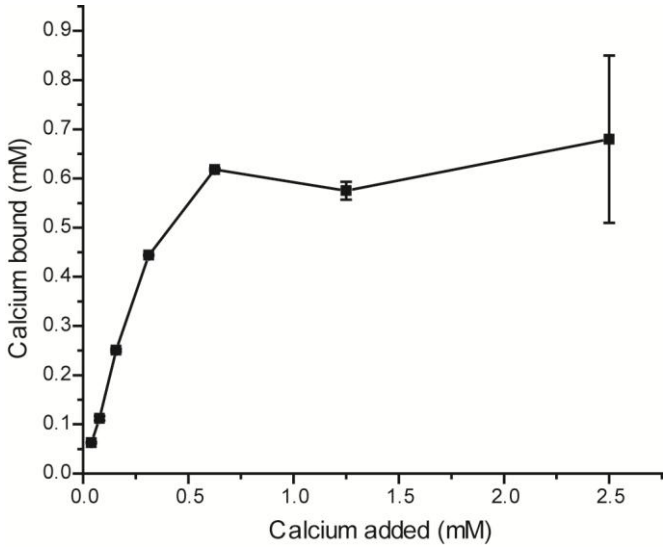

Figure 3. 4 Calcium binding of RP1137 cells

Binding of calcium to RP1137 cells increases with increasing calcium concentrations. The graph shows the amount of calcium that is bound by the same number of cells at increasing calcium concentrations. Points and error bars represent the mean and standard error respectively of three independent calcium binding reactions.

Another method of interaction cited in the literature is coordination of ions bound to one cell by another cell (44). In this method of aggregation two cells interact via bridged ions. This is similar to the commonly used nickel-NTA affinity chromatography system which binds proteins via the common coordination of a nickel ion by the 6x-His tag on a protein and a nitrilotriacetic acid residue attached to a solid substrate. The ion coordination model of aggregation predicts that algal and bacterial cells that have been preloaded with calcium separately before combination should not interact efficiently because they are both already binding ions at their cell surface and thus are less likely to bind via common ions. However, the charge neutralization model predicts a different outcome. It predicts cells preloaded with calcium before combination should interact and lead to aggregation. I tested the hypothesis that aggregation occurs by coordination of common ions by preloading algal and bacterial cells with calcium separately before mixing them. The results showed that the cells still aggregated with an average value of 74.6 ± 1.1 % algae aggregated. These results point toward the charge neutralization model of aggregation rather than the coordination model.

3.4.6 Measurement of zeta potential.

To test the hypothesis that calcium ions are causing charge neutralization, I used dynamic light scattering to measure apparent cell surface charge or zeta potential at different calcium concentrations. Zeta potential was measured for both bacterial and algal cells at different stages of growth. The data shown in Fig. 3.5 demonstrate that surface charge in both bacteria and algae decreases with increasing calcium concentration. In the absence of salt the exponential phase bacterial cells have a more negative charge at – 110 ± 6 mV compared to the stationary phase cell with a zeta potential of -72 ± 6 mV.

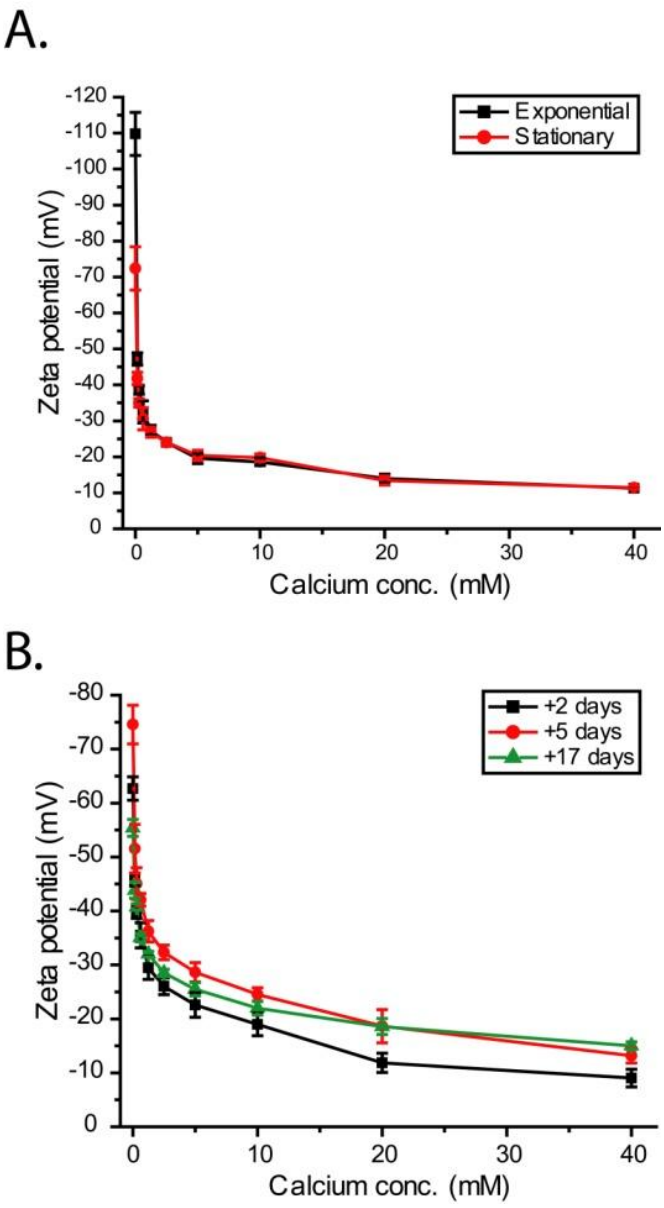

Figure 3. 5 Zeta potential of RP1137 and *Nannochloropsis* at different calcium concentrations

Surface charge (zeta potential) of RP1137 cells (A) and *Nannochloropsis* cells (B) at different stages of growth and different calcium concentrations. Charge decreases with increasing calcium concentration. Points and error bars represent the mean and standard error respectively of three biological replicates each with three technical replicates.

As calcium concentration increases the zeta potential of both exponential and stationary phase bacterial cells becomes similar, with the charge curves overlapping at 10 mM calcium which is the optimal concentration for aggregation. At this concentration, charge is - 18.6 ± 1.05 mV for exponential cells and – 19.8 ± 1.05 mV for stationary phase cells, both of which are at or below -20 mV which is often considered as the threshold where charge is no longer strong enough to separate cells by electrostatic repulsion. The surface charge of algal cells also becomes less negative as calcium concentrations increase, but compared to the bacterial cells the algae require a higher calcium concentration to get below the -20 mV threshold. This result suggests the bacterial cells have a higher affinity for calcium ions than the algal cells or that the algae have a higher number of calcium binding sites since the bacteria have a higher surface area.. The calcium binding and zeta potential measurements show bacterial cells bind calcium which results in charge neutralization. Next I aimed to determine what forces were likely mediating the binding of the RP1137 and *Nannochloropsis* cells.

3.4.7 RP1137 binding to C18 resin.

From previous work I knew that surface proteins, filament length and lectin-carbohydrate type interactions were not involved in the underlying mechanism of aggregation (41). Aggregation of multiple and distinct algae species by RP1137 also pointed toward a general instead of specific mechanism of aggregation (41). Since the cell surface charge decreased upon addition of calcium, I hypothesized that bacterial and algal cells interact via hydrophobic type interactions and thus should become more able to interact with a hydrophobic surface under these conditions. I tested this by measuring the number of individual cells that were not bound to hydrophobic C18 beads in the presence or absence

of calcium. Unbound cells were measured because it is easier to get accurate data on free cells as compared to the number of cells bound to the beads. Fig. 3.6A shows that there are 4-fold fewer unbound bacterial cells in the presence of calcium. This shows that the bacterial cells are more able to bind to a hydrophobic surface when calcium is added. The algal cells show a similar trend with 2.4-fold fewer unbound cells present in the presence of calcium (Fig. 3.6B). These data demonstrate that the algal cells are also more able to interact with a hydrophobic surface in the presence of calcium. It should be noted that calcium may bind the silica substrate to which the C18 moieties are attached. However, if this binding occurs it is unlikely to change the results of the experiment since the surface of the beads should still remain hydrophobic. Together these data support the hypothesis that bacterial and algal cells interact at least in part through hydrophobic interactions. Hydrophobic interactions are often involved in aggregation (43), so this result fits with what others have found. If both bacterial and algal cells can interact with a defined hydrophobic surface then I propose they could interact with each other. This mechanism of interaction suggests that I should be able to inhibit the interaction by coating the cells with an anionic detergent prior to the aggregation process.

3.4.8 SDS inhibition of aggregation.

To test the hypothesis that an anionic detergent will disrupt an aggregation process that occurs via hydrophobic interactions I pre-coated the bacterial and algal cells with the anionic detergent sodium dodecylsulfate (SDS). SDS has a hydrophobic tail attached to an anionic sulfate group. If the bacterial and algal surface is more hydrophobic then the SDS should orient with the hydrophobic tail oriented toward the cell and the anionic sulfate residue facing the solvent (water). The cells in this setup now have an external

negative charge which should inhibit aggregation. Achieving this molecular arrangement was the reason SDS was chosen over neutral detergents. I observed that addition of SDS results in a significant decrease in aggregation ($p = 5.19E-05$), these data are shown in Fig. 3.7. Visually, aggregation appears to be completely inhibited (Fig. 3.7A), however quantitation using the aggregation assay shows that small aggregates are still formed (Fig. 3.7B). These results suggest hydrophobic interactions are involved in the aggregation process, however they do not rule out the possibility of other types of interactions such as ionic and Van der Waals interactions between the bacterial and algal cells.

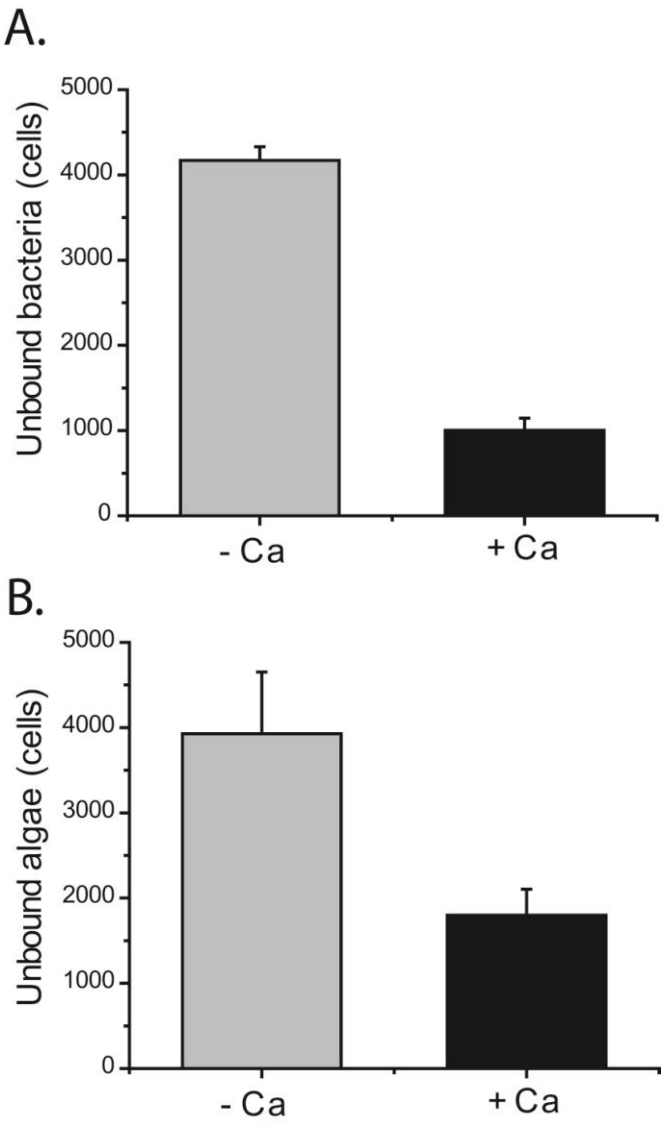

Figure 3. 6 Calcium dependent binding of RP1137 and *Nannochloropsis* to C18 beads

Binding of RP1137 cells (A) and *Nannochloropsis* cells (B) to hydrophobic C18 beads in the presence or absence of 10 mM $CaCl_2$. Both RP1137 and *Nannochloropsis* cells bind more effectively to the beads in the presence of calcium. Bar and error bars represent the mean and standard error respectively of three biological replicates with three technical replicates each.

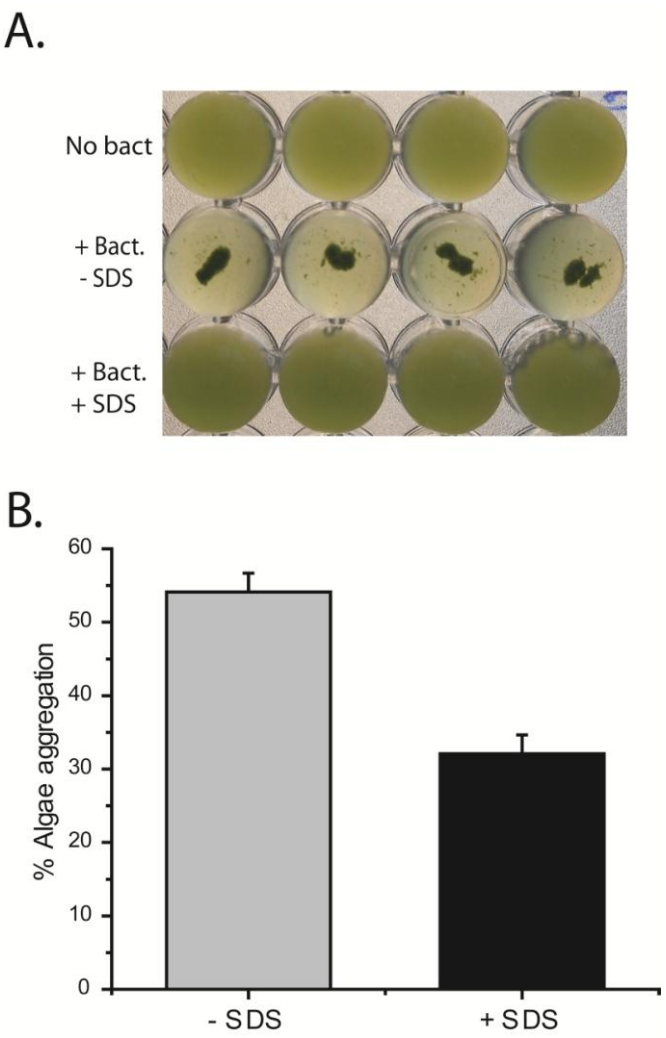

Figure 3. 7 Disruption of aggregation with SDS

Aggregation is inhibited by the presence of SDS. (A) Visual result showing the no bacteria controls, algae with bacteria and algae with bacteria and SDS. (B) Quantitation of the percent of algae aggregated with and without SDS using the filtration aggregation assay. The no bacteria sample is used to calculate the percent algae aggregation value and is therefore not shown in the bar graph. Bar and error bars represent the mean and standard error respectively of four independent aggregation reactions. A value of 100% is aggregation of all algal cells.

The aggregation assay works by removing aggregates that do not pass through a mesh with 50 µm by 50 µm square holes. Individual *Nannochloropsis* cells are spherical and have a diameter of about 3 µm. The results indicate the formation of large aggregates is inhibited but that smaller aggregates (>50 µm) are still being formed. These smaller aggregates incorporated less of the algae into the aggregates. These results indicate that the interaction between bacteria and algal cells was not completely disrupted under the conditions tested. It is possible other forms of bonding are important in the interaction between these cell types. Finally, the cells may have gained sufficient momentum when mixed by vortexing to overcome the electrostatic repulsion and allow the some of the cells to get close enough to interact. The idea that the bacterial and algal cells bind each other via hydrophobic interactions implies the cells should also self-aggregate in the absence of the other cell type; this is observed for RP1137 cells at high pH in the presence of divalent cations. *Nannochloropsis* cells do form small self-aggregates of 5-10 cells but they do not form large aggregates. The reason *Nannochloropsis* cells do not form large aggregates is unknown, however in the C18 bead assays more of the bacterial population is bound to the beads than the algae population, suggesting there are less algal cells whose cell surface is hydrophobic enough to bind the beads within the population. I speculate that the smaller the population of hydrophobic cells, the lower the chance of finding other hydrophobic cells in which they can interact. This explanation must tempered with the knowledge that up to 95% of the algal population can be harvested with RP1137, which may imply the interaction between algae and bacteria is different than the interaction of algae with other algae. Further study is needed to clarify what other forces besides hydrophobicity may be at play.

3.4.9 Determining a binding site of calcium at cell surface.

The calcium binding data indicated the ions are binding to the bacterial cells and result in charge neutralization. Teichoic acids are negatively charged and bind various cations including calcium (38), making them a plausible target for charge neutralization by calcium ions. Previous studies have shown that teichoic acids have a higher affinity for calcium relative to magnesium (38), matching data I have gathered in a previous study that showed the RP1137 has a higher affinity for calcium than magnesium (41). I tested whether calcium binds the teichoic acid residues of RP1137 using the dye pinacyanol chloride. Pinacyanol chloride binds purified teichoic acids and upon binding undergoes an absorbance shift which results in a new absorbance band centered at 485 nm (45). Interestingly, calcium competes for binding of teichoic acid with the dye. When calcium is present the dye is removed from teichoic acid and the absorbance band at 485 nm is no longer present (45). Here I use this property to determine if calcium is binding teichoic acids on RP1137 cells. The absorbance spectra of the dye alone, dye with calcium, cells and cells with dye are shown in Fig. 3.8A. The cells in the presence of the dye show the characteristic peak in absorbance at 485 nm as was observed for purified teichoic acid. The peak is not present in the cells alone, dye alone or dye with calcium. Next, the cells were stained with pinacyanol and then exposed to different concentrations of calcium. The cells are then washed to remove unbound dye and the absorbance of the cells at 485 nm is recorded. If calcium is binding teichoic acids then it should displace the dye and result in a decreased absorbance at 485 nm with increasing calcium concentration, which is what I observe in Fig. 3.8B. I must be cautious with our interpretation as the original work cited was done with purified and not cell bound teichoic acids.

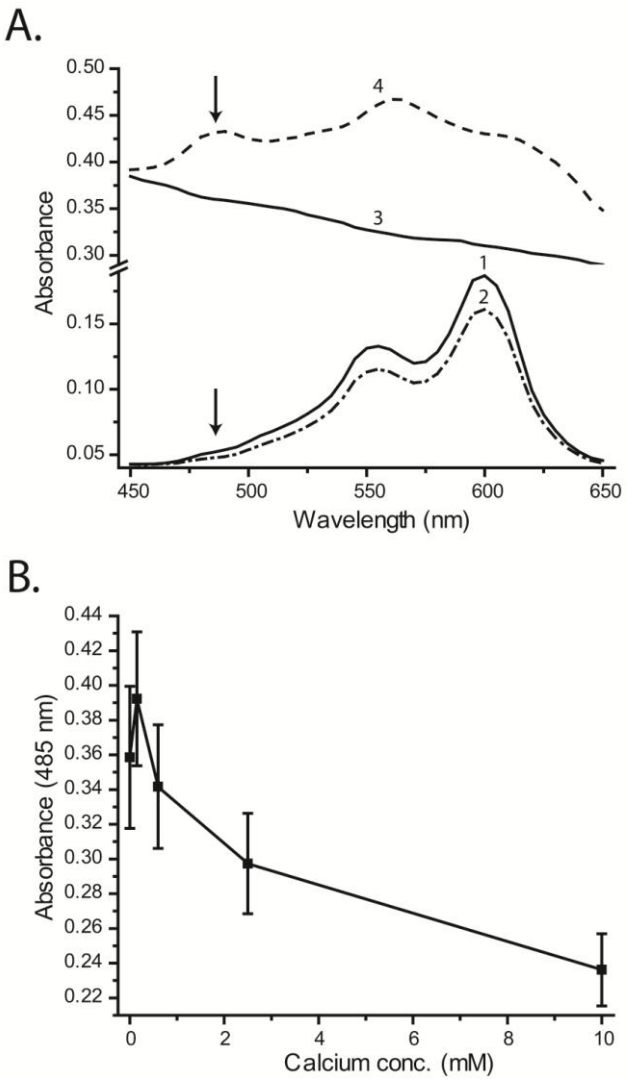

Figure 3. 8 Disruption of pinacyanol binding with calcium

Pinacyanol dye binding to RP1137 cells is disrupted by the addition of calcium. (A) Absorbance spectra of (1) Water + dye, (2) Water + dye + 10 mM $CaCl_2$, (3) RP1137 cells alone and (4) RP1137 cells + dye. Arrows indicate position of the 485 nm absorbance band indicative of pinacyanol binding teichoic acid. (B) Absorbance of pinacyanol stained cells at 485 nm with increasing calcium concentration. Points and error bars represent the mean and standard error respectively of three biological replicates each with two technical replicates.

However, this result supports the hypothesis that calcium binds to teichoic acids of RP1137 cells. The result does not rule out the possibility that calcium is also binding to other parts of the cell. Interestingly, when the pinacyanol displacement data is compare to the zeta potential and calcium binding data I see a discrepancy in calcium binding kinetics. Both zeta potential and calcium binding data suggest the RP11137 cells saturate below 1 mM calcium while the pinacyanol displacement data suggests saturation does not occur until higher concentrations. This seeming contradiction can be explained by the positive shift in the calcium dissociation that would be predicted when both calcium and pinacyanol compete for the same substrate.

Similar mechanisms of aggregation have been proposed for other aggregating bacteria, where charge neutralization with divalent cations is implicated in the mechanism of aggregation (37). Divalent cations have also been implicated in the autofloculation of some algae (40). The mechanism described here is similar to algal aggregation by *Paenibacillus kribbensis* where both high pH and calcium ions were implicated in the aggregation mechanism (22). However, in the study on *Paenibacillus kribbensis* only pH and calcium were investigated in terms of the mechanism of aggregation, whereas here I conduct a more detailed investigation. If the mechanism of aggregation in RP1137 is based on charge neutralization via calcium binding to teichoic acids then it would be expected that other related Gram-positive bacteria may demonstrate a similar aggregation phenotype. A final question that arises from this research is whether the bacterium is needed for aggregation or whether aggregation of the algae alone can occur, particularly at higher calcium concentrations and higher pH values. To test this I performed aggregation assays with the only *Nannochloropsis* cells at

different combinations of pH and calcium concentration. The results shown in Fig. 3.9 demonstrate that at pH 10 and 10 mM calcium, the optimal conditions for algal aggregation by RP1137, 5.3 ± 3.3% of aggregation can be attributed to algal self-aggregation. Self-aggregation increases with increasing pH and calcium concentration to a maximum of 34.6 ± 2.3% at pH 12 and 25 mM calcium. The conditions needed for aggregation of algal by RP1137 can be achieved in most algal production systems by simply stopping bubbling of air or CO_2 through the culture. The pH of the dense cultures used for biofuel production can easily achieve pH values greater than the minimum of pH 9 that is required for aggregation. Calcium concentrations are also usually high enough, though in cases of low salinity the bacterial cells can be charged with calcium prior to use. Higher pH and calcium concentrations can cause self-aggregation, however to achieve the 35% harvest efficiency would require addition of calcium to 2.5-fold higher concentrations than seawater and increasing pH beyond what the algae alone can achieve.

It is important to point out that the current system for harvesting algae is not economically feasible without further development. However, I speculate the chemical characteristics of the RP1137 cell surface could be used to design means of attaching the cells to solid substrates such as hydrophobic or magnetic beads to aid in recovering the cells after aggregation. In chapter 2 I show aggregation is pH dependent and reversible. If fixed RP1137 cells can be attached to beads and maintain their aggregation phenotype, then there is the possibility of reusing the cells multiple times. In this scheme the fixed cells would be attached to beads and then used to aggregate algae. The aggregates could be recovered and then pH would be lowered by either adding acid or by allowing the concentrated and thus light limited, algae to lower pH via respiration.

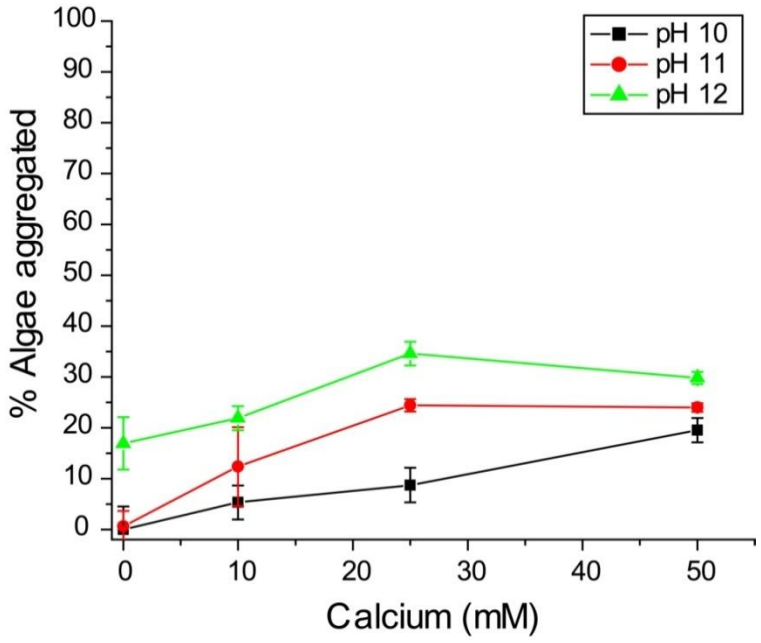

Figure 3. 9 Auto-aggregation of *Nannochloropsis* at different pHs and calcium concentrations

Nannochlorpsis cells show minimal self-aggregation under the conditions where RP1137 aggregates algae (pH 10, 10 mM calcium). Self-aggregation does increases with increasing pH and calcium concentration when compared to the negative control at pH 10 with zero calcium. Bar and error bars represent the mean and standard error respectively of four independent aggregation reactions. A value of 100% is aggregation of all algal cells.

Lowering pH reverses the aggregation process and separates the algae from the bacterium-bead complex. The bacterium-bead complex can then be separated from the algae and reused for another round or harvest. A final implication of the results presented in this study is that if the interaction between the algae and the bacteria is a hydrophobic interaction then it may be possible to simply use hydrophobic beads in place of the bacteria for harvest of algae.

Information about the mechanism of aggregation primarily is useful for predicting which algae RP1137 can harvest. The mechanistic data presented here suggests that RP1137 will be able to harvest algae where charge neutralization occurs in either sea water or fresh water with between 2-20 mM calcium ions at a pH of greater than or equal to 9. RP1137 will not likely aggregate algae that have significant negative charge (> - 30 mV) under these conditions. The data also point to charge neutralization of teichoic acids as the site where calcium binds to RP1137 cells.

Chapter 4 *Bacillus* sp. RP1137 genome sequencing and comparative genomics

4.1 Abstract

Bacillus sp. strain RP1137 is a bacterium that can rapidly and efficiently aggregate biofuel-producing microalgae. It is closely related to the industrially important bacterium *Bacillus megaterium* based on 16S rRNA gene sequence analysis. The genome of RP1137 was sequenced to better understand the molecular underpinning of the mechanism by which RP1137 aggregates algae. In this chapter I use bioinformatics to search for genes that are candidates for further targeted research into the mechanism of aggregation. This search revealed the presence of genes for capsule production and surface-associated adhesins. An S-layer protein is also present in the RP1137 genome; however I showed that it is not involved in aggregation by showing aggregation is unaffected even after S-layer removal with a lithium chloride extraction. A comparison of the aggregation efficiency of RP1137, *Bacillus megaterium* QM B1551 and *Bacillus subtilis* SMY showed that RP1137 and B1551 are equally efficient at aggregating algae while SMY does not aggregate algae. This difference in aggregation phenotypes was used to inform a genomic comparison between the three strains. This comparison revealed two putative proteins that are predicted to be bound to the cell wall and are found only in RP1137 and B1551 but not SMY. Finally, different genetic strategies are proposed for directly confirming if any of the identified genes are involved in the algal aggregation phenotype.

4.2 Introduction

The development of algal biofuels is a promising means to sustainably replace fossil fuels. One of the challenges of producing algal biofuel economically is efficiently harvesting microalgae from the water in which they are growing. *Bacillus* sp. strain RP1137, hereafter referred to as RP1137, is a bacterium that is able to rapidly and efficiently aggregate several biofuel producing microalgae (41). The bacterium was discovered as a contaminant in the culture of another algae aggregating bacterium. RP1137 is most closely related to *Bacillus megaterium* strain PPB7 on the basis of 16S rRNA gene sequence analysis (41).

Bacteria within the *B. megaterium* clade include many industrially important organisms. They have been used for the production of penicillin amidase, steroid hydrolases and the aerobic production of vitamin B_{12} (46). Organisms within this group are often genetically tractable and amenable to large scale fermentation (46). *B. megaterium* species are cosmopolitan and can be isolated from sediment, seawater, freshwater and are found in association with eukaryotes (46).

Genome sequencing can reveal information about an organism that might not be discovered otherwise. A good example is the discovery of the absence of amino acid synthesis genes in the *Buchnera* symbiont of aphids (47). This information allowed the authors to culture the bacterium and also hypothesize about the nature of the interaction between the symbiont and host. Sequencing a genome reveals the genetic potential of an organism and while that genetic potential may not be expressed or functional, it provides fruitful grounds for hypothesis generation. Knowing what might be possible with the set of genes that are present provides the opportunity for directed investigations using

genetics. Since *B. megaterium* species are typically genetically tractable (46), genome sequencing may facilitate future studies of the detailed molecular mechanism of aggregation if the responsible gene(s) can be located.

Genomes are vast territories to search, so how do I define where to look first? To narrow the area to search I looked for molecules that should be on the outside of the cell. From work presented in the previous chapters I know that the aggregation process is dependent on the chemistry at the cell surface and that even dead cells can effectively aggregate the algae. This implies that the cell surface is the key target for this bioinformatics search. Some of the molecules predicted to be on the outside of the cell can be predicted from gene annotations, including capsule polysaccharides, teichoic acids, lipotechoic acids and adhesins.

When searching for genes that might be involved in aggregation the most direct way is to check for genes encoding proteins that are known to be involved in aggregation-type phenotypes in other Gram-positives. Several proteins are known to be involved in aggregation including the co-aggregation promoting factor protein in *Lactobacillus coryniformis* DMS 20001 (48), the aggregation promoting factor gene found in *Lactobacillus gasseri* (49) and the S-layer protein from *Lactobacillus helveticus* ATCC 12046 (50). Each of these proteins has been directly linked to an aggregation phenotype and therefore were included in this investigation.

To find unknown proteins that are predicted to be localized on the outside of the cell I took advantage of signal sequences and cell wall binding motifs. Signal sequences are recognized by the Sec system, which requires several proteins including SecADEGY (51-53). As proteins are secreted they are scanned by a sortase enzyme (54). If the protein

contains an LPXTG motif, where X can be any amino acid, the sortase binds it and cleaves the protein between the conserved threonine (T) and glycine (G) residues. The sortase then attaches the protein to the cell wall (55-57). The LPXTG motif is well conserved in Gram-positive bacteria (58, 59) making it an excellent target for identifying surface associated proteins from a genome even if the function of the protein is unknown.

The purpose of this chapter is to describe the genome of RP1137 and identify potential targets in the genome that may be involved in aggregation. At the end of this chapter I will describe several strategies for determining if the identified genes are actually involved in aggregation.

4.3 Methods

4.3.1 Sequencing, assembly and annotation.

The genomic DNA from RP1137 was extracted from an overnight culture grown in marine broth 2216 (BD) at 30°C in a 125 ml Erlenmeyer flask with shaking at 180 rpm. DNA was extracted using an UltraClean microbial DNA isolation kit (MoBio, Carlsbad, CA). The DNA was sequenced using the Nextera XT kit (Illumina Inc., San Diego CA) with 250 bp paired end read sequencing on an Illumina MiSeq. The 7,878,212 reads summed to a total of 1,831,418,429 nucleotides. The reads were assembled and processed using CLC Genomics Workbench (CLC bio Inc., Cambridge, MA) and the PSU galaxy server (60-62), and resulted in 60 contigs >1000 bp with 435-fold average coverage. Annotation and prediction of genes was done using the Rapid Annotations using Subsystems Technology (RAST) server (63).

4.3.2 Nucleotide sequence accession numbers.

The draft genome sequence of *Bacillus* sp. strain RP1137 was deposited in DDBJ/EMBL/GenBank under the accession no. AXZS00000000.

4.3.3 Strains and culture conditions.

Liquid cultures of *Bacillus* sp. strain RP1137 were grown in marine broth 2216 (BD, Franklin Lakes, NJ) at 30°C in 125 ml Erlenmeyer flasks with shaking at 180 rpm. Marine broth 2216 plus 15 g/l Difco technical agar (BD) was used for solid medium. *Nannochloropsis oceanica* IMET1 was grown as described in chapter 2. Briefly, *N. oceanica* was grown in 20 ppt salinity f/2 medium (35) in 500 ml ported photo-bioreactors at 25°C with a light/dark photoperiod of 14/10.

4.3.4 Filtration aggregation assay.

A filtration aggregation assay was used to quantitate the amount of algae that were aggregated under a given condition. This assay has been described in detail in chapter 2. Briefly, the assay involves carrying out aggregation reactions with *N. oceanica* IMET1 and *Bacillus* sp. strain RP1137 in a 96-well plate. The entire volume of the reaction is then passed through a 50-µm mesh, aggregates that are larger than the mesh are retained and smaller particles pass through. Chlorophyll fluorescence is measured in the flow-through and compared to control samples without bacteria added to determine the percent of algae that are aggregated upon addition of the bacteria. Unless noted otherwise, aggregation assays were carried out in deionized water where the pH was adjusted to 10.5 with NaOH and 10 mM $CaCl_2$ had been added.

4.3.5 LiCl treatment of RP1137 cells.

Lithium chloride treatment was done according to the protocol of Lortal et al. (64). RP1137 cells were concentrated by centrifugation at 20,000 *g* for 3 min and the cell pellet was suspended in either distilled water, 5 M LiCl, 7.5 M LiCl or 10 M LiCl. Cells were incubated at these conditions for 15, 45 and 120 minutes at room temperature and then concentrated by centrifugation. The cell pellets were suspended in pH 10.5 deionized water with 10 mM $CaCl_2$ and used for aggregation assays.

4.3.6 Algal aggregation by different *Bacillus* strains.

To determine if other *Bacillus* strains share the aggregation phenotype found in RP1137, I tested the aggregation ability of *B. megaterium* QM B1551 and *B. subtilis* SMY. *B. megaterium* QM B1551 was a gift from Dr. Jacques Ravel and *B. subtilis* SMY was a gift from Dr. Harold Schreier. Cells were grown in LB medium (BD) at 37°C with 180 rpm shaking. The cells were harvested in exponential phase and fixed using the protocol listed above. Cell density normalized filtration aggregation assays were then carried out.

4.3.7 Genome comparisons.

To compare all of the predicted proteins of RP1137, *B. megaterium* QM B1551 and *B. subtilis* SMY the proteins were first downloaded from the Pathosystems Resource Integration Center (http://patric.vbi.vt.edu/) (65) and concatenated into fasta files. The files were then uploaded to Galaxy (http://galaxyproject.org/) (60-62) running on Amazon's Elastic Compute Cloud. The fasta files from each of the organisms were compared using the BLASTp algorithm with a limit of 10 hits per query. The output was a tab delimited document that was imported into Microsoft Excel for analysis. The data were parsed using logic based equations in Excel to give the top hit for each query which

was plotted. To determine if a protein was unique to a genome, the hit list generated above was used. For each protein it was determined whether there were zero, one or two hits in the other two genomes at 20, 30 and 75% sequence identity cutoffs. Proteins that were found in all three genomes were plotted, as well as proteins found in only RP1137 and *B. megaterium* QM B1551. Proteins that were found in only *B. subtilis* SMY genome were also plotted. To find sequences in the RP1137 genome that contained the LPXTG cell wall binding motif the protein sequences were searched by Mr. Taylor Carter, undergraduate intern in the Hill Laboratory, for each of the 20 possible combinations of the above mentioned motif. Sequences that contained the motif were then analyzed using the Simple Modular Architecture Research Tool (http://smart.embl-heidelberg.de/) (66) to determine if they also had the signal sequence that is needed for the protein to be exported outside the cell. The Simple Modular Architecture Research Tool was also used to identify potential domains and transmembrane regions within the proteins. The BLAST comparison dataset was used to determine if the motif containing proteins were present in *B. megaterium* QM B1551 and *B. subtilis* SMY.

4.4 Results and Discussion

4.4.1 Genome sequencing and description of the genome.

To delve deeper into the molecular mechanism of algal aggregation by RP1137, I sequenced the genome. The size of the resulting assembly was 5,878,785 bases, with a G+C content of 37.5% and an N50 of 821,973 bp. This sequence data resides on 60 contigs. A total of 6159 protein coding sequences were predicted and 14 rRNAs and 92

tRNAs were annotated. To determine which genes are responsible for the aggregation phenotype, I first performed general bioinformatics analyses and worked down to more detailed analyses. At each stage potential targets were identified and are described below. At the end of the results and discussion section I will discuss approaches for testing the various targets.

The annotation of the genome is shown in Figure 4.1. Of particular interest in the annotation are the genes coding for proteins or cell wall constituents that would be exposed to the extracellular environment, because these are the molecules that may be interacting with the algal cells. The annotation suggests RP1137 has the capacity to produce a capsule and a variety of extracellular polysaccharides. From these data I can also see that RP1137 may have the capacity to produce adhesins. All of these products are potential targets for experimental work. A more detailed examination of the gene annotations revealed the presence of the Streptococcal hemagglutinin protein. This protein was originally identified in *Streptococcus gordonii* and was found to bind to sialic acids and cause agglutination of red blood cells (67). The genome also encodes the proteins needed for secreting proteins (SecADEFG) and the sortase protein that cleaves secreted proteins and bonds them to the cell wall.

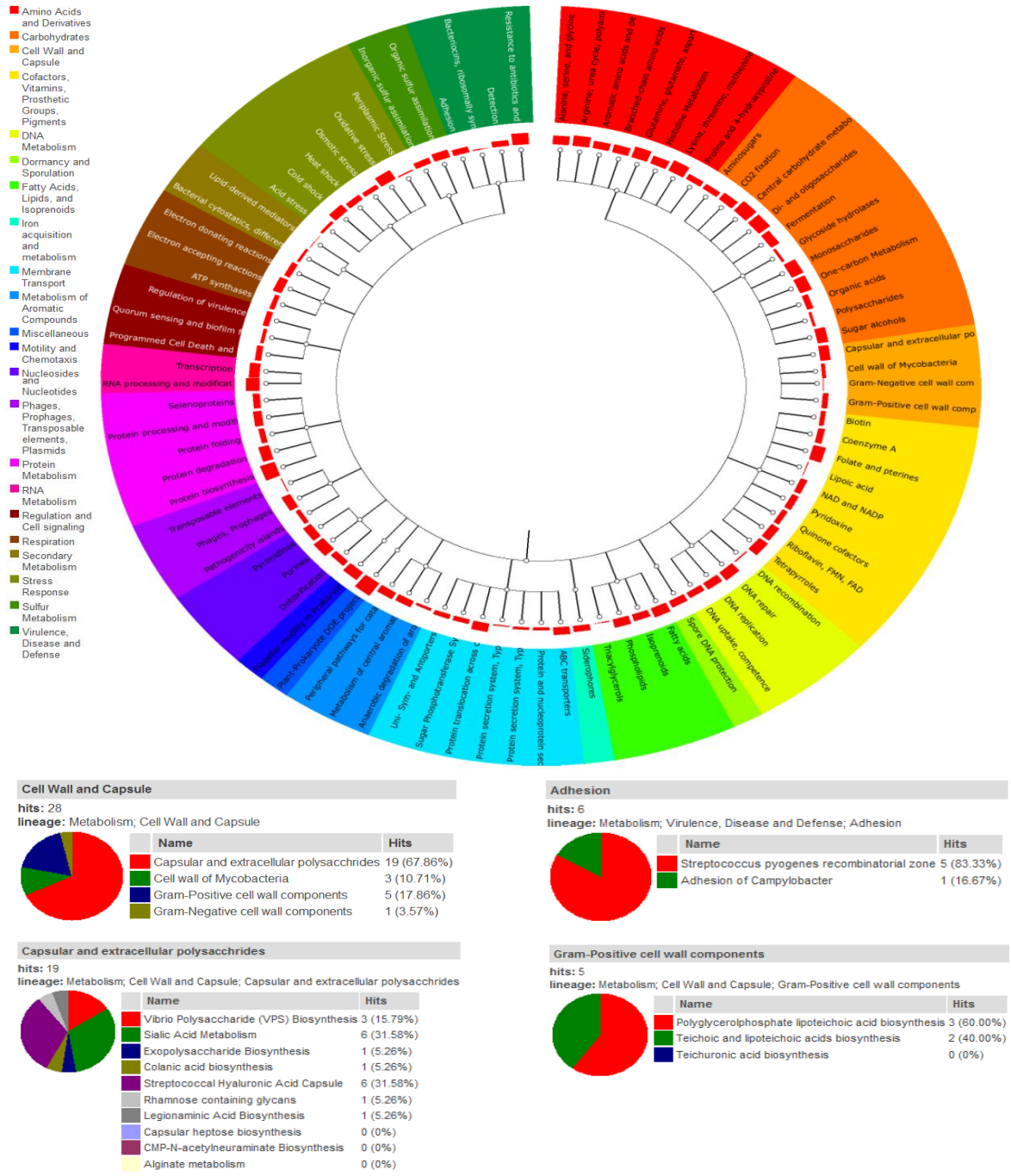

Figure 4. 1 Annotation of RP1137 genome

Annotation of the *Bacillus* sp. RP1137 genome and breakdown of predicted cell wall components. The tree indicates classification and sub-classification groups. The red bars at branch terminus indicate relative number of genes within a group.

4.4.2 Search for known aggregation factors in the RP1137 genome.

The next strategy I employed was to check for proteins that have been directly linked to aggregation phenotypes in other Gram-positive bacteria. If any of these proteins are present then they may be responsible for the algal aggregation phenotype. In the literature I found the co-aggregation promoting factor protein in *L. coryniformis* DMS 20001 (48), the aggregation promoting factor gene in *L. gasseri* (49) and the S-layer protein from *L. helveticus* ATCC 12046 (50). The sequences of these proteins were obtained from NCBI. The BLASTp algorithm on the Galaxy server was used to search for these proteins in the RP1137 proteome. No significant matches were found using a 25% identity and 50% coverage cutoff. While I was not able to find significant matches for proteins that have been directly linked to aggregation phenotypes I did find a distinct S-layer protein within the RP1137 genome.

4.4.3 LiCl treatment to remove S-layer proteins.

From my previous work, presented in Chapter 2, I showed that proteinase K treatment of the cell surface did not significantly decrease aggregation, suggesting that surface proteins were unlikely to be involved in aggregation (41). While proteinase K can cleave surface proteins (68), it may not cleave proteins that do not have an exposed cleavage site. S-layer proteins are often involved in adhesion of Gram-positive bacteria to either biotic or abiotic surfaces and can be involved in aggregation (50). S-layer proteins are also typically attached to peptidoglycan via electrostatic interactions and can be removed by LiCl treatment (64). To test if the S-layer is involved in the aggregation mechanism, RP1137 cells were treated with 5, 7.5 and 10 M LiCl for 15, 45 and 120 minutes. The treated cells did not have a significant decrease in their aggregation ability under any of

the conditions tested (Fig. 4.2), suggesting that the S-layer proteins are not involved in the aggregation phenotype. However, it is important to note that while stringent conditions were used for removal of the S-layer proteins, it unknown from these experiments whether the S-layer was actually removed. A lack of known aggregating proteins in the genome and the negative results from the LiCl experiments suggests that the mechanism of RP1137 algal aggregation may be different from previously characterized mechanisms described in the literature.

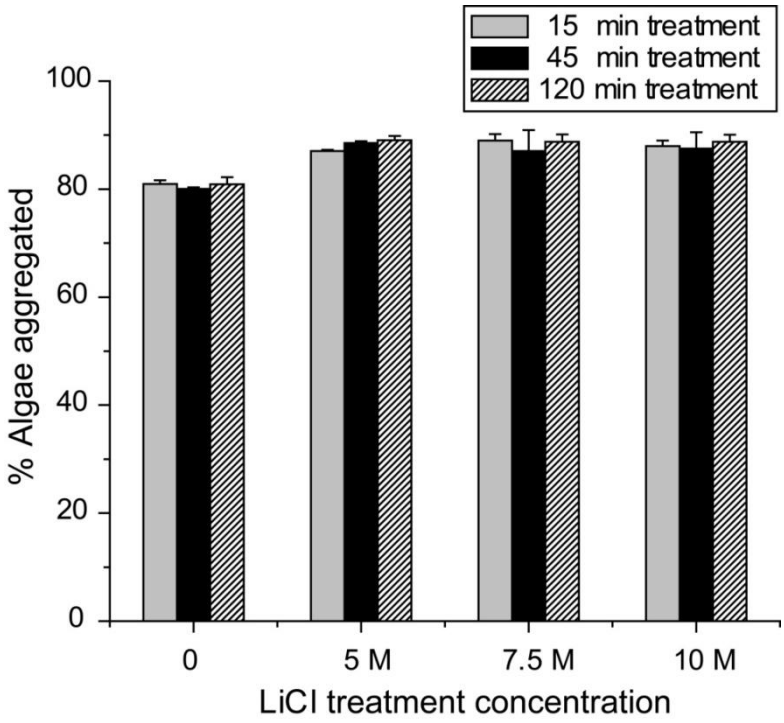

Figure 4. 2 Lithium chloride treatment of RP1137 cells

Removing S-layer proteins from RP1137 cells with lithium chloride does not inhibit aggregation. Cells were treated with different concentrations of LiCl with different treatment times and then used in aggregation assays with *Nannochloropsis*. Bar and error bars represent the mean and standard error respectively of three independent aggregation reactions. A value of 100% is aggregation of all algal cells.

4.4.4 Comparison of *Bacillus* aggregation phenotypes.

From initial examination of the genome it was unclear which factors may be responsible for the aggregation phenotype, so the next step was to incorporate a comparison of the aggregation ability of other sequenced Bacilli to inform a comparative genomic analysis. For this comparison I chose *B. megaterium* QM B1551 and *Bacillus subtilis* SMY which both have sequenced genomes. *B. megaterium* QM B1551 is closely related to RP1137 with a 16S rRNA gene identity of 99%. *B. subtilis* SMY is more distantly related to RP1137 with a 16S rRNA gene identity of 93%. The algal aggregation phenotypes of both strains were compared to RP1137. The results shown in Figure 4.3 demonstrate that *B. megaterium* QM B1551 has the same algal aggregation efficiency than RP1137. On the other hand, *B. subtilis* SMY has little or no algal aggregation activity. The difference between these strains allowed a comparative analysis of the genomes since the closely related strains both aggregate algae, but the more distantly related *B. subtilis* strain does not. In the next sections I will compare these three genomes to determine the genomic basis for the aggregation phenotype.

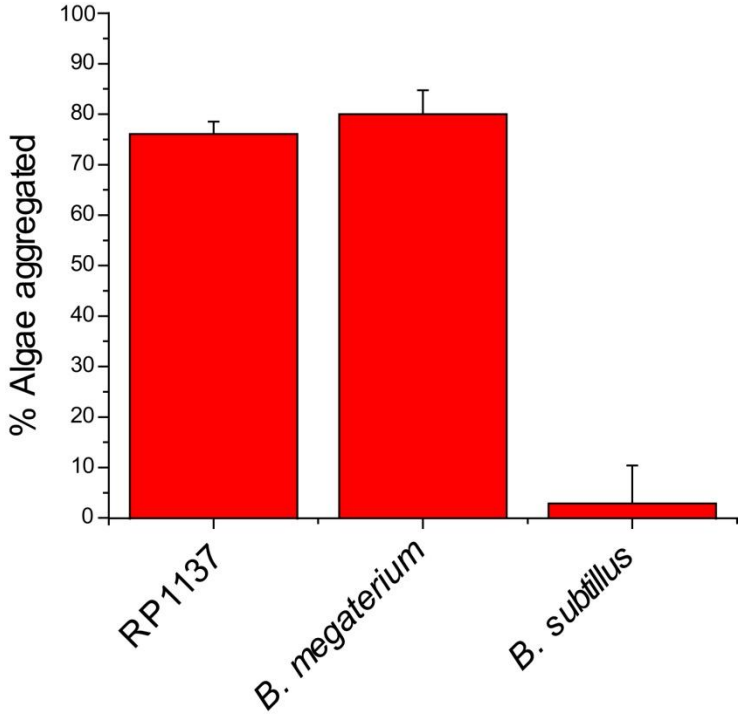

Figure 4. 3 Aggregation efficiencies of RP1137, *B. megaterium* and *B. subtilis*

RP1137 and *B. megaterium* QM B1551 have similar aggregation efficiencies while *B. subtilis* SMY has low or no aggregation activity. Bacterial concentrations were normalized between samples. Bar and error bars represent the mean and standard error respectively of three biological replicates for each strain and four independent aggregation reactions per biological replicate. A value of 100% is aggregation of all algal cells.

4.4.5 Comparative genomic analysis.

Both RP1137 and *B. megaterium* QM B1551 are able to aggregate algae while *B. subtilis* SMY cannot. The RP1137 genome size is predicted to be 5.9 Mb with 6159 predicted protein coding sequences. The *B. megaterium* QM B1551 genome size is 5.5 Mb in size and predicted to have 5609 protein coding sequences. The *B. subtilis* SMY genome size is 4.2 Mb and is predicted to have 4314 protein coding sequences. To compare the genomes I started with a general approach and then worked toward more specific comparisons. In the first comparison I did an all-versus-all protein BLAST between the each of the three proteomes. In this analysis I was looking for proteins that were present in the RP1137 and *B. megaterium* proteome, but not in the *B. subtilis* proteome. I also searched for proteins that were present in the *B. subtilis* genome but not in the RP1137 and *B. megaterium* genome. The results of this search are shown in Figure 4.4 where the number of hits versus the percent identity of the hits is shown. Of the proteins in the RP1137 genome 6133/6159 (99.6%) had a hit in the *B. megaterium* genome. Of these hits 39% had a 100% identity, 80% had a 95% identity or greater, 86% had a 70% identity or greater and 99.6% had a 25% identity or greater. This distribution is shown in Figure 4.4A. This result is expected since the two organisms are closely related. Of the proteins in the RP1137 genome 3549/6159 (57.6%) had a hit in the *B. subtilis* genome. Of these hits >0.1% had 100% identity, 0.03% had a 95% identity or greater, 7.6% had a 70% identity or greater and 57% had a 25% identity or greater. This distribution is shown in Figure 4.4B. These results show that RP1137 and the *B. subtilis* have significantly different protein coding profiles. As a final comparison the *B. megaterium* genome was compared to the *B subtilis* genome. Of the proteins in the *B. megaterium* genome

5450/5609 (97.2%) had a hit in the *B. subtilis* genome. Of these hits 0.1% had 100% identity, 0.25% had a 95% identity or greater, 16.3% had a 70% identity or greater and 96.4% had a 25% % identity or greater. This distribution is shown in Figure 4.4C. These results show *B. megaterium* has more hits in the *B. subtilis* genome than RP1137, however most of those hits have a low percent identity. The difference between in the number of hits of *B. megaterium* and RP1137 in the *B. subtilis* genome can be explained by the difference in number of predicted proteins, 5609 for *B. megaterium* versus 6159 in RP1137, and also by the quality of the annotation of those proteins. Both more proteins and the presence of potentially invalid predictions of open reading frames would cause less hits when the RP1137 genome is compared to the *B. subtilis* genome. This comparison gives an initial measure of the similarity of these three genomes. It shows that the RP1137 and *B. megaterium* genomes are more similar to each other than the *B. subtilis* genome. These differences offer the opportunity to determine which genes may be important for aggregation.

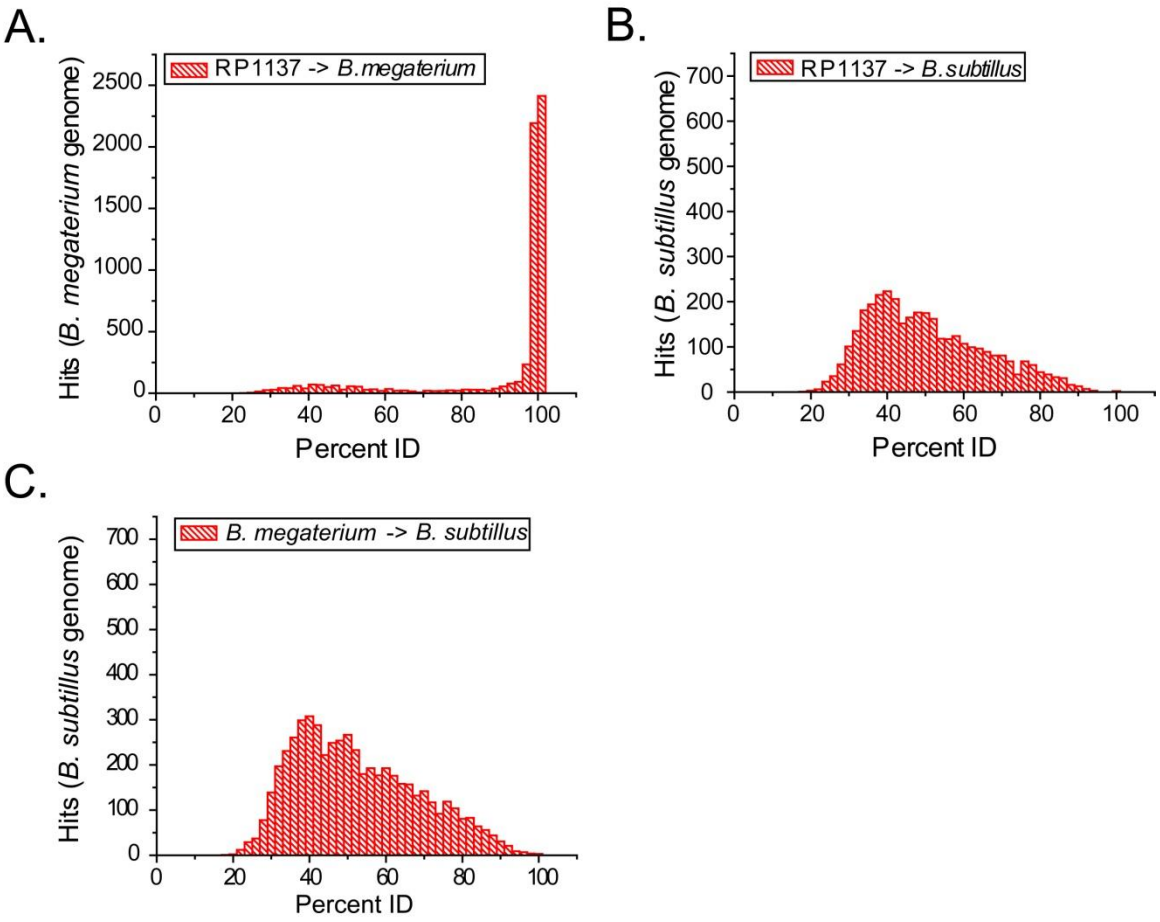

Figure 4. 4 All versus all comparison of bacilli genomes

All versus all Protein BLAST comparison of RP1137, *B. megaterium* QM B1551 and *B. subtilis* SMY genomes. Percent identity is shown on the X-axis and number of hits in the specified genome is shown on the Y-axis. (A) Results of a BLAST of RP1137 proteins against the *B. megaterium* QM B1551 proteome. (B) Results of a BLAST of RP1137 proteins against the *B. subtilis* SMY proteome. (C) Results of a BLAST of *B. megaterium* QM B1551 proteins against the *B. subtilis* proteome.

In the next step of the genome analysis I checked which proteins are unique to the RP1137 and *B. megaterium* genomes and which proteins are unique to the *B. subtilis* genome. To do this I used the BLAST dataset to count which RP1137 proteins were found in the *B. megaterium* genome and which *B. subtilis* proteins were not found in either the RP1137 or *B. megaterium* genome. This analysis was run at 20, 30 and 75% identity thresholds. Figure 4.5 shows the number proteins that are found in only RP1137 and *B. megaterium* as well as the number of proteins that are found in all three strains. This result shows that even at a low identity threshold there are many proteins that are found only in RP1137 and *B. megaterium*. While interesting, this does not help to narrow the list of potential proteins that may be involved in aggregation enough to be useful. Figure 4.6 shows the number of proteins that are unique to *B. subtilis* at different percent identity thresholds. While this figure presents fewer potential targets there are still too many proteins to reasonably test without further narrowing the list of targets. In the next section I use the predicted location of the proteins encoded in each of these genomes to narrow the list of candidate aggregation proteins.

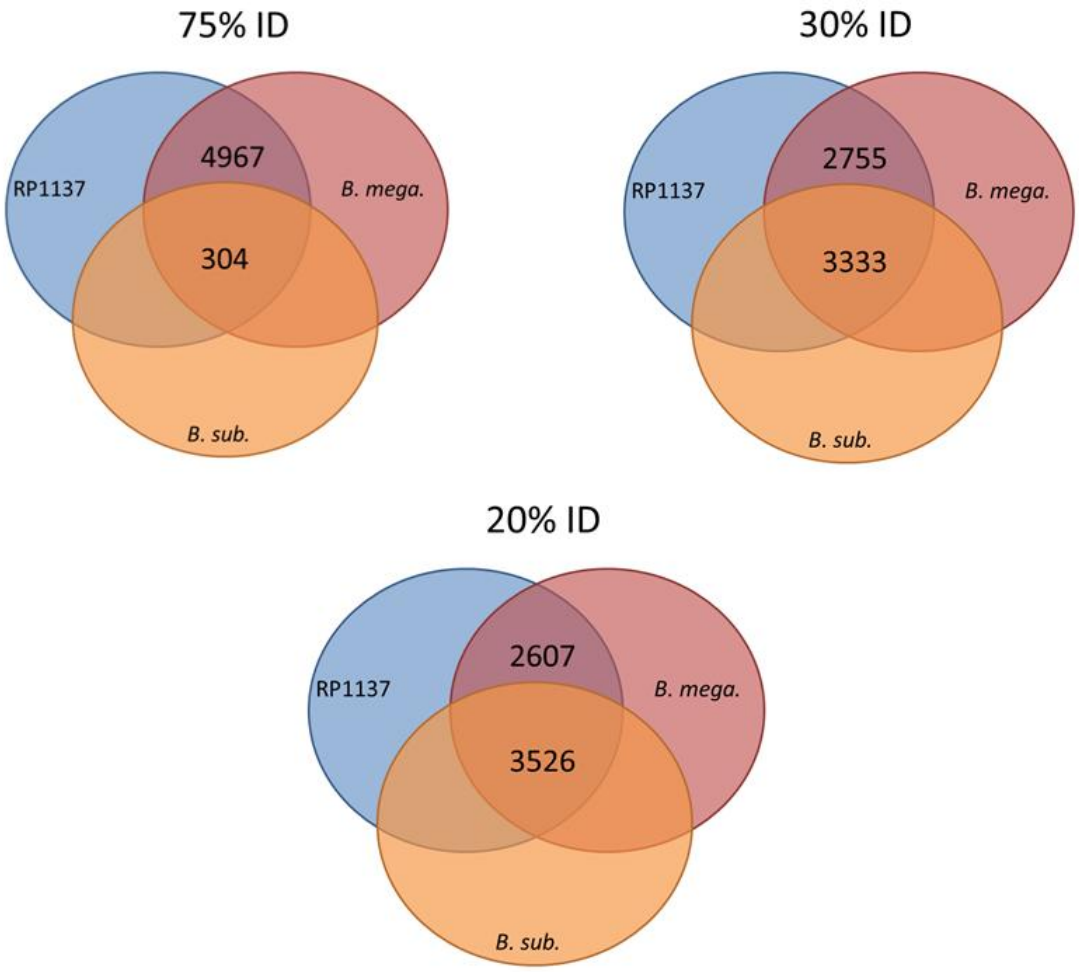

Figure 4. 5 Number of proteins that are unique to RP1137 and *B. megaterium*

The number of proteins that are shared by all three species and that are unique to RP1137 and *B. megaterium* at different percent identity cutoffs. The results show that even at the lowest percent identity cutoff there are still a large number of proteins that are unique to both RP1137 and *B. megaterium* and are not found in *B. subtilis* SMY.

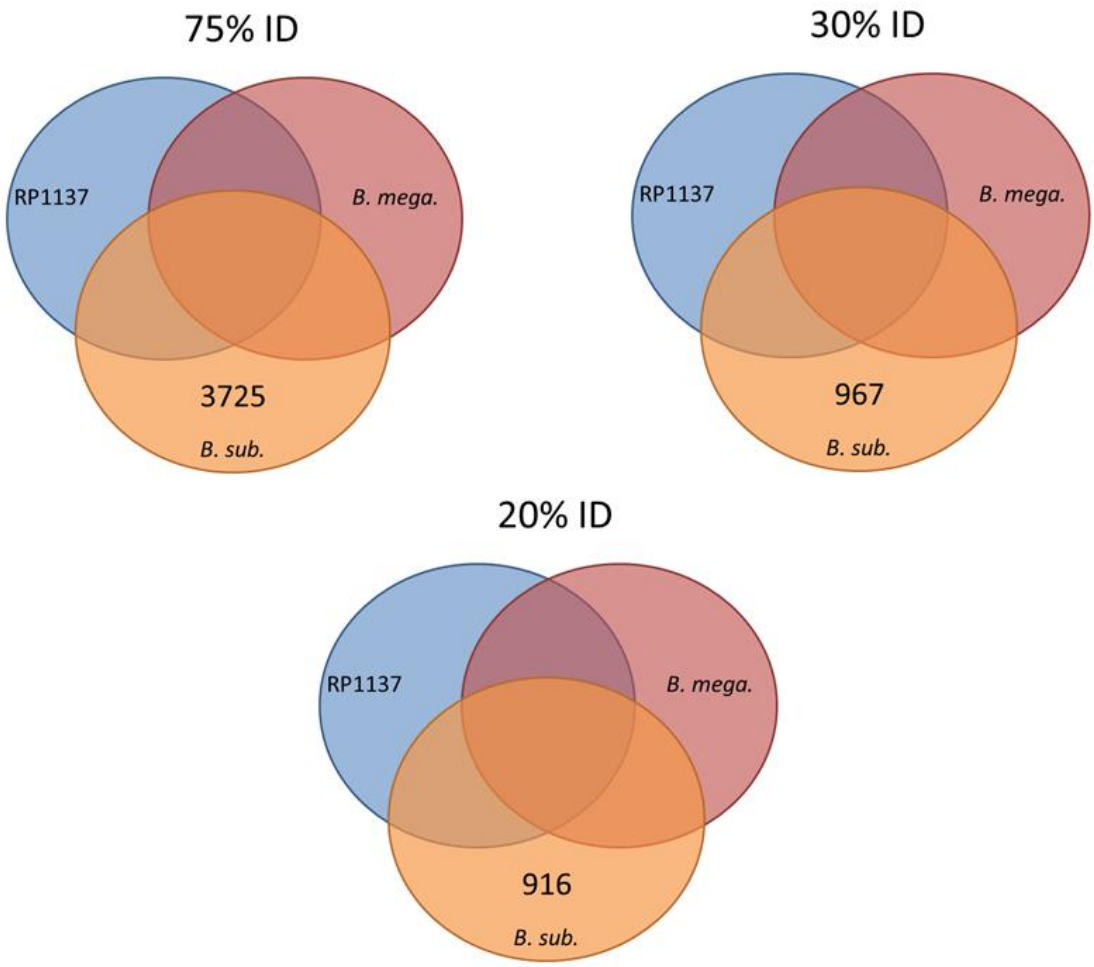

Figure 4. 6 Number of proteins that are unique to *B. subtilis*

Numbers of proteins that are unique to *B. subtilis* SMY and not found in RP1137 and *B. megaterium* QM B1551 at different percent amino acid identity cutoffs. The results show that even at the lowest cutoff there are still a significant number of proteins that do not have a match in either of the other two strains.

4.4.6 Comparative genomics for secreted and cell wall attached proteins.

While many candidate proteins were found that may be responsible for aggregation due to their presence in only an aggregating or non-aggregating strain, the total number of possible proteins was still too high to be experimentally tractable. The goal of this section is to reduce that list of proteins to a number that can be targeted experimentally. To do this I searched for proteins with motifs indicating that they may be secreted out of the cell and subsequently be bound to the peptidoglycan. Binding of proteins to the peptidoglycan can be accessed bioinformatically by looking for the conserved LPXTG PG-binding motif (58, 59). The presence of this motif and a signal sequence on a protein predicts that it could be localized outside of the cell and bound to the peptidoglycan layer. This process is shown in Figure 4.7 from Olaf et al. (69). The genome of RP1137 is predicted to have the necessary genes for exporting proteins out of the cell and transporting them to the peptidoglycan, including the sortase enzyme, StrA, and the secretion proteins SecADEGY. The genome of RP1137 was searched for proteins that contained the LPXTG motif. A total of 24 proteins were found to contain the motif and are shown in table 4.1. These proteins were then searched for signal peptides using the Simple Modular Research Tool. Of the original 24, seven were predicted to have a signal peptide which suggests that these proteins can be both exported outside of the cell and attached to the peptidoglycan layer. These proteins are potential candidates that may be involved in the aggregation process. The seven proteins were examined further by checking if any of them were exclusively present in RP1137 and *B. megaterium* or *B. subtilis*. Proteins unique to RP1137 and *B. megaterium* and not present in *B. subtilis* are candidates for being responsible for the aggregation phenotypes that were observed.

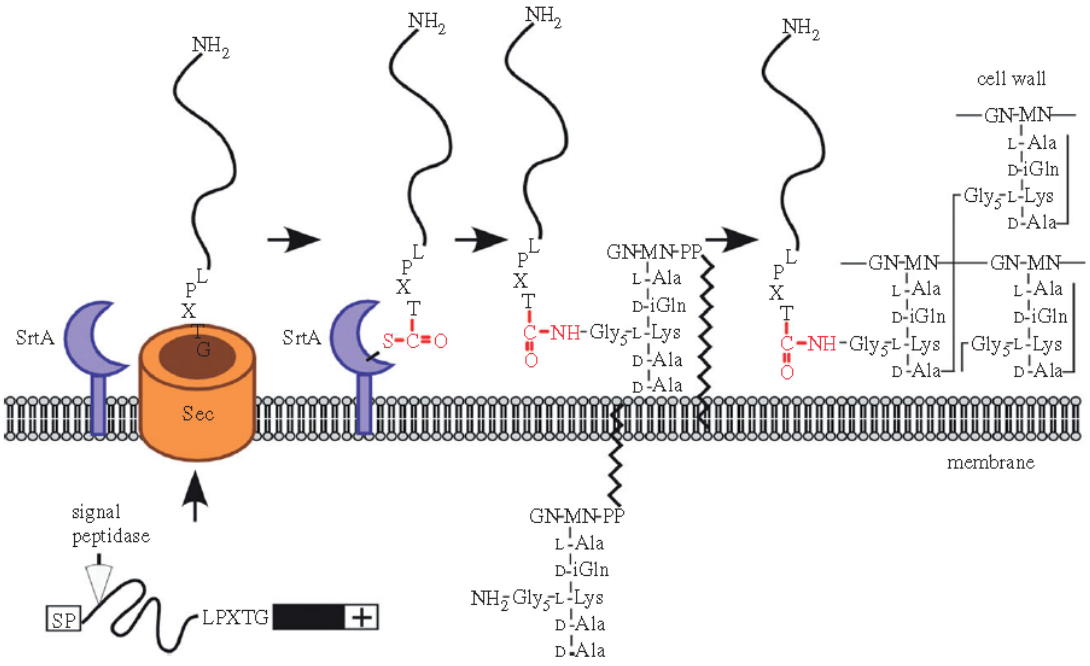

Figure 4. 7 Protein secretion in Gram-positives

Schematic of protein export and binding to the peptidoglycan via the sortase enzyme as presented by Olaf *et al*. (69). Permission to reproduce through the Creative Commons License. The presence of a signal sequence at the N-terminus of the protein routes the protein out of the cell through the secretion system. Prior to secretion the signal peptide is cleaved. The modified protein is transported across the membrane via energy derived from the SecA ATPase. Once outside of the cell, proteins with the LPXTG domain are cleaved by the sortase after the threonine (T). The cleaved protein is then attached to the cell wall.

The results shown in Table 4.1 indicate that two proteins have a PG binding motif, a signal sequence and are only found in RP1137 and *B. megaterium.* The proteins are annotated as a sodium/solute symporter and a Stage V sporulation protein B. The sodium/solute symporter is predicted to have 13 transmembrane regions and three regions of low complexity. Low complexity regions are thought to be involved in protein-protein type interactions and flexibility of the protein (70). The sodium/solute symporter protein is 497 amino acids long and the sortase is predicted to cleave this protein after the 225nd amino acid. If the protein is cleaved at this point and anchored to the peptidoglycan then seven transmembrane regions remain and the N-terminus of the protein is predicted to be facing the inside of the cell with three loops exposed to the outside of the cell. The three loops facing outside of the cell are between amino acids 22-43, 97-117 and 181-188. While this protein is predicted to be a sodium/solute symporter it is important to note that the domain predicted for that function is from 33-428. If the protein is cleaved at AA 225 by the sortase then it is unlikely to have this function in vivo. Therefore, this protein represents a rational target for experimental work. The second protein identified is annotated as a Stage V sporulation protein B. This protein is 516 amino acids long. A SMART search reveals four potential domains. These domains are listed in order of confidence (with their location in the protein in parentheses) as a polysaccharide biosynthesis motif (4-306), two domains within the multi antimicrobial extrusion (MATE) family (11- 168 and 252-403) and finally an MviN motif (114-495). This protein is predicted to have 14 transmembrane regions and four regions of low complexity.

Table 4. 1 Predicted cell wall binding proteins

ORF#	Motif	Annotation	Signal peptide	Present in *B. megaterium*	Present in *B. subtilis*
180	LPVTG	ABC transporter ATP-binding protein	+	+	+
440	LPRTG	Amino acid permease in 4-hydroxyproline catabolic gene	-	+	+
441	LPRTG	Amino acid permease in 4-hydroxyproline catabolic gene	-	+	+
751	LPITG	Cell division protein	-	+	+
752	LPITG	Cell division protein	+	+	+
943	LPATG	Cyanophycinase	-	+	+
1004	LPYTG	D-3-phosphogylcerate dehydrogenase	-	+	+
1857	LPKTG	Gluconate permease	+	+	+
1857	LPGTG	Gluconate permease	-	+	+
2855	LPRTG	Hypothetical protein	-	+	+
3246	LPYTG	Hypothetical protein	+	+	+
3719	LPNTG	Isopentenyl-diphosphate delta-isomerase, FMN-dependent	-	+	+
3741	LPATG	Lanthionine biosynthesis protein LanB	+	+	+
4180	LPKTG	Na^+/solute symporter	+	+	-
4212	LPLTG	NAD synthetase	-	+	-
4556	LPATG	Phoysphopantothenoylcystein decarboxylase	-	+	-
4582	LPLTG	Phytoene synthase	-	+	-
5006	LPITG	Retron-type RNA directed DNA pol	-	+	-
5438	LPTTG	Stage V sporulation protein B	-	+	-
5439	LPTTG	Stage V sporulation protein B	+	+	-
5474	LPLTG	Succinyl-CoA:3 ketoacid-coenzyme A transferase subunit B	-	+	-
5605	LPLTG	Transcriptional regulator	-	+	-
5649	LPVTG	Transcriptional regulator	-	+	-
6097	LPLTG	Xanthine dehydrogenase	-	+	-

The sortase is predicted to cleave this protein at amino acid 239. If the protein is cleaved at this point then only the multi antimicrobial extrusion family motif will remain. The protein is then predicted to have six transmembrane domains with N-terminus facing the outside of the cell and the C-terminus anchored to the peptidoglycan. Two loops at amino acids 61-82 and 138-159 are exposed to the outside of the cell and represent potential points of interaction for aggregation along with the exposed N-terminus. This protein represents the second direct target for experimental work to determine the factor involved in algal aggregation.

4.4.7 Steps involved in testing bioinformatics predictions.

The next step is to directly test the proteins that were found by bioinformatics for their effect on aggregation by using genetics to delete the genes. Since both RP1137 and *B. megaterium* QM B1551 have equivalent algal aggregation phenotypes either could be used as a genetic model system to ask questions about which, if any, of these proteins are involved in aggregation. *B. megaterium* QM B1551 is the better choice for these experiments because it already has a well-developed genetic system (46). The bioinformatic prediction is that one of these proteins may be involved in aggregation. Therefore, if these proteins are deleted in *B. megaterium* QM B1551, then the mutant with the protein effective in aggregation deleted will be observed to have a phenotype of lower aggregation efficiency. If disruption of the protein results in reduced aggregation efficiency then the next step would be to reintroduce the gene for the protein in trans to confirm that adding the protein back to the system recovers the aggregation phenotype. Following the successful completion of this set of experiments the next step is to do site directed mutagenesis to identify the protein domain(s) that are involved in the

aggregation process. The main target here would be the loops that are predicted to be on the outside of the cell and which are potential sites of interaction with the algal cells. If the algal and bacterial cells are interacting via hydrophobic-type interactions then mutation of hydrophobic amino acids to charged residues would be predicted to have a step wise decrease in aggregation efficiency as fewer hydrophobic amino acids are available for interaction. Another possibility is that one or more predicted hydrophobic transmembrane domains are not actually located within the cytoplasmic membrane but instead are looped out of the membrane and are available for mediating hydrophobic interactions with algal cells. This hypothesis can be tested by mutating these stretches of hydrophobic amino acids to charged amino acids. If they are involved in aggregation then the strain with the mutated sequence should have lower aggregation efficiency.

It is possible that neither of the proteins are involved in the aggregation process. If this is the case then the next step is to determine if any protein on the outside of the cell is involved in aggregation. There are two approaches to doing this. The first is to knock out the gene for the sortase in *B. megaterium*. If any of the proteins that are anchored to the peptidoglycan by the LPXTG motif are involved in aggregation then the mutated strain should be deficient in aggregation. The second approach is to knock out the protein secretion system. This can be done by deleting the secA gene, which is the cytoplasmic ATPase used to power protein secretion (52). If the aggregating protein is secreted through this system the resulting mutant should be deficient in the aggregation phenotype. If neither of these approaches yield aggregation deficient mutant then the next step would be to begin deleting the genes involved in exopolysaccharide production one by one to see if any of these genes are involved in the aggregation process. Finally, it is

possible that none of the identified genes are involved in aggregation. At this point a random mutagenesis approach would need to be employed to "blindly" screen the genome for mutants with a phenotype of loss of aggregation activity.

Another option for determining the important molecules embedded in the cell surface would be to examine the components by GC MS. Here the surface components would be removed by digesting the peptidoglycan with lysozyme. The components of RP1137 in exponential versus stationary phase could be examined since aggregation ability decreases in stationary phase. It may also be useful to compare the three different bacilli to see if any of the cell wall components jump out as being clearly associated with the aggregation phenotype.

In this chapter I describe the genome of RP1137 and identified putative proteins encoded in the genome that might be involved in the aggregation phenotype. This was aided by comparing the algal aggregation abilities and genomes of *B. subtilis* SMY and *B. megaterium* QM B1551 to that of RP1137. The comparison revealed that *B. megaterium* and RP1137 have similar aggregation phenotypes and share many common genes. By narrowing the search for proteins that are expected to be anchored to the peptidoglycan on the outside of the cell, two candidate genes were identified. Finally, the steps to confirm if these proteins are involved in the aggregation phenotype were outlined along with alternative strategies if the identified proteins are not involved.

Chapter 5 Conclusions and future directions

5.1 Conclusions and summary

In this final chapter I summarize the data presented in my dissertation and synthesize what those data mean. I also outline remaining questions and how these questions might be answered by subsequent work. I state the contributions of this work and its significance.

The research that I undertook started with the isolation of an algal aggregating bacterium designated *Bacillus* sp. strain RP1137. This study includes a description of the conditions necessary for aggregating algae and the mechanistic details of how the aggregation process happens. I discovered RP1137 serendipitously as a contaminant in the culture of another bacterium that is able to aggregate bacteria. The original source of the strain is unknown and will likely remain so. The key characteristic of RP1137 is the speed at which it can aggregate diverse algae. Aggregation occurs in seconds rather than the hours or days that have been described for other algae aggregating bacteria (22, 30, 31). Other key findings are that the aggregation is sensitive to pH and divalent cation concentration. Specifically, algal aggregation by RP1137 requires a pH of 9 or greater and the presence of magnesium or calcium ions at a concentration of 10 mM or more. In the absence of these conditions RP1137 will not aggregate algae. I also showed that both live and dead RP1137 cells fixed with paraformaldehyde are equally effective at aggregating algae. This means that the cell surface chemistry is the determining factor in the mechanism of aggregation. To understand the mechanism of aggregation I performed a large number of experiments many of which produced negative, but still informative, results. For example, I showed that temperature has no effect on aggregation and that the RP1137 filament length does not have a significant effect on algal aggregation. I showed

that aggregation cannot be inhibited by digesting surface proteins from whole cells with proteinase K or by inhibition of potential lectin-carbohydrate type binding through the addition of sugars. These results outlined the conditions that are necessary for aggregation and began to reveal what may and may not be the mechanism of aggregation.

My next focus was on defining the mechanism of aggregation. I determined the aggregation efficiency at different times in the bacterial and algal growth phase. I found both RP1137 and *Nannochloropsis* cells aggregated most efficiently in the exponential phase of growth with a decrease in efficiency as the cells entered stationary phase. This result suggested that the surface chemistry of RP1137 cells may be changing over the growth period. The surface chemistry of RP1137 cells was investigated by measuring the relative number of titratable residues at the cell surface in both exponential and stationary phase cells. Here I found stationary phase cells have more deprotonatable residues than exponential phase cells. In this same line of investigation I showed calcium ions bind directly to RP1137 cells and that the addition of calcium causes a decrease in the surface charge of both RP1137 and *Nannochloropsis* cells. Both cell types initially have a negative surface charge. Stepwise addition of calcium leads to a decrease of surface charge with the charge of both cell types approaching an effectively neutral charge of –20 mV at 10 mM calcium. These data are consistent with the optimal concentration of calcium for aggregation which is also near 10 mM. At this stage, I had therefore determined that cell surface chemistry was important and that binding of calcium to RP1137 resulted in charge neutralization. To determine where this charge neutralization was occurring at the cell surface I used the dye pinacyanol to show that, at least in part, the charge neutralization was occurring at the negatively charged teichoic acids that are

embedded in the cell wall. The next question was: how does this charge neutralization lead to aggregation? Typically, negative surface charge causes electrostatic repulsion between cells keeping them from contacting each other. With that surface charge decreased the cells could now get close enough to interact. My data shows that the interaction is likely mediated by hydrophobic type interactions. I showed this by first demonstrating that more RP1137 and *Nannochloropsis* cells bind to hydrophobic C18 beads in the presence of calcium than in its absence. This demonstrates that the cells are individually capable of hydrophobic type interactions. To show that the aggregation process is dependent on these interactions I tested whether SDS is able to disrupt this interaction. My prediction was that if the interaction is hydrophobic in nature then I should be able to disrupt the interaction with an anionic detergent. Aggregation was disrupted by the addition of SDS, supporting the hypothesis that a hydrophobic-type interaction is involved in the aggregation process.

As a next step I looked to define the other unknown players that were involved in aggregation at the RP1137 cell surface. To find the genes that may be linked to aggregation I sequenced the RP1137 genome. The sequences were assembled into 60 contigs that were at least 1000 bp in length and with an average of 435-fold coverage. The estimated genome size was 5.9 Mb with a 37.5% G+C content. A total of 6159 protein coding sequences were predicted. With this genome I now had a way to delve into the genetic potential of this strain for aggregation. As a first analysis, with the assistance of Taylor Carter, an intern in the Hill lab, we checked for genes that coded for proteins with high homology to those known to be involved in aggregation, including the co-aggregation promoting factor protein in *Lactobacillus coryniformis* DMS 20001 (48), the

aggregation promoting factor gene found in *Lactobacillus gasseri* (49) and the S-layer protein from *Lactobacillus helveticus* ATCC 12046 (50). No significant matches were found using a 25% ID and 50% coverage cutoff. This result reduced the likelihood that aggregation of algae by RP1137 was mediated by specific proteins that have been previously described. My next step was to do a comparative analysis to other sequenced bacilli. I first tested the aggregation ability of the sequenced bacteria, *Bacillus megaterium* QM B1551 and *Bacillus subtilis* SMY. I found that *B. megaterium* QM B1551 was equally effective at aggregating *Nannochloropsis* cells as RP1137 whereas *B. subtilis* SMY showed minimal or no aggregating activity with this alga. These data provided the opportunity for comparative analysis of the genomes of the three organisms to try to locate genes that were correlated with the aggregation phenotype. From this comparison I found that RP1137 and QM B1551 have 2607 proteins that are not found in the SMY strain. I also found that SMY has 916 proteins that are not found in QM B1551 and RP1137. This result shows that a simple comparison of the proteomes of these organisms was not sufficient to narrow the potential list of candidate proteins to a number low enough to be experimentally tractable. However, an analysis of those proteins that are expected to be exported outside of the cell and attached to the cell wall successfully narrowed the list to two putative proteins that may be linked with aggregation. These proteins are annotated as a sodium/solute symporter and a Stage V sporulation protein B, though based on a predicted sortase cleavage site they are unlikely to have those functions. A summation of the key results of my dissertation can be found in Figure 5.1.

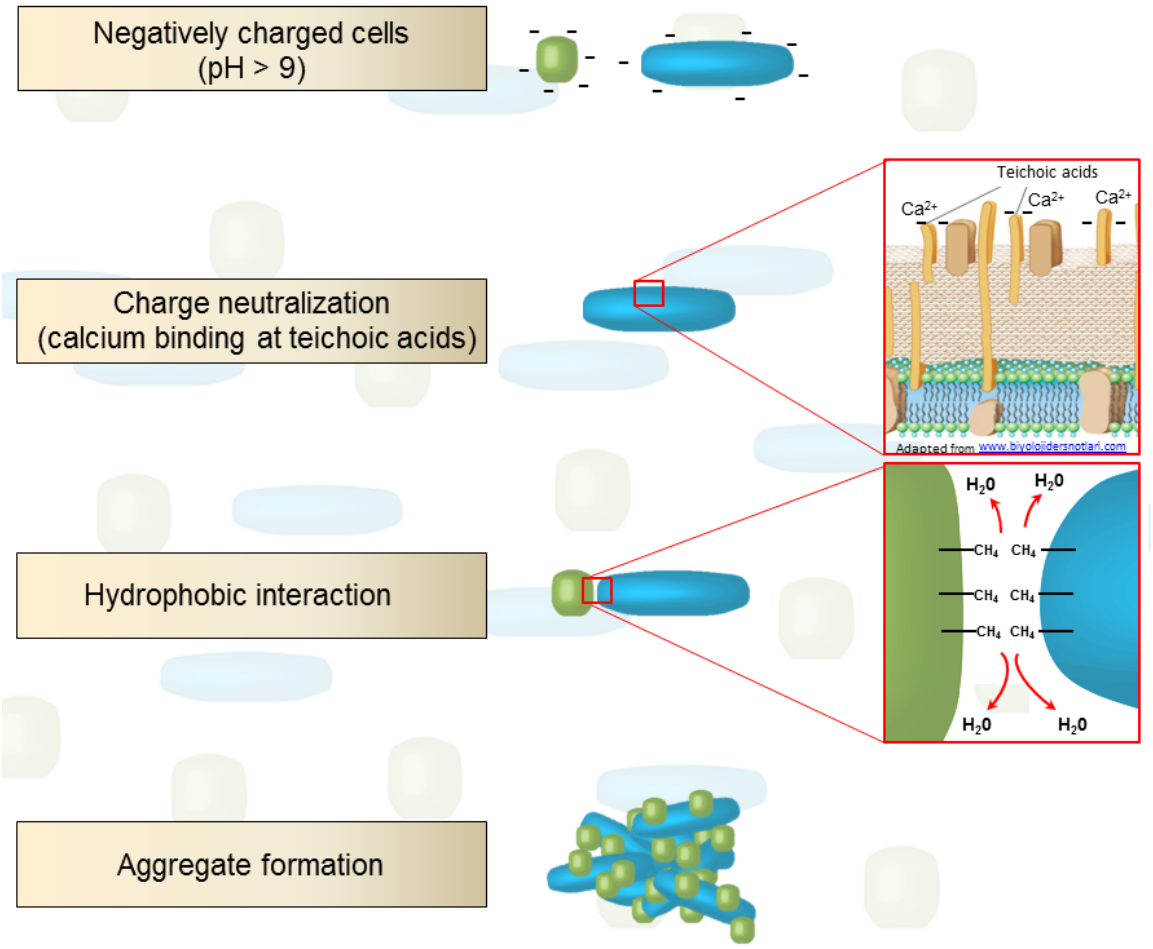

Figure 5. 1 Mechanism of algal aggregation by RP1137

Model of the aggregation of RP1137 with algal cells. At a pH of 9 or greater both cell types have a negative charge. Calcium binds to the teichoic acids on RP1137 cells and to an unknown site on the algal cells. This neutralizes the negative charge and removes the electrostatic repulsion that normally keeps the cells separated. The cells can then bind via hydrophobic type interactions where water is excluded and entropy increases. This process repeats with more cells causing the creation of bacterial/algal aggregates.

In combination, these data yield the conditions under which RP1137 will aggregate algae and mechanistic details of the aggregation process. It is important to note that mechanistic work was done with *Nannochloropsis*, so while it is likely that RP1137 aggregates other algae in a similar manner further work is needed to confirm this. The most direct implication of this work is that it provides a starting point for anyone interested in using this strain in practical applications. By knowing what is involved in the aggregation process and which algae are likely to be amenable to aggregation, this dissertation provides the necessary information to use RP1137 to harvest algae. My data also provide a mechanism of interaction between Gram-positive bacteria and algae that may be potentially broadly applicable. This mechanism provides testable hypotheses for anyone working on physical interactions between Gram-positive bacteria and algal cells. The mechanism may also be applicable to other systems in which Gram-positive bacterial cells interact with eukaryotic cells. This work adds to what is known about the binding of ions to Gram-positive cell surfaces and the effect that this binding has on surface charge and surface chemistry which will be useful to those who study the cell wall and how it interacts chemically with the surrounding environment.

5.2 Questions still to be answered and ideas for future work

As with any scientific endeavor, this study has raised a number of questions that are worth pursuing. In this section I will describe questions that remain unanswered and the work that might be done to answer those questions. These questions can be loosely divided into three categories: 1. Details of the mechanism of aggregation; 2. The role of

the aggregation phenotype, if any, in the environment; and 3. What is needed for successful practical application of RP1137 for harvesting of microalgae.

5.2.1. Details of the mechanism of aggregation

Some key questions remain unanswered about the actual mechanism of aggregation of algae by RP1137 cells. In this section I will explore questions about how these cells actually interact at the molecular level by building upon what has been presented in this dissertation. The first question is: what is the exact molecular entity on the bacterial surface that allows aggregation? This may be one component or the sum effects of several components at the cell surface. There are several possible approaches to address this question. The first and perhaps most direct is to characterize the cell surface of RP1137 when it is in exponential phase versus stationary phase. From my work, it is now clear that the aggregation efficiency is higher during exponential phase than stationary phase, suggesting there is a change in the cell surface chemistry. Zeta potential measurements show that the cells have a more negative surface charge during exponential phase than stationary phase and base titration shows the cells also have fewer deprotonatable residues at this time. Both of these results support the notion of a change in surface chemistry between cells in exponential versus stationary phase. The question is then narrowed to what are the residues that are responsible for those changes? If I hypothesize that the change in aggregation efficiency is due to a change in the composition of proteins found on the outside of the cell, then a possible approach is to characterize these proteins by proteomics. This could be done by digesting whole cells with lysozyme to depolymerize the peptidoglycan and to release the attached proteins. The surface proteins extracted from exponential and stationary phase cells could be

compared on a 2D gel with the goal of finding spots that appear, disappear or change in concentration between the two growth phases. Any spots of interest could be identified by N-terminal protein sequencing. The amino acid sequences could then be mapped back to the genome using the predicted proteins sequences from the genomic sequence data set to identify the protein and the genomic locus where it resides. Analyzing the genes and sequences around the protein coding region will reveal a wealth of information about potential regulation of the protein and what other proteins are likely co-expressed. This data will also point out which other organisms might also express this protein and thus also potentially have the aggregation phenotype. To link the correlation of the discovered protein(s) of interest to actual causation, genetics can be employed in either RP1137 or *Bacillus megaterium* QM B1551. Developing a genetic system in RP1137 should be possible because several of its close relative have working genetic systems (46). However, if B. *megaterium* QM B1551 has the same protein(s) of interest, then the question of whether the discovered proteins are responsible for aggregation can be answered in this organism in which a genetic system has already been developed. The final step in this sequence of experiments would be to knock out the protein(s) of interest and see if this disrupts the aggregation phenotype. If the protein(s) of interest is coded by an essential gene and cannot be knocked out it may still be possible to ascertain its function by adding an additional copy of the gene in trans on a plasmid. If the protein is responsible for aggregation then it may be possible to express it in stationary phase and restore the aggregation phenotype. This set of experiments would directly determine if a specific protein or set of proteins is involved in the aggregation phenotype. If a protein cannot be correlated with the aggregation phenotype then other macromolecules at the

surface of the cell need to be explored. Another potential target would be the density of teichoic and lipoteichic acids in the cell wall. Teichoic acid residues contribute to the negative charge associated with the cell wall and my data indicate that neutralization of these negative charges occurs when calcium is added to the cells. However, teichoic acids alone cannot explain the observed results as both exponential and stationary phase cells can be equally neutralized by addition of calcium. This result suggests that some additional factor is required. If teichoic acid residues alone were responsible then equally neutralized cells should have equivalent aggregation phenotypes which is not what is observed. To elucidate this unknown factor it would best to employ random mutagenesis with a screen for loss or increase in aggregation to find the unknown factor. Since my results show that different Gram-positive bacteria have different aggregation phenotypes it is likely that the phenotype is encoded on the genome.

The next question that remains unanswered is what is the molecular entity on the algal cell surface that allows it to interact with RP1137 cells? To begin to answer this question I could take advantage of the fact that my main model alga, *Nannochloropsis oceanica*, was recently sequenced (71). To find out what algal genes are involved in aggregation, one approach would be to select for a mutant *Nanochloropsis* strain that cannot be aggregated by RP1137 and then sequence the strain to find the mutation. The alga would be grown normally and at each subculture it would be harvested with RP1137 cells. The non-harvested cells would be used to start the next culture. This process would be repeated several times. If a spontaneous mutant arose that was not able to be aggregated it would soon come to dominate the culture because the aggregatable cells would be removed in each growth cycle. A decrease in aggregation efficiency would

indicate the presence of a significant population of this type of mutant. Once the culture reaches this state the cells could be plated and individual *Nannochloropsis* colonies picked and grown up to ensure that only a single genetic background is present. The colonies would be used to start cultures which would be tested for the defect in aggregation. If the defect is still present the strain would be sequenced using Illumina sequencing. The resulting sequences would be mapped back to the original genome sequence data to look for mutations. Identified mutations could then introduced back into the original strain using a recently developed targeted gene replacement technique for *N. oceanica* (72). If the introduced mutation caused the defect in aggregation then the mutated gene would be directly linked to the aggregation phenotype. This data could be used as a starting point for identifying the components of the cell that are involved in aggregation.

Another open question is what is the range of algae that RP1137 can aggregate? Within this study I tested several diverse algae.. However, further characterization should include diatoms and dinoflagellates as well as additional microalgae. A better understanding of the scope of organisms which can be aggregated by RP1137 will inform the mechanism of action as well.

One curious result from this research is that RP1137 can form large aggregates in the absence of *Nannochloropsis* but the *Nannochloropsis* cells cannot form large aggregates in the absence of RP1137 cells. My data suggest that the cells are interacting, at least in part, via hydrophobic type interactions once the cells surface charge has been neutralized by divalent cations. This mechanism of interaction suggests that both pure bacterial cultures and pure algal cultures should form self-aggregates. While

Nannochloropsis cells do form small aggregates of 5-10 cells at high pH in the presence of divalent cations, they do not form macroscopic aggregates. This is interesting because it suggests that there is more to the story than simple hydrophobic-type interaction. The simplest explanation for this is that there is a difference in the degree of hydrophobicity at the surface of RP1137 cells as compared to *Nannochloropsis* cells. In this model RP1137 cells bind more tightly to both other RP1137 cells and *Nannochloropsis* cells because the surface of the RP1137 cell is more hydrophobic. The less hydrophobic *Nannochloropsis* cells are still able to interact with the RP1137 cells but interact only weakly with other *Nannochloropsis* cells. Another potential explanation may have to do with the shape of the two cell types. *Nannochloropsis* cells are spherical and therefore when they interact with each other they, like two balls, only touch at a relatively small surface area. This smaller contact surface would have a smaller binding force. The RP1137 cells are bacilli which may have a stronger binding strength by interacting along the long surface of the cell. While this physical model predicts the results observed by the self-self type interactions, it does not explain why *Nannochloropsis* cells effectively interact with RP1137 cells, as in this type of interaction the cells have a similar contact area as when two *Nannochloropsis* cells interact. This suggests cell morphology alone cannot explain the observed results. There must be some difference in the actual binding strength. But how do we determine that binding strength? Hydrophobicity seems to play a role in the binding process and so understanding the strength of the hydrophobic interaction is one way to get at the binding strength. A simple way to test this is to measure how much force it takes to remove the cells from a hydrophobic surface. If RP1137 cells can bind to hydrophobic surfaces more tightly, then it should take more

force to remove them from the surface than *Nannochloropsis* cells. To do this the amount of fluid flow that it takes to remove the cell from a surface can be measured. The cells would first be bound to the inner surface of a small plastic tube with a hydrophobic surface to mediate that binding. Once the cells are bound the tube is connected to the input sip of a flow cytometer. The other end of the tube is submerged in pH 10 water with 10 mM $CaCl_2$, which are the conditions in which RP1137 aggregates algae. In this setup the flow cytometer does double duty by controlling the flow rate and also counting the cells that are washed off the tubing. The flow cytometer is started at the lowest flow rate and run until the counts from cells washed off of the tubing drops to zero. This process is repeated at successively higher flow rates. By adjusting the tube size the effective flow rate on the cell can be increased or decreased. This experiment can directly measure the binding strength of RP1137 and *Nannochloropsis* cells to a hydrophobic surface with a high n-value. If desired the exact binding strength can be calculated by using the flow rate and cell geometry to calculate the hydrodynamic drag on the cell. The prediction is that RP1137 cells will bind more tightly to a hydrophobic surface than *Nannochloropsis* cells. If this proves to be the case then a second experiment can be done with the same setup to calculate the binding force between RP1137 and *Nannochloropsis* cells. Here RP1137 cells are first bound to the tubing. Then *Nannochloropsis* cells are introduced to bind to the stationary RP1137 cells. The flow rate is adjusted, as before, to determine the flow rate at which the *Nannochloropsis* cells become detached from the RP1137 cells. Chlorophyll fluorescence and forward scatter will allow separation of single algal cells and algal cells that are still attached to RP1137 cells, so only the removal of single algal

cells is counted. These experiments will yield a clearer picture of the forces involved in the interactions between the algal and bacterial cell.

5.2.2. What was the original role of aggregation phenotype and why did it evolve?

An interesting question is why does RP1137 have this phenotype? After all, while it binds algae quite efficiently, the reason it has this activity is unknown. Since the isolate was originally a contaminant I do not know the original environment where this isolate evolved. Other *B. megaterium* species can be found in many different environments including freshwater and marine habitats so it is possible that binding to algal cells provides an adaptive advantage to the *Bacillus* sp. in its natural environment. In these habitats being able to bind to an algal cell may give RP1137 a selective advantage by giving the cell near-exclusive access to the sugars that may be excreted by the alga. This hypothesis can be tested by adding RP1137 cells to different algal cultures at a low dosage and seeing how well RP1137 persists over time. To facilitate easy quantitation a rifampicin resistant mutant of RP1137 could be selected and used in these assays. If RP1137 originally used this phenotype to bind to algal cells then it would be expected that the strain should be persistent within the culture over successive subculturing of the algae. If the population of RP1137 cells declined to zero it would refute this hypothesis. Evidence for this role of the aggregation phenotype could also be gathered by looking at bacterial community datasets collected from freshwater and marine algal blooms. If RP1137 like strains are found associated with the blooms then it strengthens the possibility that the algal binding phenotype was originally selected because it provided an advantage in association with algae in its natural environment.

While it is possible that the algal aggregation phenotype was originally selected for, it is more likely that generic binding to a variety of hydrophobic surfaces was the selective force. Work on the aggregation of Gram-positive bacteria and their binding to abiotic surfaces reveals that many organisms related to RP1137 are capable of forming self-aggregates (48, 50, 64). By comparing the aggregation activity of *B. megaterium* QM B1551 and *B. subtilis* SMY, I found that the aggregation phenotype is conserved in the closely related *B. megaterium* QM B1551 strain but not the more distantly related *B. subtilis* SMY strain. This suggests that if the aggregation phenotype evolved due to a specific selection pressure then it likely fills the same role for *B. megaterium* QM B1551, which was originally isolated from soil. The ability of RP1137 to bind algae and hydrophobic surfaces may then be interpreted not as binding algae in the water column but perhaps promoting interactions with soil associated algae, other eukaryotic cell or hydrophobic particles of soil.

5.2.3. What research is needed for successful practical use of RP1137 for algal harvest?

Whether this bacterium can actually be used to harvest algae at a practical scale is perhaps the most relevant question for anyone reading this dissertation. The short answer is that this technology is currently not feasible for harvesting algae for biofuels due to the costs involved in growing the bacteria. I calculated the cost of using RP1137 to harvest algae, if only the cost of the growth medium is considered, to be $0.25/liter of dilute algae harvested. This could be reduced by perhaps 10-fold by using an inexpensive industrial growth medium, however that is still not cheap enough for harvesting algae on a very large scale for biofuel production. It is certainly inexpensive enough for harvesting

algae for high value products such as pigments and nutraceuticals. However, fuel is cheap and requires an equally cheap harvesting method. If the algal biomass is converted to crude oil via hydrothermal liquefaction and the crude oil is sold at the current market value of $100/ barrel then the algal biomass must be produced and converted to crude oil for under $0.35 per kilogram of concentrated algae. As a frame of reference, if RP1137 is used to harvest one kilogram of algae at a 1 g/L biomass concentration it would currently cost $25. This figure includes only the cost of the inexpensive industrial growth medium and does not include other production costs. This clearly demonstrates that more development is needed for RP1137 to be used for cost-effective harvest of algae. To get anywhere near the $0.35 per kilogram mark, it is essential that the bacterial cells be used more than once. My work shows that the aggregation process can be reversed by lowering the pH. This opens the door to recovering the RP1137 cells after the algae has been harvested. If 90% of the cells can be recovered, then the cost for each subsequent round of harvesting drops to 10% for a given mass of algae harvested. This 10% is the amount of bacteria that must be replaced in each subsequent harvest cycle. A 90% recovery rate drops the price to $2.50 per kilogram of algae harvested which is still too expensive. However, if 99% of the cells can be recovered after each harvesting run the cost for subsequent runs drops to 1% of the original or $0.25. This is now below the cost barrier for economic harvest of algae for fuel. However, this harvest cost only includes the price of the medium needed to grow the algae meaning that in practice the harvest cost will be significantly higher. Another drawback is that this estimate includes only the cost for harvest and not the rest of the production and conversion system, which in

practice all must be done for less than $0.35 per kilogram of concentrated algae. To get to this cost-point, a very efficient means of reusing the cells would have to be developed.

If such a cell recovery system could be developed, what are the next logical steps in the development of this technology? The most pressing step would be to test the aggregation process at a greater scale. Currently, I have tested the aggregation of algae at a 20 L scale; however, it is important to test the system at 1,000 and 10,000 liter scales to ensure there are no unexpected problems at these increased volumes. Another key project would be to genetically engineer RP1137 to have a lower calcium requirement for harvest of freshwater algae. RP1137 requires at least 2 mM calcium or magnesium for aggregation. In seawater this is not a problem but some freshwater systems do not have this concentration of calcium or magnesium and would require the addition of these ions. From my model, I predict that the calcium ions are needed to neutralize negatively charged teichoic acids. Reducing the number of teichoic acid residues in the cell wall should in theory reduce the concentration of calcium needed to neutralize these residues. While deletion of genes for teichoic acids is not lethal, cells are severely inhibited and do not grow well as has been shown in other studies (73, 74). Therefore the genes for teichoic acids cannot simply be knocked out; instead the level of expression must be lowered by altering the promoters or Shine-Dalgarno sequences. While difficult this should be possible and will yield a version of the RP1137 strain that could be used for the harvest of algae in freshwater systems. An alternate and simpler approach would be to pretreat the RP1137 cells with calcium before use. My data show that several washes with deionized water are required to completely remove ions bound to the cells. Therefore if the cells are recharged with calcium ions after each use they should work

well in any salinity. This method also would use much less calcium as the cells could be treated in a small volume instead of altering the calcium concentration of a large body of water.

Overall, in this dissertation I describe the isolation and characterization the algae aggregating bacterium *Bacillus* sp. strain RP1137. I provide mechanistic details of how the aggregation process works and lay the groundwork for more detailed studies into the mechanism of action. This work also lays out the conditions for using this bacterium to harvest algae in practice and what improvements are needed for this strain to be used for the economic harvest of algae for biofuel production

Appendix 1 Characterization of the microbial community associated with the alga *Scenedesmus* sp. HTB1 grown in air, flue gas and 15% CO_2

Ryan J. Powell,[a] Leah Blasiak,[a] Li Zheng,[b] Diane Sumutka,[c] Donald Belle,[d] Zheng Liu,[a] Feng Chen[a] and Russell T. Hill[a*]

Institute of Marine and Environmental Technology,

University of Maryland Center for Environmental Science, Baltimore, Maryland, USA[a];

Marine Ecology Research Center, First Institute of Oceanography,

State Oceanic Administration of China, Qingdao, Shandong, China[b];

Joppatowne High School, Joppa, Maryland, USA[c]; and Gwynn Park High School, Brandywine, Maryland, USA[d]

[*]Corresponding author.

Mailing Address: Institute of Marine and Environmental Technology
University of Maryland Center for Environmental Science
701 E. Pratt St. Suit 326 Baltimore MD, 21202

Phone: (410) 234-8802

Fax: (410) 234-8818

E-mail: hill@umces.edu

ABSTRACT

Production of fuel from microalgal biomass is a promising means of generating a sustainable source of liquid fuels. Significant effort has focused on optimization of various steps of the microalgal biofuel production process; however, little research has been devoted to understanding the microbial community associated with microalgae. Bacteria can dramatically affect algal growth positively through nutrient cycling and production of vitamins, whereas algicidal bacteria can negatively impact algal growth and viability. In this study, I characterized the bacterial community associated the alga *Scenedesmus* sp. HTB1 grown with air, flue gas and 15% CO_2 using fluorescence microscopy, flow cytometry, denaturing gradient gel electrophoresis, 454 sequencing of 16S rRNA genes and culturing of associated bacteria. Bacteria were found as free living cells, as single cells associated with individual algal cells and in large aggregates composed of multiple bacteria and algae. Bacteria to algal cell ratios varied between 1:1 and 10:1. *Proteobacteria* and *Bacteroidetes* dominated the relatively simple bacterial community which had approximately 25 operational taxonomic units at 3% difference based on 16S rRNA gene sequences. 16S rRNA gene sequences representing the *Porphyrobacter* genus comprised 56% of those found in algal cultures grown with flue gas and 85% of the sequences found from algae grown in air. This is the first study on how the microbial community in an algal photobioreactor is affected by growth with flue gas compared with air.

INTRODUCTION

In nature, algae are never found as axenic cultures. They are surrounded by other microorganisms that may promote, inhibit or have no effect on growth. Most of the focus within the algal biofuel community has been on pure cultures of algae grown under highly controlled conditions to prevent bacterial contamination or on unialgal cultures that contain associated bacteria that remain uncharacterized and unstudied. Use of axenic algal cultures can yield highly productive cultures, though at the cost of a more complex and expensive system that is needed to keep the culture pure. In outdoor culture systems, algae with few or no bacteria will come in contact with environmental bacteria and other microorganisms that are ubiquitous outside of the laboratory. Rather than attempting to keep bacteria out of algal cultures, I believe the opposite approach warrants attention, which is to fully colonize the available niches within the algae-associated microbial community with beneficial or commensal bacteria. Filling these niches may promote a resistant and resilient community and make it more difficult for "undesirable" microbes to become established within the culture. This approach is analogous to the growing realization of the importance of the human microbiome and its role in suppressing colonization by pathogens (75).

To actively construct a resilient algal community, I first need to understand the composition of the bacterial community and the function of the bacteria within the community and in association with the microalgae. To date, most research has focused on naturally occurring algal communities that are important in the environment and for human health, as in harmful algal blooms. From these studies, I know that bacterial communities associated with algae have a direct impact on algal growth and survival by

regenerating inorganic and organic nutrients (76, 77). Bacteria can also provide vitamins, trace metals, metal chelators and phytohormones (78-80). Vitamin B_{12} or cyanocobalamin is required by all algae but only about 50% of free-living eukaryotic algae are able to synthesize their own vitamin B_{12} while the rest rely on symbiotic bacteria to produce this key cofactor (79). Although bacteria can benefit algae in many ways certain bacteria have been implicated as algicidal agents that can terminate algal blooms (81, 82). These bacteria can directly and indirectly kill (83-85). Some algicidal bacteria indirectly inhibit algae by competing for limiting nutrients (86, 87) while others alter the environment in ways that prevent algal growth (88).

The microbial community can thus have a dramatic impact on algal viability, productivity and stability. However, little work has been done on the bacterial communities associated with algae cultured for biofuels. Lakaniemi *et al*. describe the bacterial communities associated with non-axenic cultures of the fresh water alga *Chlorella vulgaris* and the marine alga *Dunaliella tertiolecta* in a photobioreactor (89-91). *Proteobacteria*, *Bacteroidetes* and *Actinobacteria* were found in the *Chlorella* cultures, while only *Proteobacteria* and *Bacteroidetes* were found in the *Dunaliella* cultures (89-91). In a comprehensive metagenomic analysis of the biofilm community associated with cultures of *C. vulgaris* and *Scenedesmus obliquus* grown in photobioreactors, the bacterial community was found to be relatively simple with approximately 30 bacterial groups and was composed mostly of *Proteobacteria* and *Bacteroidetes* (92). A high number of genes for lipid metabolism, including esterases and lipases, were present in the bacterial genomes, suggesting that the associated bacteria

may metabolize some of the lipid produced by the microalgae. The metagenomic analysis also revealed many bacterial genes that encoded for essential B vitamins.

These studies characterized the microbial communities associated with microalgae grown in cultures bubbled with air or a combination of air and flue gas. There is interest in the use of microalgae to sequester the CO_2 present in the flue gases discharged by power plants. Flue gas is the exhaust from burning oil, coal, natural gas or other carbon containing fuels. Culturing algae under CO_2 or flue gas stimulates growth by providing increased inorganic carbon for reduction to biomass. Flue gas may provide nitrogen from nitrogen oxide (NO_x) compounds and limiting trace metals for algal growth. To our knowledge, no one has investigated how flue gas and high CO_2 concentrations influence the bacterial community associated with algae. Both flue gas and CO_2 will decrease the growth medium pH which may also significantly impact the bacterial community structure. Since some algal species cannot live without their bacterial symbionts or the products provided by them, I expect that shifts in the bacterial community could have major unintended consequences on the viability, productivity or stability of algal cultures.

Scenedesmus sp. HTB1 is a freshwater alga isolated from the Back River near Baltimore Maryland, USA (93). *Scenedesmus* sp. are members of the phylum *Chlorophyta* and have been adopted by several groups as model organisms for algal biofuels due to their rapid growth rate, lipid accumulation and tolerance to high CO_2 concentrations (94-96). In this study I characterized the bacterial community associated the alga *Scenedesmus* sp. HTB1 when grown with air, flue gas and 15% CO_2. I used denaturing gradient gel electrophoresis (DGGE), 454 pyrosequencing of 16S rRNA genes and culturing of bacterial isolates to gain a better understanding of the composition of the

algal-associated bacterial community under these conditions. We screened the isolates for production of quorum sensing molecules to determine if cell-to-cell signaling could play a role in regulating the phenotypes expressed by members of the bacterial community. We also added the pure isolates back to the algal cultures and monitored their effect on algal growth.

METHODS

Strains and culture conditions. *Scenedesmus* sp. HTB1 was isolated from the Back River near the effluent of the Back River Waste Water Treatment Plant in Baltimore, Maryland USA (93). This strain was selected from several hundred isolates due to its high biomass productivity, tolerance to high CO_2 concentrations (up to 20% CO_2) and ability to grow at elevated temperature (40°C) (93). I were unable to cryopreserve *Scenedesmus* sp. HTB1 and therefore maintained continuous culture stocks for experiments. Stock cultures were routinely cultured in in 2 L Erlenmeyer flasks in 0.22 µm filtered BG11 medium (97) without added vitamins. Algae were grown with a 14/10, light/dark photoperiod with constant shaking at 180 rpm at 20°C under 83.3 µmol/sec/m^2 illumination from 30 watt white fluorescent lights. The *Scenedesmus* sp. HTB1 stock culture was used to start experiments which were grown under the conditions described in subsequent sections.

Flow cytometry. Algal and free bacterial cell numbers were determined using an Accuri C6 flow cytometer. Samples of algal culture were stained with 1x SYBR green I nucleic acid stain (Molecular Probes, Life Technologies, Grand Island NY) and diluted in BG11

with 1x SYBR green to be within the linear range of the flow cytometer (< 2500 events/sec). SYBR green was used to distinguish cells from non-DNA containing debris. Filtered BG11 medium with 1x SYBR green was used to calibrate the flow cytometer to remove non-cellular events. Events with a signal of less than 1000 on FL1 (SYBR green channel, excitation 488 nm, emission 533/30 BP filter) or less than 1000 for FL3 (chlorophyll channel, excitation 488 nm, emission 670 LP filter) were discarded. Algal cells were counted as events with a signal greater than 100,000 in the chlorophyll channel (FL3). Bacteria were considered as events with a signal of between 1000-100,000 in the FL3 channel.

Fluorescence microscopy. Algae and bacteria within *Scenedesmus* sp. HTB1 cultures were visualized by staining with 1x SYBR green I nucleic acid stain and by natural chlorophyll autofluorescence. Both signals were observed using a filter cube with a 470/40 BP excitation filter, a FT 495 dichroic mirror and a 525/50 BP emission filter on a Zeiss Axioplan microscope with excitation from a Zeiss X-Cite 120Q Iris FL light source.

Cultured based bacterial community analysis. To analyze the cultivable microbial community, samples from the stock algal culture were serially diluted in R2A liquid medium (BD, Franklin Lakes, NJ) and spread onto R2A agar plates with 15 g/L Difco Technical Agar (BD). Plates were incubated at 30°C and colonies were picked as they appeared over a three week period. For each colony morphotype observed we picked two colonies for isolation into pure culture. Colonies were repeatedly streaked to obtain pure cultures. A single colony from each pure culture was used to start a liquid culture in R2A broth for cryopreservation. Cultures were incubated at 30°C with 180 rpm shaking until

turbid and preserved by adding sterile glycerol to a final concentration of 20% and freezing the samples at -80°C. Samples were tested for recovery from cryopreservation by streaking onto solid R2A agar plates with incubation at 30°C. Only bacterial isolates that were recoverable from cryopreservation were used in subsequent experiments. We identified these isolates by sequencing their 16S rRNA genes. PCR was performed using whole bacterial cells as the source of template DNA. Primers 27F and 1492R (36) were used with standard reaction conditions. The resultant PCR products were purified using the Qiaquick PCR purification kit (Qiagen, Valencia, CA) and sequenced using primer 27F. The resulting trimmed sequences (599-827 bp) were identified using the Seqmatch function of the Ribosomal Database Project website (98).

DGGE based microbial community analysis under different atmospheres. I cultured *Scenedesmus* sp. HTB1 in air, flue gas and 15% CO_2 to understand the impact of differing atmospheric conditions on the bacterial community associated with the microalga. Flue gas was derived from the exhaust of electrical generators burning methane at the Back River Waste Water Treatment Plant. This methane was generated via anaerobic digestion of solid waste that is processed at the plant. The flue gas contains 10-12% CO_2. The 15% CO_2 atmosphere was obtained by supplementing ambient air with pure CO_2. Algae were grown in 12-well tissue culture plates under Agro-Lite R20, 50 W, Philips lights at 25 µmol /m^2/sec at room temperature with continuous illumination. Culture plates were incubated inside GasPak™ EZ bags (BD) filled with the atmosphere being tested (Zheng et al. 2013). A sample from the initial inoculum (grown in air) was used to start all samples. For each atmospheric condition three replicates were used. Samples were collected during exponential and stationary phases of growth. The samples

were harvested by centrifugation at 20,000 *g* for 5 minutes, supernatants were aspirated and the cell pellets were stored at -20°C. DNA was extracted from cell pellets using the Ultra Clean Microbial DNA isolation kit (MoBio, Carlsbad, CA). Extracted DNA was quantitated by spectroscopy and samples were diluted so all samples had the same concentration. These normalized DNAs were used to PCR-amplify 16S gene fragments for DGGE (99). Briefly, primers P2 and P3 were used to amplify a fragment within the bacterial 16S rRNA gene (99). Fragments were separated on a denaturing gradient polyacrylamide gel with a denaturant gradient of 40-70% for 16 hours at 60 volts. The gel was stained with 1x SYBR green I nucleic acid stain and visualized on a UV transilluminator. Individual bands were identified by excising the band with a clean scalpel and then transferring the band to a clean 1.5 ml tube. The band was washed twice with sterile DNA-free deionized water. 50 µl of sterile DNA-free deionized water was added and the band was ground into small pieces and then incubated at RT for 30 minutes. The acrylamide fragments were removed from suspension by centrifugation at 20,000 *g* for 3 minutes. 2.5 µl of the supernatant was used as template for a second PCR using high fidelity Phusion DNAP (New England BioLabs, Ipswich, MA) with the same reaction conditions as the original DGGE PCR. To ensure the correct band was amplified these DNA fragments were run on a new DGGE gel along with the original samples to confirm a single product ran at the expected location. The amplified samples were purified using the Qiaquick PCR purification kit and sequenced using primer P2. The resulting trimmed sequences (100-150 bp) were identified using the Seqmatch function of the Ribosomal Database Project website (98).

454 based microbial community analysis under different atmospheres. DNA purified from the algal cultures grown under air and flue gas (described above) was used for 16S rRNA gene PCR amplification and 454 sequencing based characterization of the microbial community. Three biological replicates from each condition were prepared and processed separately. DNA samples were amplified with primers 341F (5′-XXXXXXXX-CCTACGGGAGGCAGCAG-3′, where X is a unique barcode) and 907R (Table S1). PCR amplification and 454 pyrosequencing was performed by Research and Testing Laboratory (Lubbock, TX) on a 454 Life Sciences GS FLX+ instrument (Roche Diagnostics, Branford, CT). Sequence quality filtering and data processing were performed using Mothur (100). Raw flowgrams were denoised with PyroNoise (101) implemented in Mothur. Sequences with ambiguous bases, primer or barcode mismatches, or homopolymers > 8 were discarded. All sequences were trimmed to exactly 280 bases. Chimera removal was performed with UCHIME (102) in Mothur, and sequences were classified with RDP 9 (103) using an 80% bootstrap cutoff. A pairwise distance matrix was calculated in Mothur followed by average neighbor clustering at 3% difference to give operational taxonomic units (OTUs). Sequences were subsampled to 2300 sequences per sample to allow comparisons across samples with equal sampling coverage.

Comparison of cultured isolates to 454 data. I were interested in seeing if the bacteria I cultured matched the dominant organisms identified by 454 sequencing. By sequencing the same region of the 16S rRNA gene in both the isolates and in the metagenomic 454 dataset I was able to directly compare whether I cultured dominant members of the community. The pooled, un-subsampled 454 dataset was used to generate a searchable

database using Standalone BLAST (version 2.2.27+) (104). Individual isolate sequences were searched against the 454 database using the Blastn algorithm with the minimum percent identity set to 99%, 7 bp word size and maximum target sequences returned set to 100,000. Matches with coverage of less than 267 bp were discarded. Matches for each isolate at 99.3% (~2 bp mismatch) and 100% identity were counted and plotted.

DGGE assessment of community stability. Samples were taken from the continuously cultured stock of *Scenedesmus* sp. HTB1 13 months apart, representing roughly 400 generations. Samples were processed for DGGE as described above.

Effect of bacterial isolates on algal growth under high CO_2. Bacterial isolates were added back to *Scenedesmus* sp. HTB1 cultures to assess the effect of each isolate on algal growth. I attempted to prepare axenic algal cultures for these experiments using cell sorting, dilution to extinction, different antibiotic treatments alone and in combination, differential centrifugation, mild bleach treatment and UV treatment. None of these procedures provided axenic and viable algal cultures. By differential centrifugation I were able to obtain a 10-fold reduction in free bacteria and maintain algal viability and so I used this method to prepare algal cultures for "add-back" experiments. *Scenedesmus* sp. HTB1 culture was centrifuged at 100 *g* for 3 min which pelleted the algal cells and left most unattached bacteria in the supernatant. The supernatant was aspirated and the algae were suspended in sterile BG11 medium. Centrifugation, aspiration and suspension in fresh BG11 were repeated to obtain the reduced bacteria samples. Bacterial isolates were prepared by streaking onto R2A agar plates from cryostocks. Single colonies were picked into R2A broth and incubated at 30°C with 180 rpm shaking. Flow cytometry was used to determine the concentration of cells in the algal cultures and in the bacterial pure cultures

using the parameters listed above in the flow cytometry section. Algal cells were diluted to a final concentration of 1 x 10^4 cells/ml and 180 µl of the algae was transferred into the wells of clear, flat bottom 96-well plates. Each bacterial isolate was added at ratios of bacteria to algae of 10:1, 1:1 and 1:10 while holding the final concentration of the algae constant. Four replicates for each ratio were used. Controls without added bacteria were also set up in each plate. 96-well plates with algae were grown in sealed BD EZ-GasPak chambers with a 15% CO_2 atmosphere. Evaporation was minimized by maintaining a humidified atmosphere. The chambers were incubated at 20°C with a 14/10 light/dark photoperiod with 142 µmol/sec/m^2 illumination from 30 watt white fluorescent lights. Growth of the algae was measured in black 96-well plates using chlorophyll fluorescence in a Spectromax M5 microplate reader with an excitation wavelength of 488 nm, a 515 nm cutoff filter and an emission wavelength of 685 nm. Chlorophyll fluorescence was used to specifically measure algal growth. Samples were measured daily for 10 days which was sufficient for the cultures to reach stationary phase. Treatments that gave statistically significant differences relative to controls were repeated in subsequent experiments with 24 replicates.

Screening isolates for AHL production. All isolates were screened for AHL production using the *Agrobacterium tumefaciens* based biosensor system developed by Zhu et al. (105). Isolates were spotted onto two R2A agar plates and grown for three days at 30°C. The *Agrobacterium* reporter strain KYC55 was prepared by growing it in 1x ATGN minimal medium (106) with 100 µg/ml spectinomycin dihydrochloricle pentahydrate, 4.5 µg/ml tetracycline and 100 µg/ml gentamicin at 30°C with 180 rpm shaking. A subculture was made in the same medium with an initial 1 to 500 dilution of the cells. The

subculture was grown under the same conditions and harvested when the optical density at 600 nm reached of 0.35. The cells were harvested by centrifugation at 15,000 *g* for 10 minutes. The cell pellet was suspended in sterile 30% glycerol to a calculated optical density of 12. One milliliter aliquots of the cells were stored at -80°C. The reporter overlay was prepared by cooling 90 ml of 0.6% agar to 45°C and adding 5 ml of 20× AT salts (15 mM $(NH_4)_2SO_4$, 0.6 mM $MgSO_4 \cdot 7H_2O$, 0.06 mM $CaCl_2 \cdot 2H_2O$ and 0.0071 mM $MnSO_4 \cdot H_2O$) , 5 ml of 20× AT buffer (79 mM KH_2PO_4, pH 7.0), 1 ml of 50% (w/w) glucose, 200 µl of 20 mg/ml X-gal and 1 ml of the prepared the KYC55 cells. This reporter strain mixture was poured over one of the colony containing plates. The other replica plate received the same overlay mixture except the reporter strain was not included. This served as a control for non-AHL dependent cleavage of X-gal, which may occur if an isolate produces β-galactosidase. Isolates deemed positive for the production of AHLs were further tested to determine the number of AHL species produced using a thin layer chromatography reporter overlay assay (105). A 20 ml culture of each isolate was grown to stationary phase in R2A medium in a 125 ml Erlenmeyer flask at 30°C with 180 rpm shaking. The cultures were extracted three times with 20 ml of dichloromethane on ice. The dichloromethane extracts were evaporated in glass petri dishes and then dissolved in 2 ml ethyl acetate (0.01% acetic acid). A speedvac was used to dry the ethyl acetate and the resulting dried extract was suspended in 200 µl ethyl acetate (0.01% acetic acid) giving a 300 fold concentration from the original extracts. Extracts were spotted onto C18 reverse phase thin layer chromatography (TLC) plates (Mallinckrodt Baker, Philipsburg, NJ) and developed with 60% methanol in the mobile phase. TLC plates were dried, placed in a large square sterile petri dish and the AHL

reporter overlay, described above, was poured on top of the plate. The plate was incubated at 30°C overnight to allow the development of blue color associated with the presence of AHLs.

RESULTS

Visualization and enumeration of associated bacteria. Microalgae are receiving considerable attention for their potential use as a means of sequestering CO_2 and also for generating renewable fuels. While much research has been devoted to the study and isolation of new algal strains, relatively little work has been done on the microbial communities associated with these algae. In this study, I aimed to characterize the microbial community associated with an alga, *Scenedesmus sp.* HTB1. I was first interested in looking at the number of unassociated bacterial cells found relative to the number of algal cells. Flow cytometry was used to count both bacteria and algae. Bacterial concentrations varied from a 1:1 ratio of bacteria to algal to as high as ten bacteria for every one algal cell. Fluorescence microscopy confirms the presence of large numbers of free bacteria (Fig. 1). Algae were found as single cells with no associated bacteria, single cells with one or few surface associated bacteria and in large aggregates composed of multiple bacterial and algal cells. Aggregates ranged in size from 10 µm to greater than 100 µm. Bacteria associated with the aggregates had diverse morphologies, suggesting different microorganisms were present. The data show that bacteria within the algal culture are found in distinct niches.

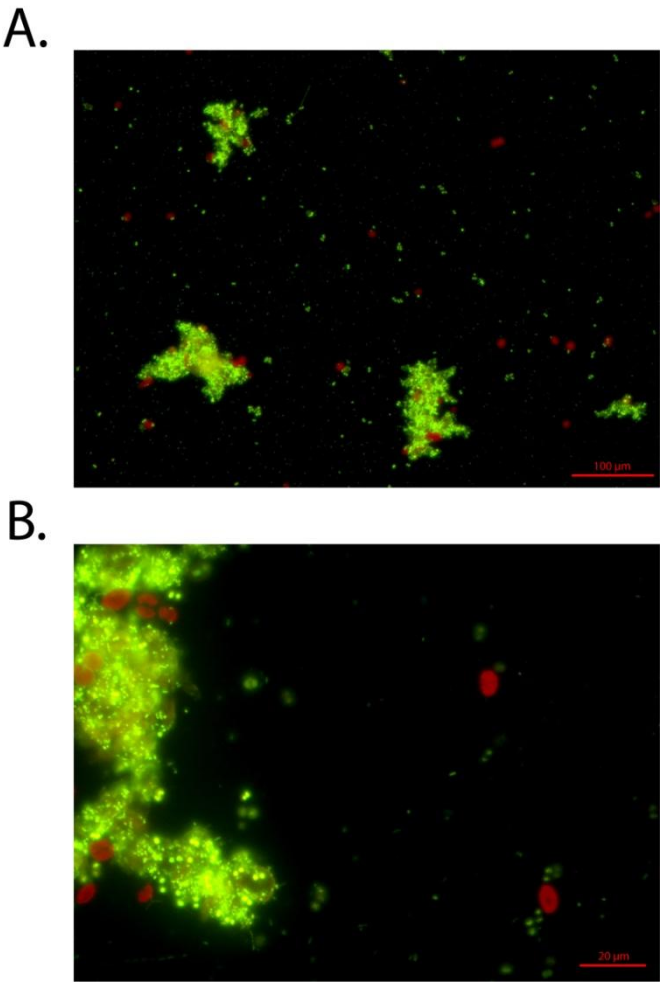

FIG 1 Fluorescence microscopy images of *Scenedesmus* sp. HTB1 algal cultures showing free living algal and bacterial cells, single algal cells with one or a few associated bacteria and aggregates of algal and bacterial cells. Algae are shown in red and bacteria in green. (A) A culture at 10X magnification. (B) A culture at 40X magnification.

Bacteria are found as free-living cells where they must depend on diffusible nutrients for growth. They are also found associated with the surface of the algae, where a single bacterium or few bacteria are associated with a single algal cell and may take advantage of extracellular polymeric substances produced by the algal cell. Also, the bacteria are found within aggregates with other bacteria and algal cells. Here the cells likely have access to extracellular polymeric substances and also metabolites produced by other bacteria.

Bacterial community characterization under different atmospheres. Shifts in the bacterial community were monitored using DGGE with universal 16S rRNA gene primers. The bacterial community was monitored under atmospheres of air, flue gas and 15% CO_2. The flue gas contained on average 12% CO_2 and also contained NO_x and SO_x compounds. Samples were collected from three biological replicates of algal cultures and associated bacteria over a growth cycle. DGGE banding patterns between the replicates were nearly identical. A representative sample from each treatment is shown in the gel in Fig. 2. Bands were excised, amplified and sequenced to reveal the identity of the bands. Bands that were successfully sequenced are numbered in Fig. 2.

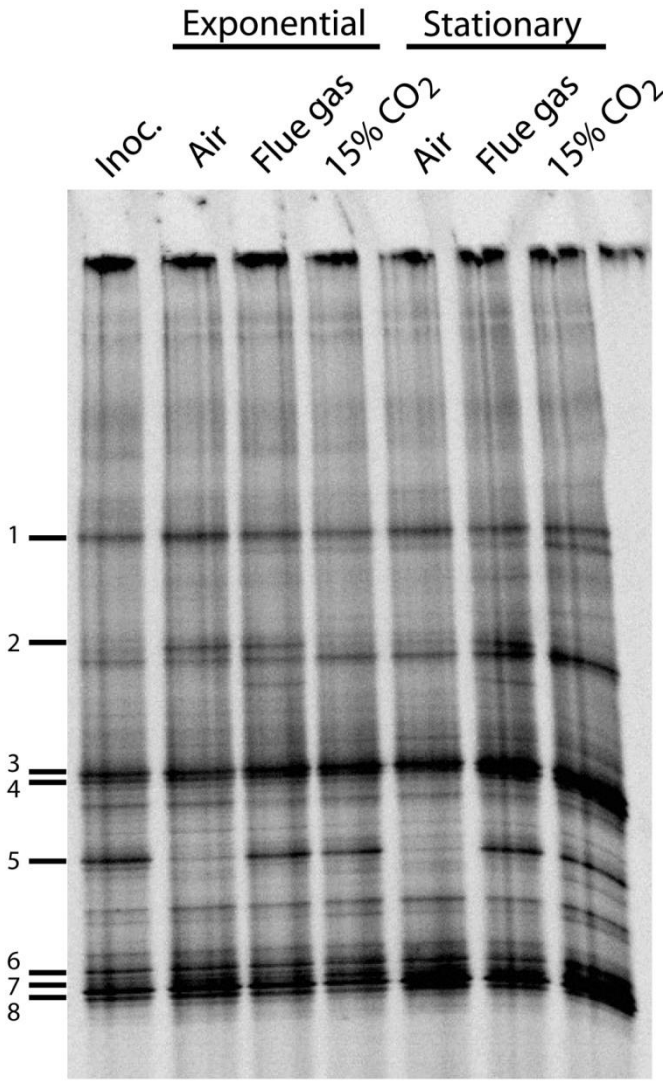

FIG 2 Denaturing gradient gel electrophoresis analysis of algal-associated bacterial communities from algal cultures grown under different atmospheres. Each sample shown has three biological replicates which were nearly identical. Only one replicate is shown in this representative gel. Numbers indicate bands that were successfully cut and identified by sequencing. *The identified bands represent organisms from the following clades, (1) genus Flavihumibacter*, (2) family *Pseudomonadaceae*, (3) genus *Porphyrobacter*, (4) genus *Flavobacterium*, (5) genus *Rhizobium*, (6) class *Alphaproteobacteria*, (7) family *Acetobacteraceae* and (8) family *Acetobacteraceae*

The sequences were identified using the Ribosomal Database Project sequence match tool (98). The identified bands represent organisms from the following clades: (1) genus *Flavihumibacter*, (2) family *Pseudomonadaceae*, (3) genus *Porphyrobacter*, (4) genus *Flavobacterium*, (5) genus *Rhizobium*, (6) class *Alphaproteobacteria*, (7) family *Acetobacteraceae* and (8) family *Acetobacteraceae*. Note that bands 7 and 8 have identical sequences. Due to the short sequence length and location of the amplicon on the 16S rRNA gene, classification is unreliable beyond the genus level. The DGGE gel shows that most of the community remains constant under the different atmospheric conditions with a few minor shifts.

454 sequence-based bacterial community characterization. To further characterize the microbial community associated with the algal culture, I performed 454 sequencing of 16S rRNA gene amplicons. For this in-depth analysis, I choose to compare the microbial community from three biological replicates of algae grown with air to three replicates grown with flue gas. Details of the sequence processing are shown in Table S1. A rarefaction curve showing sequencing depth is shown in Fig. S1. The results of the 454 sequence analysis showed many of the same types of organisms that were found in the DGGE analysis (Fig. 3). The three biological replicates of flue gas and air each grouped more closely with samples of the same type as shown in Fig. 3. There were 18-21 OTUs in the air samples and 26-33 OTUs in the flue gas samples at a cut off of 3% 16S rRNA gene sequence difference. Bacterial communities in algal cultures grown with flue gas were found to be significantly more diverse than those grown with air with an inverse Simpson's index of 2.63 ± 0.07 for flue gas compared with 1.34 ± 0.02 for air.

Supplementary Table 1. Sequence reads obtained for each 454 sequencing run for analysis of bacterial communities associated with microalgae grown with air and flue gas, designated "A" and "F", respectively

.

454 Sample Name	Barcode	Raw seqs	Final quality Filtered Seqs
A1	CAGCTACA	7178	2331
A2	CAGCTCGA	10027	3627
A3	CAGCTGTA	11898	4225
F1	CAGGACCA	11621	5659
F2	CAGGAGGA	5429	2559
F3	CAGGATTA	12365	5957

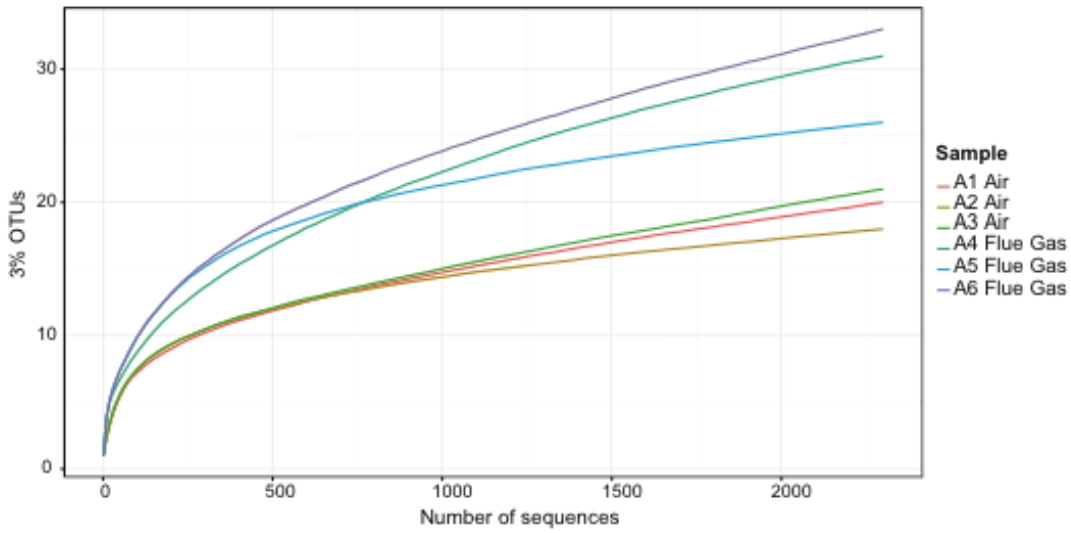

Fig S1 Rarefaction curve of 454 sequence data from algal cultures grown in air and flue gas.

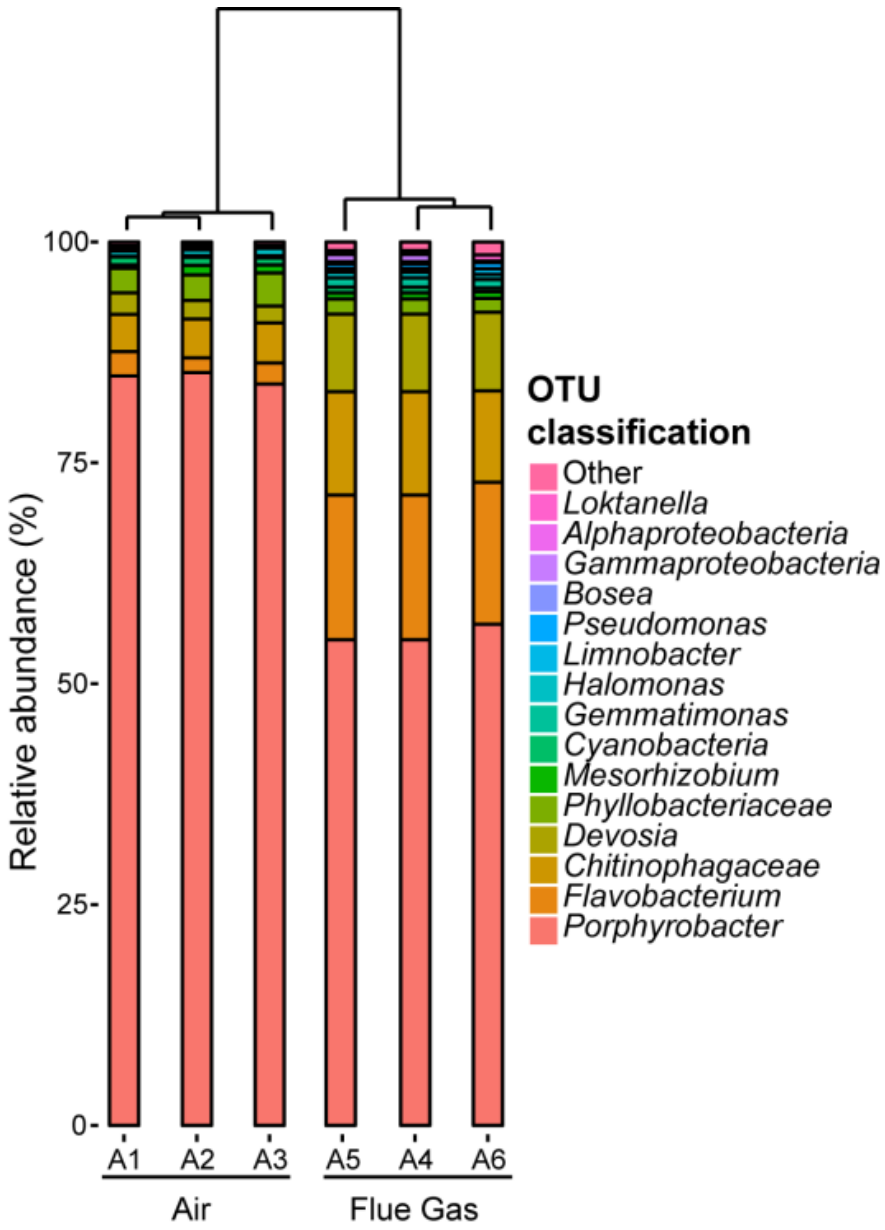

FIG 3 Relative abundance of sequences in 3% OTUs under air (A1-A3) and flue gas (A4-A6). OTUs containing less than 0.1% of total sequences were grouped as “Other”. The tree shows hierarchical clustering of samples based on Bray-Curtis dissimilarities calculated on 3% OTUs.

The increase in diversity was due to an increase in OTU richness for the flue gas samples, despite a small but significant difference in evenness (Smith Wilson's evenness index 0.518 ± 0.001 for flue gas, 0.527 ± 0.003 for air). The dominant sequenced organisms in both air and flue gas cultures were found to be *Porphyrobacter* spp.. This group comprised 56 ± 0.5 % of the sequences in the flue gas samples and 84.6 ± 0.4 % of sequences in the air samples. Other organisms representing greater than 1% of total sequences in flue gas include those in the *Flavobacterium* (16.4 ± 2.4 %), *Chitinophagaceae* (10.9 ± 0.4 %), *Devosia* (9.1 ± 3.0 %), *Limnobacter* (6.5 ± 0.2 %), *Phyllobacteriaceae* (1.5 ± 0.1 %) and *Gemmatimonas* (1.1 ± 0.1 %) clades. Other organisms representing greater than 1% of total sequences in air samples include those in the *Chitinophagaceae* (4.4 ± 0.1 %), *Phyllobacteriaceae* (3.1 ± 0.3 %), *Flavobacterium* (2.2 ± 0.3 %) and *Devosia* (2.1 ± 0.2 %) clades. Groups that were significantly more abundant in air samples than flue gas include the *Porphyrobacters* ($p < 0.001$) and *Phyllobacteriaceae* ($p = 0.022$). Groups that were significantly more abundant in flue gas than air include the *Flavobacterium* ($p = 0.007$), *Devosia* ($p = 0.008$), *Chitinophagaceae* ($p = 0.022$), *Gemmatimonas* ($p = 0.019$) and *Limnobacter* ($p = 0.026$).

Isolation of algae-associated bacteria. With the bacterial community characterized by DGGE and 454 sequence analysis, I next set out to culture members of the bacterial community. While molecular methods have become increasingly powerful for characterizing which bacteria are present in a community, obtaining pure isolates in culture opens up many avenues of investigation into the roles of the identified organisms. Bacteria were isolated from algal cultures on R2A agar plates. A total of 96 isolates were obtained, and of these 52 were recoverable from cryo-storage. The 16S rRNA gene of

these isolates was PCR amplified, sequenced and the closest cultured relative identified using the RDP sequence match function. A summary of the isolated organisms is shown in Fig. 4 and the complete list can be found in Table S2.

BLAST comparison of isolates to the 454 dataset. A stand-alone BLAST search was used to compare the isolates in the culture collection to the 454 data. The result of this search at a 100% and 99.3% identity threshold are shown in Fig. 5. Many of the isolates have a 100% match to sequences within the 454 data set, indicating these isolates are likely the same organisms that were identified by molecular methods. A total of 35 of the 52 isolates have at least a 99.3% match in the 454 dataset. The *Flavihumibacter* and *Flavobacterium* isolates are well represented within the 454 dataset, which suggests these bacteria may be abundant in the algal microbial community. *Porphyrobacter* strain RP1180 was the organism with the most hits at a 99.3% cutoff with 15,763 hits. Several Pseudomonads were present in the culture collection and also represented in the 454 dataset. All isolates with hits in the database at 100% identity had more hits at 99.3% identity. This may indicate a combination of sequencing errors and additional, uncultured diversity within a given group. These two possibilities cannot be distinguished with the current dataset, though more abundant sequences are less likely to be errors. The BLAST search does confirm that many of the bacteria that were isolated are also present by independent molecular analyses.

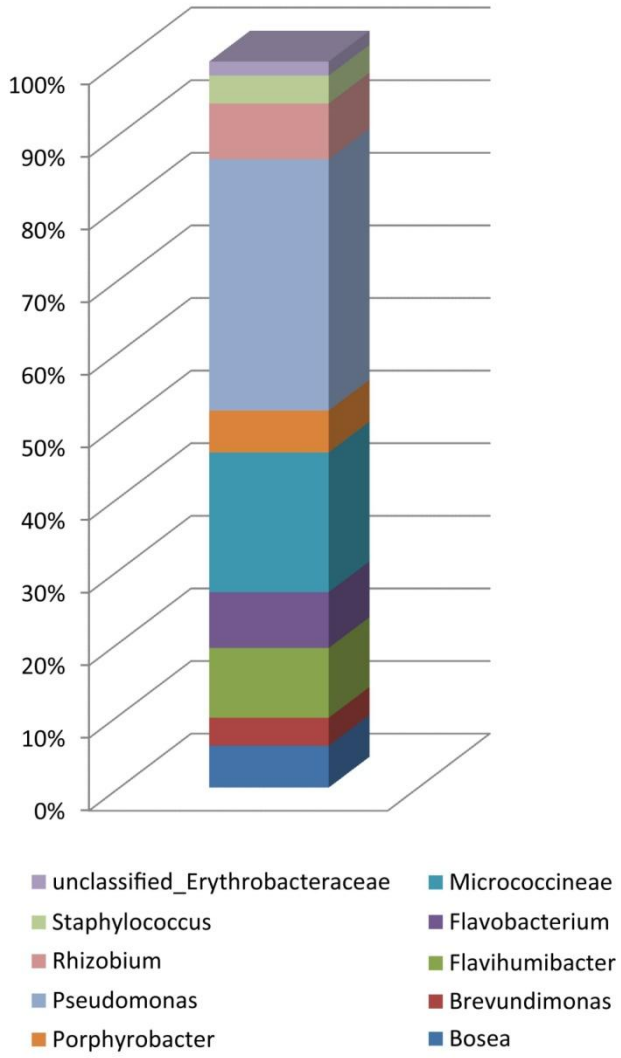

FIG 4 Percent abundance of the 52 bacteria isolated from the algal community. Isolates were identified by sequencing the 16S rRNA gene, identifying the sequences using RDP and by classifying the isolates at the genus level. Data show percentages of isolates of that fall into the listed genera.

Supplementary Table 2. Cultivable bacteria isolated from microalgae cultures.

Strain	Closest match in RDP database	AHL production
RP1138	*Pseudomonas nitroreducens*; 0802	-
RP1139	*Pseudomonas* sp. USTB-04	-
RP1140	*Pseudomonas* sp. PASS-camb	-
RP1141	*Pseudomonas* sp. PASS-camb	-
RP1142	*Pseudomonas nitroreducens*; 0802	+
RP1143	*Brevundimonas diminuta*; DSM 1635	-
RP1144	*Microbacterium maritypicum* (T); type strain: DSM 12512	-
RP1145	uncultured bacterium; sls1369	-
RP1146	*Rhizobium radiobacter*; UP-3	+
RP1147	*Micrococcus luteus*; Ballarat	-
RP1148	*Pseudomonas* sp. PASS-camb	-
RP1149	*Pseudomonas pseudoalcaligenes*; KF710	-
RP1150	*Pseudomonas* sp. LOB-2	-
RP1151	*Pseudomonas* sp. PASS-camb	-
RP1152	*Pseudomonas* sp. PASS-camb	-
RP1153	*Pseudomonas alcaliphila*; D11	-
RP1154	*Pseudomonas* sp. PASS-camb	-
RP1155	uncultured bacterium; sls1369	-
RP1156	*Brevundimonas diminuta*; DSM 1635	-
RP1157	uncultured bacterium; sls1369	-
RP1158	*Janibacter* sp. BQN4P5-02d	-
RP1159	*Micrococcus* luteus; Ballarat	-
RP1160	*Pseudomonas luteola*; Marseille	+
RP1161	*Bosea* sp. STM 358	-
RP1162	uncultured alpha proteobacterium; Alchichica_AQ2_1_1B_61	-
RP1163	*Rhizobium radiobacter*; UP-3	+
RP1164	*Rhizobium radiobacter*; UP-3	+
RP1165	uncultured bacterium; sls1369	-
RP1166	*Pseudomonas nitroreducens*; 0802	-
RP1167	uncultured alpha *proteobacterium*; Alchichica_AQ2_1_1B_61	-
RP1168	*Micrococcus luteus*; Ballarat	-
RP1169	*Micrococcus luteus*; Ballarat	-
RP1170	*Rhizobium radiobacter*; UP-3	+

RP1171	*Micrococcus luteus*; Ballarat	-
RP1172	uncultured bacterium; ncd522d11c1	-
RP1173	uncultured bacterium; sls1369	-
RP1174	*Pseudomonas nitroreducens*; 0802	-
RP1175	*Pseudomonas* sp. LOB-2	-
RP1176	*Pseudomonas* sp. PASS-camb	-
RP1177	*Staphylococcus epidermidis*; BBEB-03d	-
RP1178	*Microbacterium oxydans*; WR53	-
RP1179	*Porphyrobacter* sp. J3-AN66	-
RP1180	uncultured bacterium; 5-67	-
RP1181	*Erythromicrobium ramosum* (T); DSM 8510	-
RP1182	*Pseudomonas* sp. PASS-camb	-
RP1183	*Microbacterium maritypicum* (T); type strain: DSM 12512	-
RP1184	*Porphyrobacter donghaensis* (T); SW-132	+
RP1185	*Flavobacterium lindanitolerans* (T); IP10	-
RP1186	*Flavobacterium lindanitolerans* (T); IP10	-
RP1187	*Flavobacterium lindanitolerans* (T); IP10	-
RP1188	*Staphylococcus* sp.; 1F-09	-
RP1189	*Flavobacterium lindanitolerans* (T); IP10	-

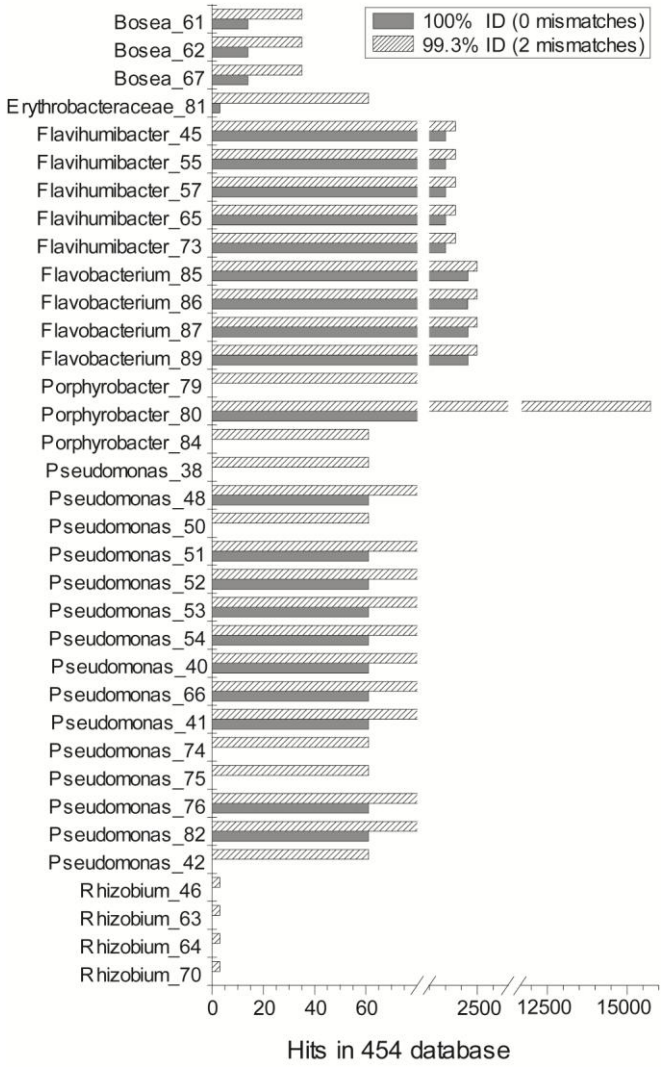

FIG 5 Comparison of cultured isolates to the culture independent 454 sequence data set. Putative isolate classification and strain ID are shown on the y-axis where the last two numbers correspond to the last two digits in the strain ID format of RP11xx. The comparison was done by doing a BLAST search with 16S rRNA gene sequence of each isolate against the 454 dataset. Hits at 99.3% (hatched bars) and 100% (solid bars) are shown.

Observation of community stability over time. Microbial communities can often be dynamic with some community members consistently present while others are only transiently detected. A stable association with the alga suggests an essential role in the community while a transient member is less likely to be essential. To gain insight into the dynamics of the bacterial community, I used 16S DGGE to compare fingerprints of samples that were separated by 56 weeks of culturing. Algal cultures were continuously subcultured every two weeks between the compared samples. This represents a separation of about 400 algal generations. The initial (t = 0) DNA sample was the same sample shown in Fig. 2, where bands had been cut and identified. DNA from the t = 0 and t = 56 weeks cultures was compared by 16S DGGE on the same gel so the bands could be directly compared. This allowed identification of the organisms that are likely changing between the two time points. The results shown in Fig. 6 demonstrate that some organisms are more stably associated with the algae and some represent transient members of the community. Overall the second time point has more bands than the first one, indicating the presence of more bacterial phylotypes. The *Flavihumibacter* and *Porphyrobacter* bands are present in both time points. Bands six and seven, which represent organisms from the *Alphaproteobacteria* class and the *Acetobacteraceae* family respectively, are also conserved.

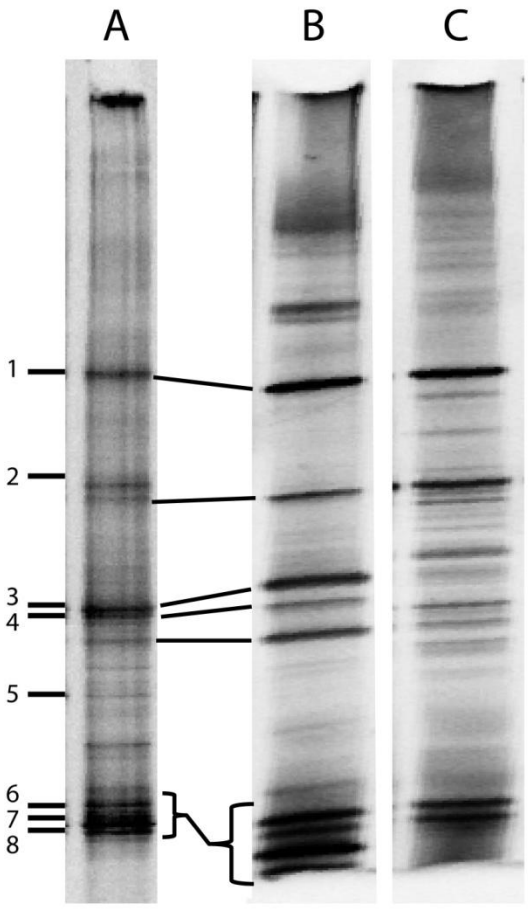

FIG 6 DGGE of bacterial 16S rRNA gene fragments from the same algal culture separated by 13 months of subculturing (~400 algal generations). The same DNA sample shown in Fig. 2 as the air sample is used here (lane A and B). Numbering represents the bands that were cut and identified from this sample. Lane C is the sample after 13 months.

Determination of the effect of pure isolates on algal growth. With some of the bacterial community members isolated into pure culture, I was interested in trying to determine what roles these isolates were playing within the community associated with the algae. An ideal experiment would separate the effect of each isolate by adding back individual isolates one at a time to axenic algae cultures. I was unable to obtain axenic HTB1 cultures despite extensive efforts including cell sorting, dilution to extinction, different antibiotic treatments alone and in combination, mild bleach treatment and UV treatments. These methods were tried with BG11 medium alone and with the addition of vitamins. All treatments either resulted in failure to remove the bacteria or death of the algae. These results provide circumstantial evidence that the bacteria may be important for algal survival. I was able to achieve a consistent 10-fold reduction of the unassociated microbial community by differential centrifugation. I decided to investigate the effect of adding the bacteria back to cultures with 10-fold reduced bacterial populations. Specifically, I asked whether addition of the bacteria would increase, decrease or have no effect on the final density of the algal culture. Though less direct than working with axenic cultures, I speculated that if a bacterium was beneficial for algal growth, for example by providing an unknown cofactor, then addition of that bacterium to an algal culture depleted of bacteria could provide a growth benefit. Alternatively, if a bacterium was inhibitory to algal growth then addition of this bacterium should result in a decrease in growth. The effect of all of the isolates on final algal density was tested by adding them individually at ratios of bacteria to algae of 10:1, 1:1 and 1:10. These ratios were chosen because flow cytometry data showed that the free bacterial population can be up to ten times higher than the algal population. The experiments were carried out in 96-well

plates to achieve higher numbers of replicates. The algal cultures were also grown at 15% CO_2 to replicate what is found in the photo-bioreactors. Flue gas was not used due to the variability of the gas which would introduce significant variability into the growth of the algae. The experiment was repeated on three separate occasions. The effect of adding bacteria back to the algal cultures was not consistent in these different experiments with the exception of two isolates, RP1178 and RP1181, which showed minor reductions in final algal density of 20-25%. For most of the isolates an effect that was observed in one experiment was not reproducible in the next trial.

Screening for quorum sensing activity. From fluorescence microscopy observations it is clear that the bacteria form dense communities in close association with the algal cells. Within this type of environment quorum sensing often plays a role in coordinating the phenotypes of individual bacteria within a species. To determine if quorum sensing is active within the algal cultures we screened all of the bacterial isolates for the production of quorum sensing compounds, specifically acyl-homoserine lactones (AHLs), and we also screened spent algal culture media for AHLs. The isolate screening results are shown in Table S2 and show that 13.5% (7/52) isolates were positive for AHL production. Algal cultures were positive for AHLs, except in one case where negative results were observed. This negative result was likely due to the growth phase of the algal culture though further work is needed to confirm this. TLC in combination with the AHL bioassay was used to characterize the number and general hydrophobic character of the produced AHLs. In the HTB1 culture there was one major species of AHL and a second minor species which is more hydrophobic (Fig. S2). Strains RP1142 and RP1170 produced similar patterns of AHLs and were identified as being most closely related to

Pseudomonas nitroreducens and *Rhizobium radiobacter* respectively. Both RP1160 and RP1184 produced three species of AHLs. Of the AHL positive isolates, three proved recalcitrant to TLC bioassay characterization. When extracts from RP1146, RP1163, RP1164 were assayed the entire overlay layer consistently turned blue, and these extracts are therefore not shown in Fig. S2. Quorum sensing can control the formation of aggregates by bacteria in pure culture as in the well-studied strain *Burkholderia thailandensis* (107). Several of the AHL-positive isolates from the algal culture formed aggregates in pure culture (Fig. S3). I hypothesize that quorum sensing may control the formation of the large algal bacterial aggregates that are readily observed in HTB1 cultures which has important implications for algal biofuels.

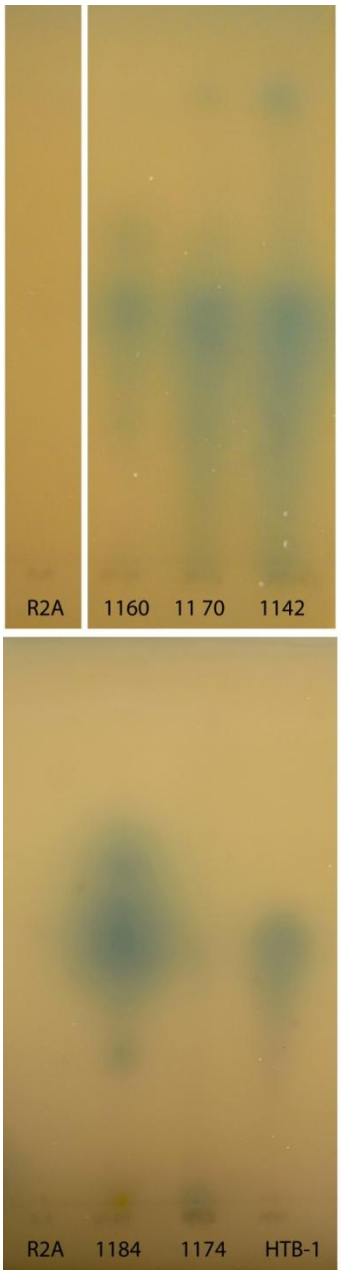

Fig S2 AHL reporter overlay assay showing the number of AHL compounds produced by different bacterial isolates and in the HTB1 culture. R2A is the media control..

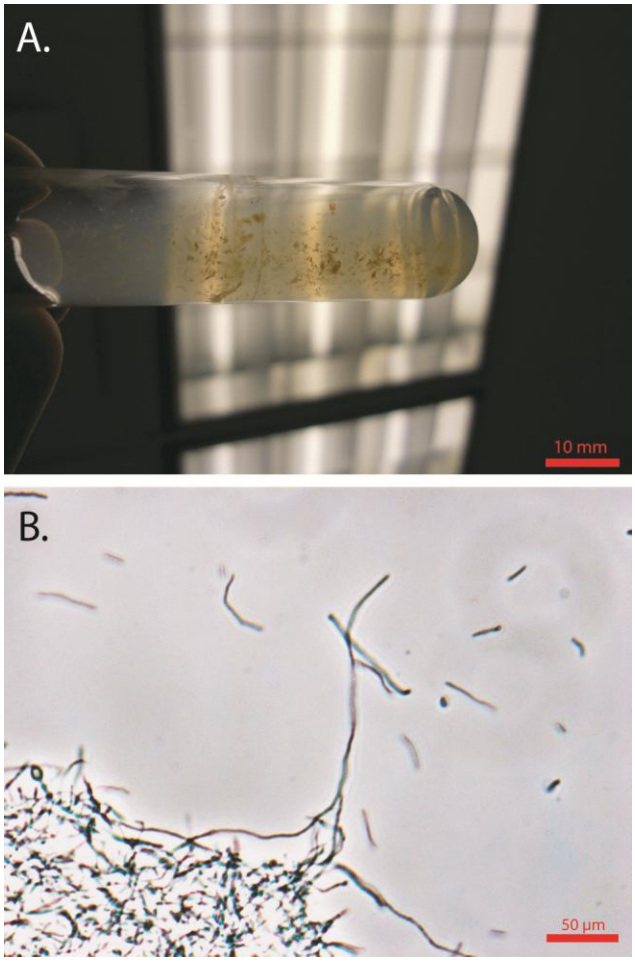

FIG S3 Aggregate formation phenotype in isolate RP1184. (A) Formation of aggregates in pure culture upon reaching stationary phase. (B) Phase contrast microscopy of RP1184 aggregates at 40x magnification.

DISCUSSION

In this study, I set out to describe the microbial community associated with the alga *Scenedesmus* sp. HTB1 and determine how this community changes when exposed to different atmospheric conditions. Most research in the field of algal biofuels focuses on finding productive algal strains and efficient systems to grow algae. Often these systems are designed to keep algal cultures axenic. However, at the production scales required to produce meaningful quantities of fuel, full exclusion of microbes is almost impossible. Thus, I propose that understanding the microbial community associated with healthy, growing algal cultures could lead to the development of an algal probiotic that could improve growth and stability of algal cultures.

As a first step, I determined the ratio of the algae *Scenedesmus* sp. HTB1 to free-living bacteria and found that cultures regularly had one to ten free-living bacterial cells for every algal cell present. I obtained similar results with flow cytometry and visually inspection of the cultures with fluorescence microscopy. Bacteria were also found attached to the algal cell surface, which suggests an intimate association between these community members. The exact role of the bacteria is currently unknown, but the observation that algal cultures continue to grow well in the presence of these bacteria indicates they are unlikely to be algicidal pathogens. An excellent review by Geng et al. describes several potential types of interactions between algal and bacterial cells (108). Bacteria are known to synthesize vitamin B_{12} which often is essential for algal growth but cannot be synthesized by about 50% of known algae and must be obtained from bacteria (79). Bacterial siderophores have also been cited as a means of providing trace metals to the algal host by bacterial symbionts. The algal host, on the other hand, often provides

carbon and energy rich photosynthate which the associated bacteria utilize (108). In the case of *Scenedesmus* sp. HTB1 I do not yet know which if any of these interactions are involved in the relationship between the algal and bacterial cells, though circumstantial evidence from a failure to obtain axenic cultures suggests the bacteria may play a key role in the growth of HTB1.

To begin to understand what roles the microbial community may play, I set out to characterize the microbial community using molecular and culture-based methods under conditions that would be expected to occur in biofuel production. Similar to other reported studies, I found relatively few bacterial groups to be associated with the algal culture. I observed 18-33 OTUs at 3% difference, which is similar to what was observed by Krohn-Molt *et al.* (92). The *Proteobacteria* and *Bacteroidetes* phyla were the dominant groups in the 454 dataset which is similar to previous reports on the bacterial communities associated with freshwater algae in photobioreactors (89, 91, 92). These results suggest that the community structure of the algae studied so far is rather simple and involves similar groups of bacteria. Within our study, the dominant sequences in the 454 data set were classified as *Porphyrobacter* spp.. This group was also detected as a major band on DGGE gels (band 3) and represented about 4% of the cultured isolates. The *Porphyrobacter* DGGE band was also present in DNA purified from the algae culture after more than a year of subculturing. Together these data suggest that porphyrobacters are a present in significant numbers in the HTB1 algal culture. *Porphyrobacter* spp. belong to the *Alphaproteobacteria clade* and are known for aerobic anoxygenic phototrophy which can be used to generate ATP from light energy. This feature would be useful to an organism living in a well-illuminated environment such as

the photobioreactor where *Scenedesmus* sp. HTB1 is cultured. At a high density, these organisms may even compete for light with HTB1 resulting in decreased algal growth. *Porphyrobacter* strains have also been implicated in the aggregation of *Microcystis aeruginosa* blooms in natural waters (109). *Flavobacteriaceae* strains, which are abundant in HTB1 cultures, have also been associated with *Microcystis* aggregates (109). These results suggest the aggregates found in HTB1 cultures may be due to the presence of *Porphyrobacter* and *Flavobacteriaceae* strains, though further work is needed to test this hypothesis.

I observed changes in bacterial community membership and relative abundance within algal cultures grown in air and flue gas. In general, flue gas samples contained a higher diversity of bacterial OTUs than samples from algal cultures grown in air. The most dramatic difference between the two treatments was the change in percent abundance of bacteria within the *Porphyrobacter* group. In the air samples this group was dominant and made up nearly 85% of all of the sequences compared to 56% in the flue gas samples. This suggests either the flue gas inhibits bacteria within this group or that it is stimulating the growth of other groups such as the *Chitinophagaceae*, *Flavobacterium* and *Devosia* whose abundance within the population increased in the presence of flue gas. If the *Porphyrobacters* are competing for light with the algae then these results suggest that using flue gas may lessen their impact. However, the 454 data are not absolute counts but relative percentages, meaning that it is possible that the actual concentration of *Porphyrobacters* may not have changed, but instead the concentration of other cell types may have simply increased in the presence of flue gas. Further work would be necessary to quantitate these changes in absolute terms.

Bacterial communities can be dynamic and change in community membership and abundance over time. To begin to understand if the community I characterized was stably associated with the HTB1 algal culture, I performed DGGE on the community more than a year after the initial characterization. I found that some members of the community were still present while others were no longer detected. The bands that were conserved were identified as belonging to the *Porphyrobacter, Flavihumibacter, Alphaproteobacteria* and *Acetobacteraceae* lineages. These results are far from defining the core microbial community associated with HTB1, though they do provide some initial evidence of which members of the community are more stable.

Often when doing molecular and culture based analyses, the bacteria that are identified by molecular methods not overlap well with those identified by culture based methods (110). In this study, I was fortunate that several of the major members of the bacterial community were identified by both molecular methods and in the culture collection. Ideally, I would like to test the effects of each isolate on algal growth in the absence of other bacteria, however despite many attempts I was not able to get viable and axenic cultures of *Scenedesmus* sp. HTB1. I was able to deplete the free bacterial community by about 10-fold. I hypothesized that if some of the isolated bacteria provide vitamins or other growth-promoting factors to the algae then I should still be able to see an effect on growth upon adding these bacteria back relative to bacteria-depleted controls. Conversely, growth inhibition may occur if the overabundance of a particular isolate detrimentally disrupted the bacterial community. While I did observe statistically significant effects in individual trials, these effects generally were not reproducible upon subsequent replication of the experiments. This occurred even when using a relatively

high number of replicates and was somewhat surprising. Perhaps the most likely explanation for this result is that the bacterial community was not altered sufficiently by depletion of the bacteria to see any reproducible effect of adding back isolates. These negative data may also be explained by growth variability of the parent culture used in each trial. The average peak density of individual control trials ranged from 122 to 178 relative fluorescence units with a mean of 146.7 and standard error of 18.2 relative fluorescence units over eight independent trials. This variability may be responsible for masking minor effects caused by the addition of the bacterial isolates. While the lack of a major effect upon adding back the bacterial isolates did not yield a direct positive result, it does suggest the algal/bacterial community is somewhat resistant to disruption. In the bacterial "add-back" experiments, individual isolates were added at 10 times the algal cell concentration. However, in no case did this result in a large disruption of growth. In future research it would be interesting to compare the effect of addition of algicidal bacteria to algal cultures with and without their associated microbial community to see if the community affords any protection from invasion by harmful bacteria.

Maintenance of the bacterial community and specifically individual bacterial species suggests there is a functional link between the microalga and some members of the bacterial community. By microscopy I see that some of the bacteria live at the cell surface or within large aggregates that encompass the algae cells. When bacterial cells live in close proximity there is the opportunity for cell-cell signaling. Therefore, I screened our isolates for production of AHL signaling molecules. I found 13.5% (7/52) of our isolates were positive for AHL production. AHLs are known to regulate key phenotypes in environmental bacteria (111). One readily apparent phenotype in both the

HTB1 algal cultures and in the pure cultures of the isolated bacteria was the formation of aggregates in stationary phase cultures. Regulation of aggregation by quorum sensing has been described in the literature (107). I speculate that the formation of aggregates by the bacteria associated with HTB1 may be beneficial to the bacteria by trapping more algal cells into an aggregate and thus providing exclusive access to photosynthetic products produced by the algae. If the bacteria are reciprocally providing vitamins or trace metals to the algae then this aggregation phenotype may mutually benefit both algae and bacteria at least initially. The formation of aggregates is well known to those who culture algae and in general aggregates are undesirable because they do not stay suspended in the water column and remove algae from the photic zone. The formation of aggregates can be useful when it is time to harvest microalgae because aggregates are easier to separate from the water than well-suspended single cells. If further work shows the formation of aggregates is indeed tied to the production of AHLs, then this property could be used to control the formation of aggregates. Aggregation control could be achieved by modulating the community members or through the addition of unpurified AHLs to the algal culture medium.

Algae are never found in isolated, pure cultures in nature and often cannot survive without their bacterial symbionts. The recent surge in interest in algal biofuels has prompted research into many areas of algal biofuel production; however, little is known about the roles of the bacterial communities associated with the algae. A better understanding of the structure, stability and function of these communities may provide an inexpensive route to higher algal biomass productivity and increased culture stability.

Appendix 2. Merging metabolism and power: development of a novel photobioelectric device driven by photosynthesis and respiration

Abstract:

Generation of renewable energy is one of the grand challenges facing our society. I present a new bio-electric technology driven by chemical gradients generated by photosynthesis and respiration. The system does not require pure cultures nor particular species as it works with the core metabolic principles that define phototrophs and heterotrophs. The biology is interfaced with electrochemistry with an alkaline aluminum oxide cell design. In field trials I show the system is robust and can work with an undefined natural microbial community. Power generated is light and photosynthesis dependent. It achieved a peak power output of 33 watts/m^2 electrode. The design is simple, low cost and works with the biological processes driving the system by removing waste products that can impede growth. This system is a new class of bio-electric device and may have practical implications for algal biofuel production and powering remote sensing devices.

Introduction

The search for renewable energy sources has renewed interest in finding ways to use biological systems to generate electrical energy. Specifically there is an interest in systems that use biology to convert light into electrical energy as way to use the advantages of biology to harvest a sustainable energy source. These devices are collectively known as photo-bioelectric systems. In this study I aim to develop a new photo-bioelectric system through the combination of several well-known technologies and widely conserved biological phenomena. The system is distinct from a microbial fuel cell (MFC), as it uses an aluminum oxide cell design to interface phototrophic and heterotrophic metabolisms with power production.

Many photo-bioelectric systems are modeled on microbial fuel cells and have been described (112, 113). A MFC has microbes associated with the anode oxidizing organic compounds under normally anaerobic conditions, using the anode as the terminal electron acceptor (114). Electrons are shuttled to a platinum cathode where they combine with O_2 and H^+, yielding water (114). In the closest related class of photo-MFCs, the MFC is fed organic carbon from algae (115-117) or plant root exudates (118-123). Energy stored by photosynthesis is liberated when the organic matter is oxidized by bacteria. In another design, algae are added to the cathodic side of the MFC, supplying O_2 in the electron consuming reaction (116). In both cases electrons are donated from electron transfer chains to the anode. Cyanobacteria can also donate electrons to the anode during respiration of cellular carbon reserves in dark phases with redox shuttles such as HNQ (124-126). The need for a redox shuttle to move electrons from algae to anode limits this type of cell to closed systems. Recently it was shown pure cultures of

cyanobacteria could directly donate electrons to the anode (127). The authors postulate these organisms donate electrons via nanowires when CO_2 is limiting (127). It is also possible to extract electrons from photosynthesis by using hydrogen as an intermediary (113). Hydrogen is produced by hydrogenases or nitrogenases and then oxidized at a platinum electrode, recovering the electrons (113). Ryu et al. take a different approach by inserting nano-electrodes directly into photosynthetic membranes of alga, extracting electrons using an overvoltage (128). This eliminates light to chemical energy conversion losses, theoretically increasing efficiency, but consumes energy needed by the organism for growth and sustained survival.

In this study I present a system that is distinct from established photo-bioelectric systems. It is designed around the normal processes that occur when phototrophs and heterotrophs grow and replicate. Phototrophs and heterotrophs pump carbon through ecosystems, shifting inorganic carbon equilibrium reactions and in the process affecting pH. Algae alter pH by removing CO_2 and HCO_3^-, which shift the equilibrium and produces hydroxide ions, resulting in pH values as high as 11 (39). Respiration oxidizes organic compounds to CO_2 and organic acids, reducing pH. The system extracts energy from acids and bases which are waste products of heterotrophic and phototrophic metabolism respectively. These products of metabolism are interfaced with an electrical system by using an aluminum fuel cell under the alkaline conditions. In this type of fuel cell, water and base react with aluminum to form aluminum oxides and electrons (129). In an isolated system the electrons typically reduce hydrogen ions resulting in hydrogen gas, however they can also be drawn into an external circuit with an applied voltage.

The goal of this study is to demonstrate a proof of principle of exploiting the chemical gradient that occurs when photosynthesis and respiration are separated. The mechanistic data presented focus on the algal side of the cell. I show power production in the cell is pH dependent in the absence of algae. Power production is light and photosynthesis dependent when the algae are present. Finally a cell was deployed in the field to test the robustness of the design outside of the laboratory.

Materials and Methods:

Algal cultivation: *Nannochloropsis oceanica* IMET1 was grown in f/2 medium (35) with a salinity of 20 ppt. The alga was grown in photobioreactors which consisted of 500 ml borosilicate bottles with three ports in the cap. Two ports were connected to tubes leading to the bottom of the bottle. Air was pumped into these two ports through 0.22 µm syringe filters at a rate of 5 L/min to provide constant mixing and to provide CO_2 present in the air. The third port was used as a vent. Light was provided by 215 watt Phillips white fluorescent lights with a light intensity of 275 µmol/m^2/s at the front of the bottle. Cultures were grown with a light/dark photoperiod of 14/10 at 25°C. Algae were subcultured weekly using an inoculating volume of 10%. *Scenedesmus* sp. HTB1 was grown in a photobioreactor as described above and was grown in BG11 medium (130). *Microcystis aeruginosa* LE-3 was grown in BG11 medium in 1 L Erlenmeyer flasks at 32°C with constant shaking. Light was provided with fluorescent lamps at an intensity of 100 µmol/m^2/s on a 14/10 day/night cycle.

Test cell design: The test cell was a sandwich type cell, whose structure was made of two end pieces of acrylic (100 x 90 x 13 mm each) and at least two sections of clear PVC pipe (88 mm outer diameter, 6 mm wall thickness). Unless otherwise noted two 30 mm long lengths of pipe composed the standard test cell. The cells were held together by compression from four bolts in the corners of the cell. Circular gaskets made of three layers of parafilm were placed between the junctions of each component to form a water-tight seal upon compression. A single circle of Whatman 3 filter paper (Frederick, MD) was used as the membrane separating the two sides of the cell. The Al electrode in the cell was derived from Al foil (98.5% Al) and was routinely 57 cm^2. The platinum electrode was Pt wire of 0.3 mm diameter and an exposed surface area of 4.56 cm^2. The power curve of the cell was performed with *N. oceanica* IMET1 at pH 10 on the high pH side and f/2 medium with a pH of 7 on the low pH side. Voltage was measured at set resistances between 5 – 10,000 Ω.

Salt/agar cell design: The salt agar cell is a molded cell produced by casting wells into agar using 400 ml serum bottles to form the wells. Molten agar with 5 M NaCl was poured into a plastic bin that contained the bottles separated by 2 cm. Once the agar solidified the bottles were removed leaving two separate wells. In one well *N. oceanica* IMET1 culture at pH 10.4 was added and into the other well ASW at pH 4 was added. An Al foil electrode was used on the high pH side with a submerged area of 252 cm^2 and a Pt wire electrode was inserted in the low pH side of the electrode with an area of 4.26 cm^2. A power curve was done to determine the optimal load to measure power output. Peak power output was measured at 500 ohms.

Outdoor cell design: The larger outdoor cell was made of concentric cylinders with different materials composing each cylinder. The central cylinder is structural and consists of PVC pipe (8.8 cm diameter, 42 cm length) capped with two plastic circles of 26 cm in diameter. Platinum cloth (Fuelcellstore.com) was used as the inner electrode and had a bulk area of 600 cm^2 of which 342 cm^2 (57%) was projected Pt surface area. This electrode was wrapped around the inner 88 mm diameter pipe. A secondary support with a diameter of 21.5 cm supported the paper membrane which was two layers of black poster board sealed tightly at the top and bottom of the cell. Together these formed the inner, low pH side, of the cell with a volume of approximately 12.7 L. The Al electrode was composed of Al screen wrapped around the paper membrane. The high pH side of the cell in this case was the body of water where the cell is deployed. The power curve for the cell was performed with pH 10.3 water on the outside of the cell and pH 7.8 water on the inside of the cell. Voltage was measured at set resistances between 0.2 – 10,000 Ω.

pH dependence experiment: The pH dependence of the cell was determined using the small test cell. In this experiment cell free media were used to allow more precise control of pH. The low pH side of the cell had pH 7 f/2 medium. The high pH side of the cell was set up as a flow-through system and was connected to a gradient maker that allowed pH to be precisely set by mixing high pH and low pH solutions of f/2 medium. The pH at the Al electrode was recorded every 60 seconds. Voltage from the cell was measured continuously across a 10K Ω resistor using the HOBO data logger.

Short term light/dark experiment: The smaller test cell was used for this experiment along with the circuit shown in Fig. S3. To increase the light absorption area algae were continuously pumped through the cell and a tubular type photobioreactor on top of a

fluorescent light box, giving the algae 400 cm^2 of surface area to absorb light at an average intensity of 117 μmol/m^2/s. This setup was light-proofed so only light from the light box reached the algae. Light and dark cycling was then controlled by turning the light box on and off with cycle lengths of four hours. The low pH side of the cell contained f/2 medium at pH 7. Two voltage channels were recorded on a HOBO U12 4-channel data logger (Onset Computer Corp., Bourne, MA). The first channel measures the voltage of the cell across a 10K Ω resistor and the second channel measures pH from an Orion Research pH meter using the voltage outputs on the meter. The voltage output from the pH meter was amplified using an Op-Amp circuit shown in Fig. S3 to ensure the signal was in the sensitivity range of the data logger. Voltage data was converted to pH using a standard curve generated from voltage outputs at known pH values. The grounds within the logger are tied together. To prevent interference between the cell voltage channel and the pH voltage channel an oscillator circuit was built so only one channel was being measured at any moment while the other was disconnected. It was necessary to electronically insulate the pH probe from the electrodes in the cells to prevent spurious pH readings. This was achieved by passing the algae through two drip insulators on either side of the electrode which broke any electrical connection between the pH electrode and the electrode in the cell while allowing continuous pH monitoring. Periodic samples were tested to confirm the pH values recorded reflected the pH values at the electrode.

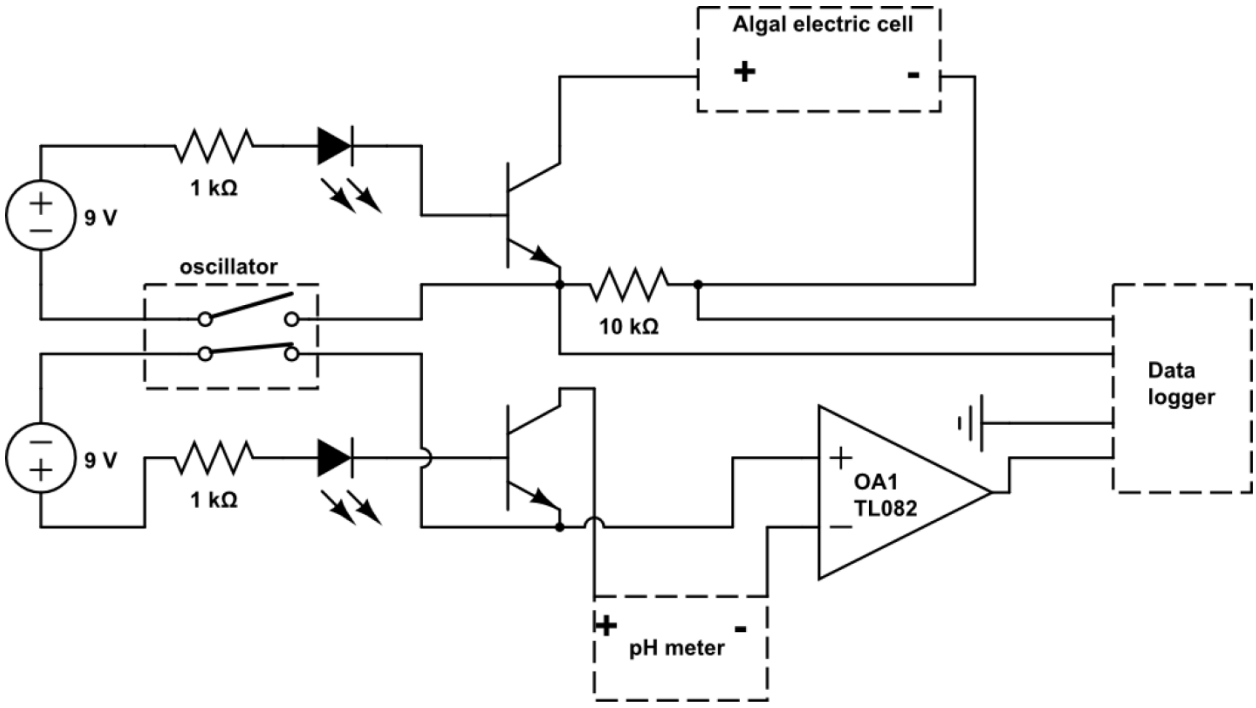

Figure S3. Diagram of the circuit used to measure pH and voltage continuously. Common grounding within the data logger requires the pH channel and the algal cell voltage channel to be alternately measured so they do not interfere with the measurement. In this circuit two 9 V sources run through an oscillator which alternately connects and disconnects each 9 V source for 30 seconds. When connected, the current activates an NPN transistor, which acts as an electronic switch, allowing the voltage from the cell to continue on to the data logger shown to the right. For pH measurement the transistor gates a low voltage output from the pH meter. This output continues on to an Op-Amp where the signal is amplified to be within the optimal voltage range of the data logger. Circuit diagram was drawn in circuitlab (www.circuitlab.com).

Long term light/dark experiment: The smaller test cell was used for this experiment. The cell was started with pH 10.4 algae on the high pH side and pH 7 f/2 medium on the low pH side. The cell was incubated in a photoperiod room with a light/dark cycle of 14/10. The algal side of the cell was illuminated with Phillips white fluorescent lights with a light intensity of 275 µmol/m^2/s. Voltage was measured continuously with a HOBO data logger over a 5K Ω resistor.

Inhibition of photosynthesis: The DCMU concentration needed to inhibit *Nannochloropsis* was determined by empirical testing to be 100 µM. This concentration was used for all experiments. Fresh 100 mM stocks of DCMU (Sigma) were dissolved in acetone prior to running each experiment. The small test cell was used and voltage was measured continuously with the HOBO data logger across a 10K Ω resistor. Experiments were done with 2 L batches of algae in polypropylene bags placed directly on a light box to maximize light exposure. The illuminated surface area was 1288 cm^2 with an average light intensity of 117 µmol/m^2/s. Voltage and pH were measured from a 100 ml aliquot of algae, sampled every 30 minutes. A fresh 100 ml aliquot of f/2 media was used at each of these time point. Between time points the cell was washed twice with pH 2 dH_2O to remove remaining algae and any Al reaction end products. DCMU was added after the midpoint of the timecourse to a final concentration of 100 µM. Acetone only was added as the control.

Electrode ionization: The small test cell was used in this experiment. Algae with pH 10.3 were added to the high pH side of the cell and f/2 medium with a pH of 7 was added to the low pH side of the cell. The two electrodes were connected directly with copper

wire with no additional resistance to facilitate electron transfer. The cell was operated continuously for ten days and the electrode was observed.

Field test of algal electric cell: The testing site was at latitude and longitude of 38.518462, -75.964653. The site is on public land and no samples were removed from the site. No permits were required to access the site. This site was chosen because periodic algal blooms occur where pH values can reach over pH 10, representing ideal conditions for the algal electric cell being tested. The cell was installed at fixed height on a dock. An aliquot of water from the pond was adjusted to pH 7 with 5 M HCl and used as the starting catholyte inside of the cell. Voltage was measured across a fixed resistance of 50 Ω every 30 seconds using the voltage input of the HOBO data logger mentioned above starting on 22nd of August to the 5th of September, 2012. Ohm's law was used to convert resistance and voltage data to power in watts. Tidal data were collected from a local NOAA tide gauge (station ID: 8571892) in Cambridge, MD.

Results and Discussion

The system is shown in Figure 1A with the proposed mechanism of action. By separating heterotrophic and phototrophic metabolism a pH gradient can be generated. This pH gradient can be used to generate power. Importantly, the presented system is effectively a photosynthesis dependent battery in the current stage of development due to the use of aluminum (Al) as the anode and does not yet constitute a standalone energy generation system. Substitution of the Al electrode with a catalyst would make it a stand-alone biologically driven power source. The cell has an algae-filled high pH side with an

Al electrode and low pH side with a platinum electrode, separated by a paper membrane (Fig. 1B). The Al reacts with basic water produced by algal carbon fixation. Al is ionized, leaving electrons on the anode which pass through an external circuit, combining with hydrogen ions at the platinum electrode producing H_2 (shown below).

$$2Al_{(s)} + 8OH^-_{(aq)} \longrightarrow 2Al(OH)_4^-{}_{(aq)} + 6e^-$$

$$6H^+_{(aq)} + 6e^- \longrightarrow 3H_{2(g)}$$

Initially I show the cell is responsive to pH by increasing pH stepwise on the basic side of the cell in the absence of algae while voltage was monitored. The data confirm increased pH results in increased voltage (Fig. 2A). Results were obtained in cell-free media, showing living cells are not necessary for pH-dependent power production. Support for the proposed Al reaction was observed by comparing electrodes before and after ten days of operation. Electrode ionization was observed near the air-liquid interface (Fig. S1). These data support hydroxide dependent production of current through the oxidation of Al. The exact mechanism of Al oxidation in our system is unknown and may proceed by several parallel reactions (129). While the intermediate steps in Al oxidation are important, here I focus on developing a process linking the biology of algae to an electron producing reaction.

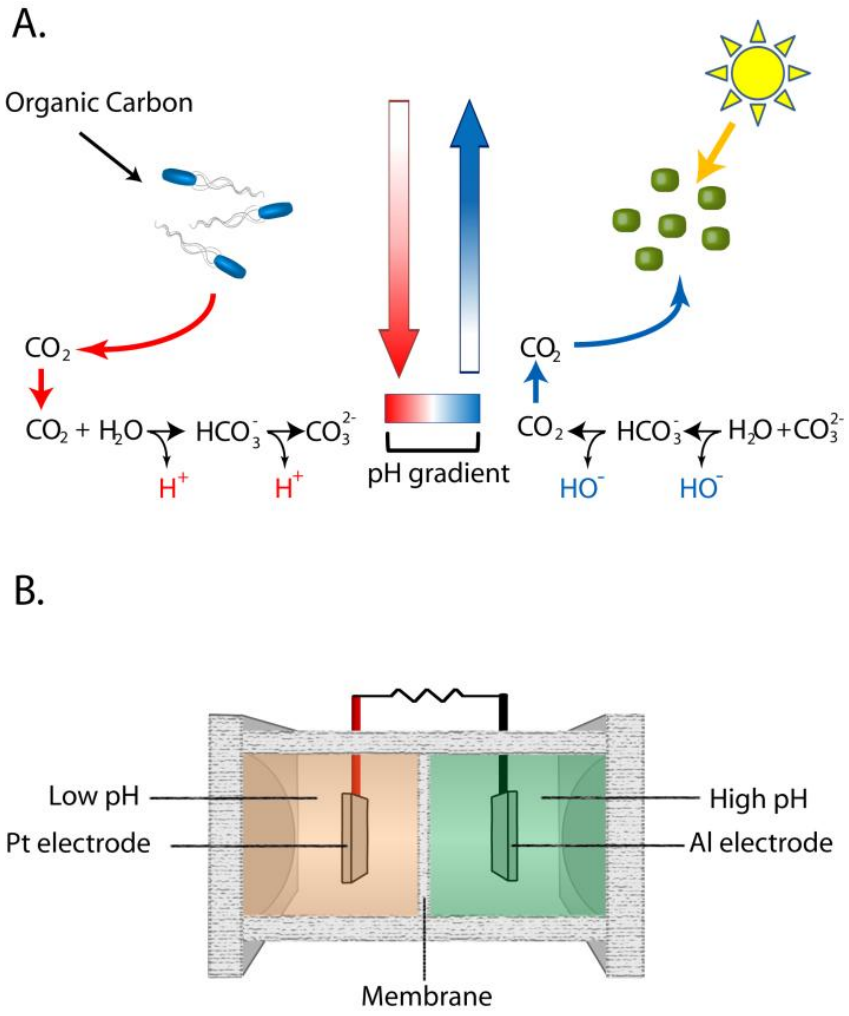

Figure 1. Principle and design of the algal electric cell. (A) Respiration decreases pH through the oxidation of organic compounds, generating CO_2 which shifts the inorganic carbon equilibrium and produces hydrogen ions. Photosynthesis increases pH by removing CO_2 and HCO_3^-, which shifts the inorganic carbon equilibrium and produces hydroxide ions, resulting in pH values as high as 11 [23]. Separation of photosynthesis and respiration results in a pH gradient which can be used to generate electricity. **(B)** Design of test cell.

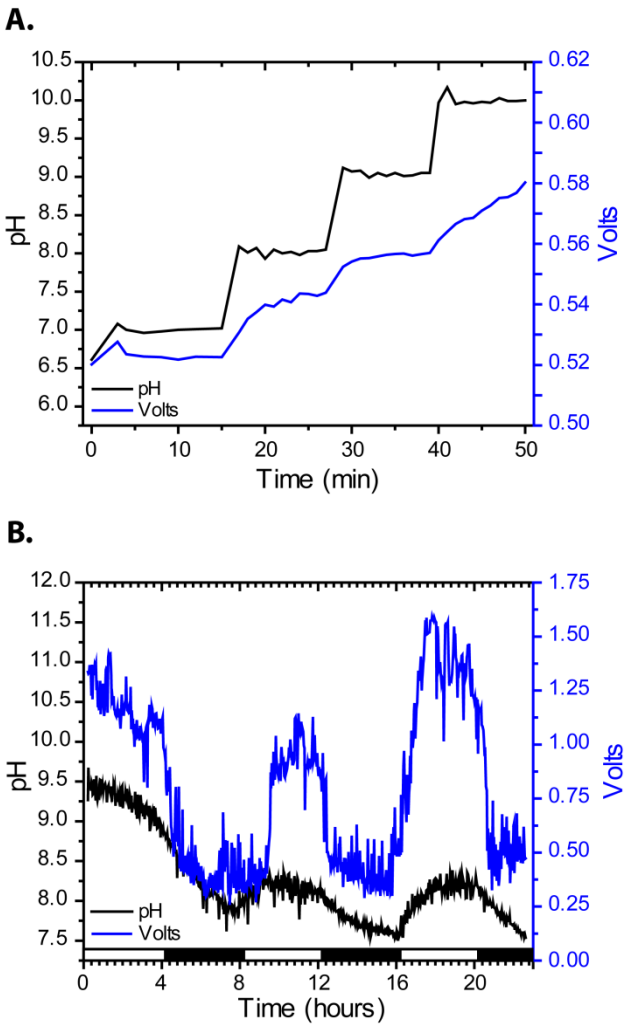

Figure 2. pH dependence of voltage and light dependence of pH and voltage. (A) Voltage is dependent on pH of the Al side of the cell. pH was adjusted stepwise in the absence of algal cells. pH was measured every minute and voltage was measured every ten seconds **(B)** Voltage and pH over light/dark cycles (white/black bar). Algal photosynthesis increases pH, increasing voltage. pH and voltage were each measured every 1.5 minutes for 24 hours. At 16 hours fresh f/2 medium was added to compensate for evaporative losses, resulting in slightly higher voltage at a lower pH due to more of the electrode being submerged. The light/dark data presented are from a single cell and are a representative dataset from four independent trials.

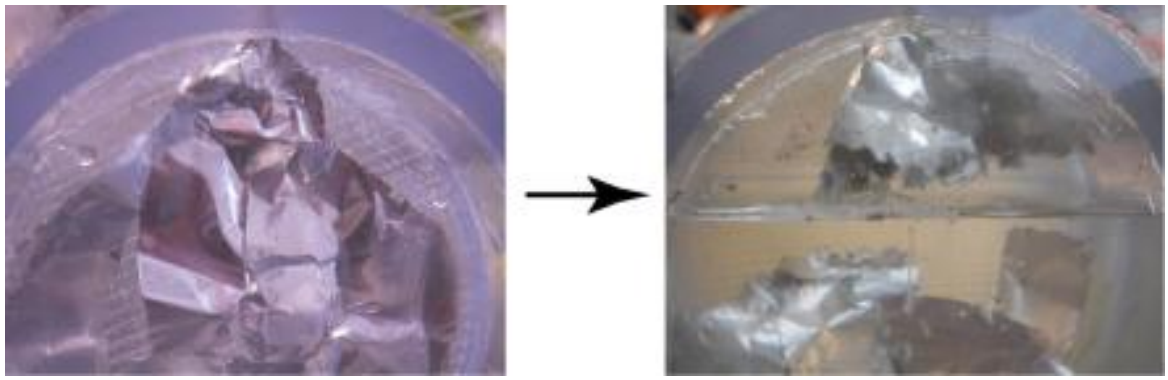

Figure S1. Ionization of the Al electrode, demonstrating solid Al metal is being dissolved. On the left is the original electrode and on the right is the same electrode after 10 days of operation. The electrode on the right has completely dissolved near the liquid interface and has small holes in the submerged portion of the electrode.

Optimal operating load was determined with a power curve, where current was measured at increasing external resistances (Fig. S2). Optimal resistance was 500 Ω, where 285 mW/m^2 Pt electrode was produced. Often in photo-bioelectric systems either algae or a bacterial intermediary must first colonize the electrode (113). In our system voltage is produced immediately upon submersion of the electrodes, showing colonization is not required, which is consistent with power generation being driven by the pH. In addition, different alga in different media with similar pH values produce similar voltages including *Microcystis aeruginosa* LE-3 (freshwater cyanobacterium), *Scenedesmus* sp. HTB1 (freshwater green alga) and *Nannochloropsis oceanica* IMET1 (marine alga).

I hypothesized production of hydroxide ions through the removal of inorganic carbon via photosynthesis drives power production. In our next set of experiments I tested if voltage is light dependent. Algae in the cell were passed through a series of light/dark cycles while voltage and pH were monitored. During light phases, pH and voltage increase (Fig. 2B). Photosynthesis likely causes the pH increase and leads to higher cell voltage. During dark phases, photosynthesis stops and voltage decreases as hydroxide is consumed in the reaction with Al. In a separate trial the light/dark dependence was tested and found to be stable over the two week course of the experiment (Fig. 3). These data show increases in voltage are light dependent and likely due to pH increases from photosynthesis. To confirm power output is dependent on photosynthesis I used DCMU (3-(3,4-dichlorophenyl)-1,1-dimethylure), a specific inhibitor of photosystem II. DCMU was added to cultures under constant illumination while voltage and pH were monitored.

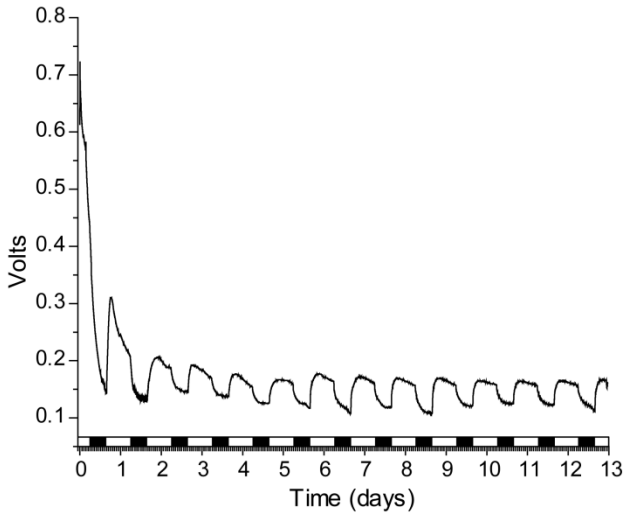

Figure 3. Change in voltage is light dependent. Algal electric cell with algae exposed to light (white) and dark (black) cycles for 13 days. Voltage increases when light falls on the algal electric cell, plateaus and then decreases in the dark

Upon addition of the inhibitor pH increase stopped, whereas the pH of the solvent control lacking DCMU continued to climb (Fig. 4A). Cell voltage resembles the pH curve, voltage increase stopped after addition of the inhibitor, while voltage continued to climb in the control (Fig. 4B). Voltage plateaued before pH in the control, potentially indicating inhibition by constraints on the cathodic reaction imposed by the size of the Pt electrode, or the internal resistance of the cell. The data show specific inhibition of photosynthesis results in lower pH and lower voltage, confirming voltage is light and photosynthesis dependent.

Next I was interested in testing the limits of this type of cell. I hypothesized power was limited by internal resistance; this was tested with a cell cast into 1.5% agar with 5 M NaCl. This setup produced a peak power output of 33 W/m^2 Pt electrode with a stable power output of 0.7 W/m^2 Pt. This peak power output is over 33 fold higher than the next highest photo-bioelectric cell (117) and nearly 6 fold higher than the highest bioelectric system (131). High power is possible due to liberation of stored energy in the Al electrode through reaction with algae-derived hydroxide. The Al electrode could be substituted with a catalyst to extract electrons from hydroxide ions such as a perovskite oxide (132). It should also be possible to increase power by decreasing the pH of the acidic side of the cell, though the focus of the current paper is on the algal side of the cell. The current device is useful for powering remote sensors in aquatic systems and for algal biofuel production to control pH and provide power for mixing ponds.

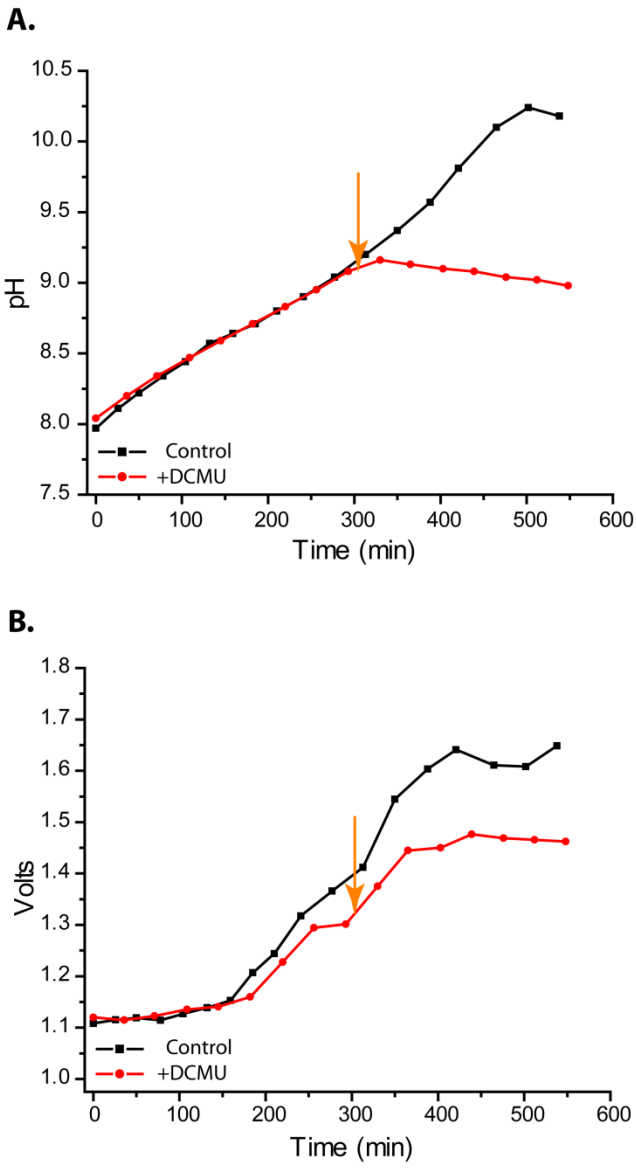

Figure 4. Voltage and pH are dependent on photosynthesis. Addition of the photosynthesis inhibitor DCMU (orange arrow) **(A)** inhibits pH increase, and **(B)** voltage increase. Control and inhibition experiments were carried out on separate algal stocks on separate days showing biological reproducibility of pH and voltage curves prior to addition of inhibitor. Data presented are from a single cell and are a representative dataset from three independent trials.

The mechanism of action suggests the cell is species neutral. The species neutral nature of the cell was tested with a larger version deployed in a Chesapeake Bay tributary. This cell incorporated the entire proposed design principle and is shown in Figure 5A. A power curve showed peak power output occurred at 50 Ω resistance (Fig. S2). Power was produced immediately upon submerging the cell at the site, where pH was 8.3. The cell interior maintained a lower pH than the surrounding water throughout the experiment. A maximum power output of 192 mW/m^2 Pt electrode was recorded shortly after start up with an average power output of 11 mW/m^2 Pt (Fig. 5B). Unlike the laboratory-scale test, the cell was affected by environmental factors including storms and tides. Power produced roughly follows the day/night cycle, deviations from this cycle correlate well with changes in tides. Changes in tides affect power output by altering the area of submerged Pt electrode. After the fourth day a storm moved over the site and stirred up sediment, correlating with a drop in power to 0.3–1 mW/m^2 Pt electrode (Fig. 5B). I speculate this was due to a pH decrease from inhibition of photosynthesis. After this period the cell recovered, and resumed power production. From these data I conclude the cell can successfully produces power with an undefined freshwater microbial community. The system I presented represents a novel class of photo-bioelectric cell, where photosynthesis and respiration are linked to electrical power production via known electrochemical reactions. This type of cell can generate high current densities and operate outside of the laboratory in a species neutral manner. Power production from different species is likely dependent on the rate at which algae removed inorganic carbon from water. This rate will differ based on the algal species present and the densities on those algae.

.

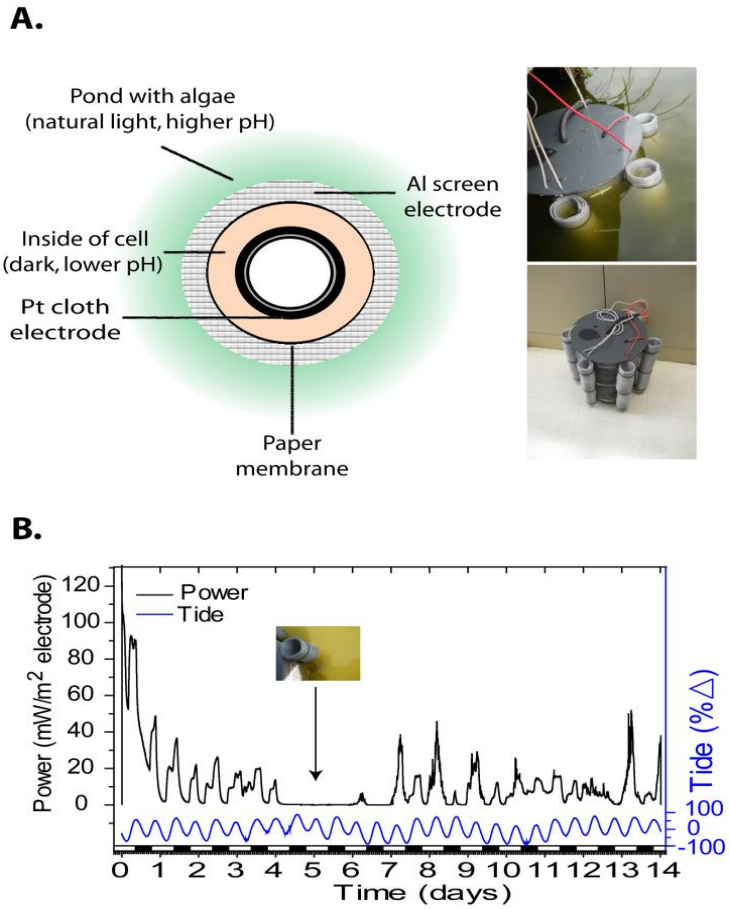

Figure 5. Design and field-testing of the outdoor photo-bioelectric cell. (A) Cutaway of the cell. Inside of the cell is water with the local biota which is kept in the dark, inhibiting photosynthesis while allowing respiration. Pt cloth electrode is wrapped around the center. Paper membrane separates the inside of the cell from the surrounding water. Al electrode is wrapped around the cell. **(B)** Power produced by the cell. Power is correlated with day/night cycle (white/black bar) and tides (blue). After day four a storm suspended sediment, likely inhibiting photosynthesis and power production. Voltage was measured every 30 seconds for two weeks over a 50 Ω resistance. Data presented are from a single cell deployed on-site.

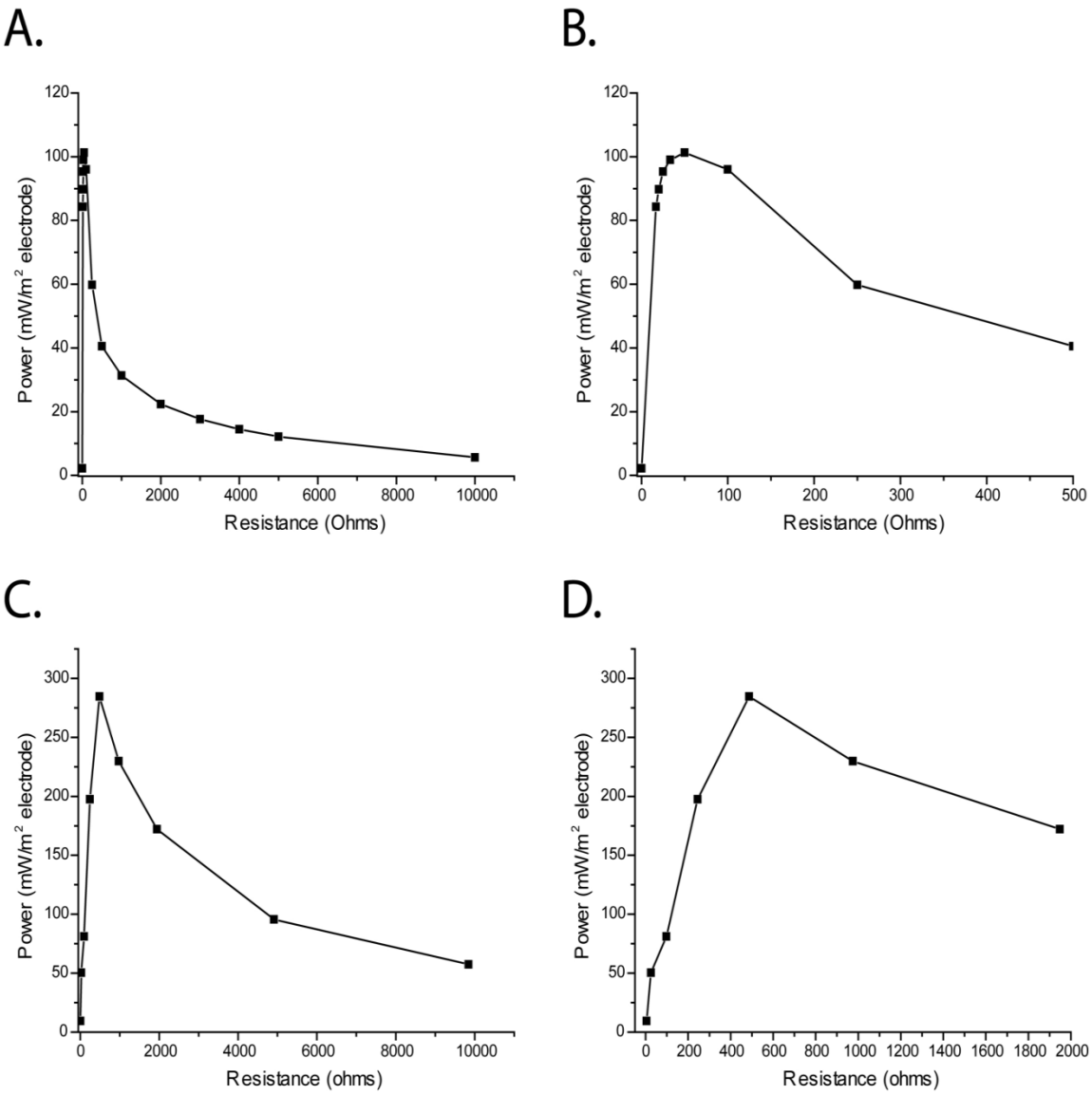

Figure. S2. Power curves for the small test cell and the large outdoor cell. **(A)** Power curve for the outdoor cell. **(B)** Rescaled view of the outdoor cell's power curve showing peak power output at 50 Ω resistance. **(C)** Power curve for small test cell. **(D)** Rescaled view of the small test cell's power curve showing peak power output at 500 Ω resistance.

To maintain a constant voltage from the system under differing conditions of algal carbon fixation the external resistance can be adjusted to obtain a desired voltage.

It is important to remember that the current cell design is dependent on oxidation of aluminum and therefore does not yet constitute a stand-alone sustainable energy source. It may however be used as a way to liberate the energy stored in the reduced metal in a portable manner. This would allow aluminum to be used effectively as an energy storage medium for transferring energy from areas that have access to large reserves of renewable energy, such as hydroelectric power, to areas that do not. Further research may allow power to be generated directly from the pH gradient that occurs when photosynthetic carbon fixation is separated from respiration.

Literature cited

1. **LLNL** 2013, posting date. Estimated Energy Use in 2012, https://flowcharts.llnl.gov/.
2. **Stocker, D. Q.** 2013. Climate change 2013: the physical science basis. Working Group I Contribution to the Fifth Assessment Report of the Intergovernmental Panel on Climate Change, Summary for Policymakers, IPCC.
3. **USDA**, posting date. Agriculture, Navy Secretaries Promote U.S. Military Energy Independence with 'Farm-to-Fleet. USDA, http://www.usda.gov/wps/portal/usda/usdamediafb?contentid=2013/12/0237.xml&printable=true&contentidonly=true.
4. **Osborn, S. G., A. Vengosh, N. R. Warner, and R. B. Jackson.** 2011. Methane contamination of drinking water accompanying gas-well drilling and hydraulic fracturing. P.N.A.S **108:**8172-8176.
5. **Kelly, E. N., J. W. Short, D. W. Schindler, P. V. Hodson, M. Ma, A. K. Kwan, and B. L. Fortin.** 2009. Oil sands development contributes polycyclic aromatic compounds to the Athabasca River and its tributaries. P.N.A.S **106:**22346-22351.
6. **IEA.** 2007. IEA Energy Technology Essentials International Energy Agency.
7. January 13th, 2013, posting date. Renewable Fuel Standard (RFS). US Environmental Protection Agency.
8. **Matsuoka, S., J. Ferro, and P. Arruda.** 2011. The Brazilian experience of sugarcane ethanol industry, p. 157-172, Biofuels. Springer.

9. **Roberts, M. J., and W. Schlenker.** 2010. Identifying supply and demand elasticities of agricultural commodities: Implications for the US ethanol mandate. National Bureau of Economic Research.

10. **Ewalt, L. H. M. H. a. D. M.** 2006. How Americans Make And Spend Their Money, Forbes.

11. **WFP** 2013, posting date. Food Security And Nutritional Status In Egypt Worsening Amidst Economic Challenges. WFP, http://www.wfp.org/node/3611/3690/443992.

12. **Pimentel, D., and T. W. Patzek.** 2005. Ethanol production using corn, switchgrass, and wood; biodiesel production using soybean and sunflower. Nat. Res. Research **14:**65-76

13. **von Blottnitz, H., and M. A. Curran.** 2007. A review of assessments conducted on bio-ethanol as a transportation fuel from a net energy, greenhouse gas, and environmental life cycle perspective. J. of Cleaner prod. **15:**607-619

14. **Uellendahl, H., G. Wang, H. B. Moller, U. Jorgensen, I. V. Skiadas, H. N. Gavala, and B. K. Ahring.** 2008. Energy balance and cost-benefit analysis of biogas production from perennial energy crops pretreated by wet oxidation. Water science and technology : a journal of the International Association on Water Pollution Research **58:**1841-1847.

15. **Waltz, E.** 2009. Biotech's green gold? Nat. Biotechnol. **27:**15-18.

16. **Chisti, Y.** 2008. Biodiesel from microalgae beats bioethanol. Trends Biotechnol. **26:**126-131.

17. **Schenk, P. M., S. R. Thomas-Hall, E. Stephens, U. C. Marx, J. H. Mussgnug, C. Posten, O. Kruse, and B. Hankamer.** 2008. Second generation biofuels: high-efficiency microalgae for biodiesel production. Bioenerg, Res. **1:**20-43.

18. **Brennan, L., and P. Owende.** 2010. Biofuels from microalgae—a review of technologies for production, processing, and extractions of biofuels and co-products. Renewable and sustainable energy reviews **14:**557-577

19. **Benemann, J.** 2013. Microalgae for Biofuels and Animal Feeds. Energies **6:**5869-5886.

20. **Schlesinger, A., D. Eisenstadt, A. Bar-Gil, H. Carmely, S. Einbinder, and J. Gressel.** 2012. Inexpensive non-toxic flocculation of microalgae contradicts theories; overcoming a major hurdle to bulk algal production. Biotechnol. Adv. **30**: 1023-30

21. **Uduman, N., Y. Qi, M. K. Danquah, G. M. Forde, and A. Hoadley.** 2010. Dewatering of microalgal cultures: A major bottleneck to algae-based fuels. J Renew. Sustain. Ener. **2:**017201.

22. **Oh, H. M., S. J. Lee, M. H. Park, H. S. Kim, H. C. Kim, J. H. Yoon, G. S. Kwon, and B. D. Yoon.** 2001. Harvesting of *Chlorella vulgaris* using a bioflocculant from *Paenibacillus* sp AM49. Biotechnol. Lett. **23:**1229-1234.

23. **Sirin, S., R. Trobajo, C. Ibanez, and J. Salvado.** 2012. Harvesting the microalgae *Phaeodactylum tricornutum* with polyaluminum chloride, aluminium sulphate, chitosan and alkalinity-induced flocculation. J Appl. Phycol. **24:**1067-1080.

24. **Lavoie, A., and J. Noüe.** 1983. Harvesting microalgae with chitosan. J. World Maricult. Soc. **14:**685-694.

25. **Divakaran, R., and V. Sivasankara Pillai.** 2002. Flocculation of algae using chitosan. J. Appl. Phycol. **14:**419-422.

26. **Pavoni, J. L., M. W. Tenney, and W. F. Echelberger, Jr.** 1972. Bacterial exocellular polymers and biological flocculation. J. Water Pol. Cont. Fed. **44:**414-429.

27. **Yuan, S. J., M. Sun, G. P. Sheng, Y. Li, W. W. Li, R. S. Yao, and H. Q. Yu.** 2011. Identification of key constituents and structure of the extracellular polymeric substances excreted by *Bacillus megaterium* TF10 for their flocculation capacity. Environ. Sci. Technol. **45:**1152-1157.

28. **Nontembiso, P., C. Sekelwa, M. V. Leonard, and O. I. Anthony.** 2011. Assessment of bioflocculant production by *Bacillus* sp. Gilbert, a marine bacterium isolated from the bottom sediment of Algoa Bay. Mar. Drugs **9:**1232-1242.

29. **Gardes, A., M. H. Iversen, H. P. Grossart, U. Passow, and M. S. Ullrich.** 2011. Diatom-associated bacteria are required for aggregation of *Thalassiosira weissflogii*. ISME J. **5:**436-445.

30. **Wang, H., H. D. T. Laughinghouse, M. A. Anderson, F. Chen, E. Willliams, A. R. Place, O. Zmora, Y. Zohar, T. Zheng, and R. T. Hill.** 2012. Novel bacterial isolate from Permian groundwater, capable of aggregating potential biofuel-producing microalga *Nannochloropsis oceanica* IMET1. Appl. Environ. Microbiol. **78:**1445-1453.

31. **Yoon, J. H., H. M. Oh, B. D. Yoon, K. H. Kang, and Y. H. Park.** 2003. *Paenibacillus kribbensis* sp nov and *Paenibacillus terrae* sp nov., bioflocculants for efficient harvesting of algal cells. Int. J. Syst. Evol. Micr. **53:**295-301.

32. **Brown, T. M., P. Duan, and P. E. Savage.** 2010. Hydrothermal liquefaction and gasification of *Nannochloropsis* sp. Energy & Fuels **24:**3639-3646.

33. **Valdez, P. J., M. C. Nelson, H. Y. Wang, X. N. Lin, and P. E. Savage.** 2012. Hydrothermal liquefaction of *Nannochloropsis* sp.: Systematic study of process variables and analysis of the product fractions. Biomass and Bioenergy **46:**317-331

34. **Richardson, J. W., M. D. Johnson, and J. L. Outlaw.** 2012. Economic comparison of open pond raceways to photo bio-reactors for profitable production of algae for transportation fuels in the Southwest. Algal Res. **1:**93-100.

35. **Guillard, R. R. L.** 1975. Culture of phytoplankton for feeding marine invertebrates. Culture of marine invertebrate animals. Plenum**:**29-60.

36. **Lane, D.** 1991. 16S/23S rRNA sequencing. Nucleic acid techniques in bacterial systematics**:**115-147.

37. **Lee, J., D. H. Cho, R. Ramanan, B. H. Kim, H. M. Oh, and H. S. Kim.** 2013. Microalgae-associated bacteria play a key role in the flocculation of *Chlorella vulgaris*. Bioresour Technol **131:**195-201.

38. **Marquis, R. E., K. Mayzel, and E. L. Carstensen.** 1976. Cation exchange in cell walls of gram-positive bacteria. Can. J. Micro. **22:**975-982.

39. **Dubinsky, Z., and J. Rotem.** 1974. Relations between algal populations and the pH of their media. Oecologia **16:**53-60.

40. **Schlesinger, A., D. Eisenstadt, A. Bar-Gil, H. Carmely, S. Einbinder, and J. Gressel.** 2012. Inexpensive non-toxic flocculation of microalgae contradicts theories; overcoming a major hurdle to bulk algal production. Biotechnol. Adv. **30:**1023-1030.

41. **Powell, R. J., and R. T. Hill.** 2013. Rapid aggregation of biofuel-producing algae by the bacterium *Bacillus* sp. strain RP1137. Appl. Environ. Microbiol. **79:**6093-6101.

42. **Kamentsky, L., T. R. Jones, A. Fraser, M. A. Bray, D. J. Logan, K. L. Madden, V. Ljosa, C. Rueden, K. W. Eliceiri, and A. E. Carpenter.** 2011. Improved structure, function and compatibility for CellProfiler: modular high-throughput image analysis software. Bioinformatics **27:**1179-1180.

43. **Hermansson, M.** 1999. The DLVO theory in microbial adhesion. Colloid Surface B **14:**105-119.

44. **Sobeck, D. C., and M. J. Higgins.** 2002. Examination of three theories for mechanisms of cation-induced bioflocculation. Water research **36:**527-538.

45. **Pal, M. K., T. C. Ghosh, and J. K. Ghosh.** 1990. Studies on the conformation of and metal ion binding by teichoic acid of *Staphylococcus aureus*. Biopolymers **30:**273-277.

46. **Vary, P. S.** 1994. Prime time for *Bacillus megaterium*. Microbiology **140 (Pt 5):**1001-1013.

47. **Hansen, A. K., and N. A. Moran.** 2011. Aphid genome expression reveals host-symbiont cooperation in the production of amino acids. P.N.A.S **108:**2849-2854.

48. **Schachtsiek, M., W. P. Hammes, and C. Hertel.** 2004. Characterization of *Lactobacillus coryniformis* DSM 20001T surface protein Cpf mediating coaggregation with and aggregation among pathogens. Appl. Environ. Microbio.l **70:**7078-7085.

49. **Boris, S., J. E. Suarez, and C. Barbes.** 1997. Characterization of the aggregation promoting factor from *Lactobacillus gasseri*, a vaginal isolate. J. App. Micro. **83:**413-420.

50. **Garrote, G. L., L. Delfederico, R. Bibiloni, A. G. Abraham, P. F. Perez, L. Semorile, and G. L. De Antoni.** 2004. Lactobacilli isolated from kefir grains: evidence of the presence of S-layer proteins. J. Dairy Res. **71:**222-230.

51. **Gorlich, D., and T. A. Rapoport.** 1993. Protein translocation into proteoliposomes reconstituted from purified components of the endoplasmic reticulum membrane. Cell **75:**615-630.

52. **Economou, A., J. A. Pogliano, J. Beckwith, D. B. Oliver, and W. Wickner.** 1995. SecA membrane cycling at SecYEG is driven by distinct ATP binding and hydrolysis events and is regulated by SecD and SecF. Cell **83:**1171-1181.

53. **Duong, F., and W. Wickner.** 1997. The SecDFyajC domain of preprotein translocase controls preprotein movement by regulating SecA membrane cycling. EMBO J. **16:**4871-4879.

54. **Ilangovan, U., H. Ton-That, J. Iwahara, O. Schneewind, and R. T. Clubb.** 2001. Structure of sortase, the transpeptidase that anchors proteins to the cell wall of *Staphylococcus aureus*. P.N.A.S. **98:**6056-6061.

55. **Ton-That, H., K. F. Faull, and O. Schneewind.** 1997. Anchor structure of staphylococcal surface proteins. A branched peptide that links the carboxyl terminus of proteins to the cell wall. J. Biol. Chem. **272:**22285-22292.

56. **Ton-That, H., H. Labischinski, B. Berger-Bachi, and O. Schneewind.** 1998. Anchor structure of staphylococcal surface proteins. III. Role of the FemA, FemB, and FemX factors in anchoring surface proteins to the bacterial cell wall. J. Biol. Chem. **273:**29143-29149.

57. **Ton-That, H., and O. Schneewind.** 1999. Anchor structure of staphylococcal surface proteins. IV. Inhibitors of the cell wall sorting reaction. J. Biol. Chem. **274:**24316-24320.

58. **Mazmanian, S. K., G. Liu, H. Ton-That, and O. Schneewind.** 1999. *Staphylococcus aureus* sortase, an enzyme that anchors surface proteins to the cell wall. Science **285:**760-763.

59. **Ton-That, H., G. Liu, S. K. Mazmanian, K. F. Faull, and O. Schneewind.** 1999. Purification and characterization of sortase, the transpeptidase that cleaves surface proteins of *Staphylococcus aureus* at the LPXTG motif. P.N.A.S. **96:**12424-12429.

60. **Goecks, J., A. Nekrutenko, J. Taylor, and G. Team.** 2010. Galaxy: a comprehensive approach for supporting accessible, reproducible, and transparent computational research in the life sciences. Genome Biol. **11**.

61. **Blankenberg, D., G. Von Kuster, N. Coraor, G. Ananda, R. Lazarus, M. Mangan, A. Nekrutenko, and J. Taylor.** 2010. Galaxy: a web-based genome

analysis tool for experimentalists. Current protocols in molecular biology / edited by Frederick M. Ausubel ... [et al.] **Chapter 19:**Unit 19 10 11-21.

62. **Giardine, B., C. Riemer, R. C. Hardison, R. Burhans, L. Elnitski, P. Shah, Y. Zhang, D. Blankenberg, I. Albert, J. Taylor, W. Miller, W. J. Kent, and A. Nekrutenko.** 2005. Galaxy: a platform for interactive large-scale genome analysis. Genome Res. **15:**1451-1455.

63. **Aziz, R. K., D. Bartels, A. A. Best, M. DeJongh, T. Disz, R. A. Edwards, K. Formsma, S. Gerdes, E. M. Glass, M. Kubal, F. Meyer, G. J. Olsen, R. Olson, A. L. Osterman, R. A. Overbeek, L. K. McNeil, D. Paarmann, T. Paczian, B. Parrello, G. D. Pusch, C. Reich, R. Stevens, O. Vassieva, V. Vonstein, A. Wilke, and O. Zagnitko.** 2008. The RAST server: Rapid annotations using subsystems technology. Bmc Genomics **9**.

64. **Lortal, S., J. Vanheijenoort, K. Gruber, and U. B. Sleytr.** 1992. S-Layer of *Lactobacillus-Helveticus* Atcc-12046 - Isolation, Chemical Characterization and Re-Formation after Extraction with Lithium-Chloride. J. Gen. Microbiol. **138:**611-618.

65. **Wattam, A. R., D. Abraham, O. Dalay, T. L. Disz, T. Driscoll, J. L. Gabbard, J. J. Gillespie, R. Gough, D. Hix, R. Kenyon, D. Machi, C. Mao, E. K. Nordberg, R. Olson, R. Overbeek, G. D. Pusch, M. Shukla, J. Schulman, R. L. Stevens, D. E. Sullivan, V. Vonstein, A. Warren, R. Will, M. J. Wilson, H. S. Yoo, C. Zhang, Y. Zhang, and B. W. Sobral.** 2014. PATRIC, the bacterial bioinformatics database and analysis resource. Nucleic Acids Res. **42:**D581-591.

66. **Letunic, I., T. Doerks, and P. Bork.** 2012. SMART 7: recent updates to the protein domain annotation resource. Nucleic Acids Res. **40:**D302-305.

67. **Takahashi, Y., K. Konishi, J. O. Cisar, and M. Yoshikawa.** 2002. Identification and characterization of hsa, the gene encoding the sialic acid-binding adhesin of *Streptococcus gordonii* DL1. Infection and immunity **70:**1209-1218.

68. **Sabarth, N., R. Hurvitz, M. Schmidt, U. Zimny-Arndt, P. R. Jungblut, T. F. Meyer, and D. Bumann.** 2005. Identification of Helicobacter pylori surface proteins by selective proteinase K digestion and antibody phage display. J. Microbiol. Meth. **62:**345-349.

69. **Schneewind, O., and D. M. Missiakas.** 2012. Protein secretion and surface display in Gram-positive bacteria. Philosophical transactions of the Royal Society of London. Series B, Biological sciences **367:**1123-1139.

70. **Coletta, A., J. W. Pinney, D. Y. Solis, J. Marsh, S. R. Pettifer, and T. K. Attwood.** 2010. Low-complexity regions within protein sequences have position-dependent roles. BMC Systems Biology **4:**43.

71. **Wang, D., K. Ning, J. Li, J. Hu, D. Han, H. Wang, X. Zeng, X. Jing, Q. Zhou, X. Su, X. Chang, A. Wang, W. Wang, J. Jia, L. Wei, Y. Xin, Y. Qiao, R. Huang, J. Chen, B. Han, K. Yoon, R. T. Hill, Y. Zohar, F. Chen, Q. Hu, and J. Xu.** 2014. *Nannochloropsis* genomes reveal evolution of microalgal oleaginous traits. PLoS Genetics **10:**e1004094.

72. **Vieler, A., G. Wu, C. H. Tsai, B. Bullard, A. J. Cornish, C. Harvey, I. B. Reca, C. Thornburg, R. Achawanantakun, C. J. Buehl, M. S. Campbell, D.**

Cavalier, K. L. Childs, T. J. Clark, R. Deshpande, E. Erickson, A. Armenia Ferguson, W. Handee, Q. Kong, X. Li, B. Liu, S. Lundback, C. Peng, R. L. Roston, Sanjaya, J. P. Simpson, A. Terbush, J. Warakanont, S. Zauner, E. M. Farre, E. L. Hegg, N. Jiang, M. H. Kuo, Y. Lu, K. K. Niyogi, J. Ohlrogge, K. W. Osteryoung, Y. Shachar-Hill, B. B. Sears, Y. Sun, H. Takahashi, M. Yandell, S. H. Shiu, and C. Benning. 2012. Genome, functional gene annotation, and nuclear transformation of the heterokont oleaginous alga *Nannochloropsis oceanica* CCMP1779. PLoS Genetics **8:**e1003064.

73. **Schirner, K., J. Marles-Wright, R. J. Lewis, and J. Errington.** 2009. Distinct and essential morphogenic functions for wall- and lipo-teichoic acids in *Bacillus subtilis*. The EMBO journal **28:**830-842.

74. **Wormann, M. E., R. M. Corrigan, P. J. Simpson, S. J. Matthews, and A. Grundling.** 2011. Enzymatic activities and functional interdependencies of *Bacillus subtilis* lipoteichoic acid synthesis enzymes. Mol. Microbiol. **79:**566-583.

75. **Group, N. H. W., J. Peterson, S. Garges, M. Giovanni, P. McInnes, L. Wang, J. A. Schloss, V. Bonazzi, J. E. McEwen, K. A. Wetterstrand, C. Deal, C. C. Baker, V. Di Francesco, T. K. Howcroft, R. W. Karp, R. D. Lunsford, C. R. Wellington, T. Belachew, M. Wright, C. Giblin, H. David, M. Mills, R. Salomon, C. Mullins, B. Akolkar, L. Begg, C. Davis, L. Grandison, M. Humble, J. Khalsa, A. R. Little, H. Peavy, C. Pontzer, M. Portnoy, M. H. Sayre, P. Starke-Reed, S. Zakhari, J. Read, B. Watson, and M. Guyer.** 2009. The NIH Human Microbiome Project. Genome Res. **19:**2317-2323.

76. **Hernandez, J.-P., L. E. de-Bashan, and Y. Bashan.** 2006. Starvation enhances phosphorus removal from wastewater by the microalga *Chlorella* spp. co-immobilized with *Azospirillum brasilense*. Enzyme and Microbial Technology **38:**190-198

77. **Jiang, L., L. Yang, L. Xiao, X. Shi, G. Gao, and B. Qin.** 2007. Quantitative studies on phosphorus transference occuring between *Microcystis aeruginosa* and its attached bacterium (*Pseudomonas* sp.), p. 161-165 Eutrophication of Shallow Lakes with Special Reference to Lake Taihu, China. Springer.

78. **Amin, S. A., D. H. Green, M. C. Hart, F. C. Kupper, W. G. Sunda, and C. J. Carrano.** 2009. Photolysis of iron-siderophore chelates promotes bacterial-algal mutualism. P.N.A.S. **106:**17071-17076.

79. **Croft, M. T., A. D. Lawrence, E. Raux-Deery, M. J. Warren, and A. G. Smith.** 2005. Algae acquire vitamin B12 through a symbiotic relationship with bacteria. Nature **438:**90-93.

80. **Gonzalez, L. E., and Y. Bashan.** 2000. Increased growth of the microalga *Chlorella vulgaris* when coimmobilized and cocultured in alginate beads with the plant-growth-promoting bacterium *Azospirillum brasilense*. Appl. Environ. Microbiol. **66:**1527-1531.

81. **Adachi, M., K. Fukami, R. Kondo, and T. Nishijima.** 2002. Identification of marine algicidal *Flavobacterium* sp. 5 N-3 using multiple probes and whole-cell hybridization. Fisheries Science **68:**713-720

82. **Seyedsayamdost, M. R., R. J. Case, R. Kolter, and J. Clardy.** 2011. The Jekyll-and-Hyde chemistry of *Phaeobacter gallaeciensis*. Nature chemistry **3:**331-335.

83. **Amaro, A. M., M. S. Fuentes, S. R. Ogalde, J. A. Venegas, and B. A. Suarez-Isla.** 2005. Identification and characterization of potentially algal-lytic marine bacteria strongly associated with the toxic dinoflagellate *Alexandrium catenella*. J. Euk. Microbiol. **52:**191-200.

84. **Simon, N., I. C. Biegala, E. A. Smith, and D. Vaulot.** 2002. Kinetics of attachment of potentially toxic bacteria to *Alexandrium tamarense*. Aquatic Microbial Ecology **28:**249-256

85. **Su, J. Q., X. R. Yang, T. L. Zheng, Y. Tian, N. Z. Jiao, L. Z. Cai, and H. S. Hong.** 2007. Isolation and characterization of a marine algicidal bacterium against the toxic dinoflagellate *Alexandrium tamarense*. Harmful Algae **6:**799-810

86. **Currie, D. J., and J. Kalff.** 1984. A comparison of the abilities of freshwater algae and bacteria to acquire and retain phosphorus. Limnology and Oceanography **29:**298-310.

87. **Gurung, T. B., J. Urabe, and M. Nakanishi.** 1999. Regulation of the relationship between phytoplankton *Scenedesmus acutus* and heterotrophic bacteria by the balance of light and nutrients. Aquatic Microbial Ecology **17:**27-35

88. **Ferrier, M., J. L. Martin, and J. N. Rooney-Varga.** 2002. Stimulation of *Alexandrium fundyense* growth by bacterial assemblages from the Bay of Fundy. J. Applied Microbiol. **92:**706-716.

89. **Lakaniemi, A. M., C. J. Hulatt, K. D. Wakeman, D. N. Thomas, and J. A. Puhakka.** 2012. Eukaryotic and prokaryotic microbial communities during microalgal biomass production. Bioresour. Technol. **124:**387-393.

90. **Lakaniemi, A. M., V. M. Intihar, O. H. Tuovinen, and J. A. Puhakka.** 2012. Growth of *Dunaliella tertiolecta* and associated bacteria in photobioreactors. J. Indust. Microbiol. & Biotech. **39:**1357-1365.

91. **Lakaniemi, A. M., V. M. Intihar, O. H. Tuovinen, and J. A. Puhakka.** 2012. Growth of *Chlorella vulgaris* and associated bacteria in photobioreactors. Microbial Biotech. **5:**69-78.

92. **Krohn-Molt, I., B. Wemheuer, M. Alawi, A. Poehlein, S. Gullert, C. Schmeisser, A. Pommerening-Roser, A. Grundhoff, R. Daniel, D. Hanelt, and W. R. Streit.** 2013. Metagenome survey of a multispecies and alga-associated biofilm revealed key elements of bacterial-algal interactions in photobioreactors. Appl. Environ. Microbiol. **79:**6196-6206.

93. **Liu, Z., F. Zhang, and F. Chen.** 2013. High throughput screening of CO2-tolerating microalgae using GasPak bags. Aquatic Biosystems **9:**23.

94. **Mandal, S., and N. Mallick.** 2009. Microalga *Scenedesmus obliquus* as a potential source for biodiesel production. Appl. Microbiol. Biotechnol. **84:**281-291.

95. **Mandal, S., and N. Mallick.** 2011. Waste utilization and biodiesel production by the green microalga *Scenedesmus obliquus*. Appl. Environ. Microbiol. **77:**374-377.

96. **Kaewkannetra, P., P. Enmak, and T. Chiu.** 2012. The effect of CO2 and salinity on the cultivation of *Scenedesmus obliquus* for biodiesel production. Biotechnology and Bioprocess Engineering **17:**591-597

97. **Stanier, R. Y., R. Kunisawa, M. Mandel, and G. Cohen-Bazire.** 1971. Purification and properties of unicellular blue-green algae (order *Chroococcales*). Bacteriological reviews **35:**171.

98. **Cole, J. R., Q. Wang, E. Cardenas, J. Fish, B. Chai, R. J. Farris, A. S. Kulam-Syed-Mohideen, D. M. McGarrell, T. Marsh, G. M. Garrity, and J. M. Tiedje.** 2009. The Ribosomal Database Project: improved alignments and new tools for rRNA analysis. Nucleic Acids Res. **37:**D141-145.

99. **Muyzer, G., E. C. De Waal, and A. G. Uitterlinden.** 1993. Profiling of complex microbial populations by denaturing gradient gel electrophoresis analysis of polymerase chain reaction-amplified genes coding for 16S rRNA. Appl. Environ. Microbiol. **59:**695-700

100. **Schloss, P. D., S. L. Westcott, T. Ryabin, J. R. Hall, M. Hartmann, E. B. Hollister, R. A. Lesniewski, B. B. Oakley, D. H. Parks, C. J. Robinson, J. W. Sahl, B. Stres, G. G. Thallinger, D. J. Van Horn, and C. F. Weber.** 2009. Introducing mothur: open-source, platform-independent, community-supported software for describing and comparing microbial communities. Appl. Environ. Microbiol. **75:**7537-7541.

101. **Quince, C., A. Lanzen, R. J. Davenport, and P. J. Turnbaugh.** 2011. Removing noise from pyrosequenced amplicons. BMC Bioinformatics **12:**38.

102. **Edgar, R. C., B. J. Haas, J. C. Clemente, C. Quince, and R. Knight.** 2011. UCHIME improves sensitivity and speed of chimera detection. Bioinformatics **27:**2194-2200.

103. **Wang, Q., G. M. Garrity, J. M. Tiedje, and J. R. Cole.** 2007. Naive Bayesian classifier for rapid assignment of rRNA sequences into the new bacterial taxonomy. Appl. Environ. Microbiol. **73:**5261-5267.

104. **Altschul, S. F., W. Gish, W. Miller, E. W. Myers, and D. J. Lipman.** 1990. Basic local alignment search tool. J. Mol. Biol. **215:**403-410.

105. **Zhu, J., Y. Chai, Z. Zhong, S. Li, and S. C. Winans.** 2003. *Agrobacterium* bioassay strain for ultrasensitive detection of N-acylhomoserine lactone-type quorum-sensing molecules: detection of autoinducers in *Mesorhizobium huakuii*. Appl. Environ. Microbiol. **69:**6949-6953.

106. **Tempe, J., A. Petit, M. Holsters, M. Montagu, and J. Schell.** 1977. Thermosensitive step associated with transfer of the Ti plasmid during conjugation: Possible relation to transformation in crown gall. P.N.A.S. **74:**2848-2849.

107. **Chandler, J. R., B. A. Duerkop, A. Hinz, T. E. West, J. P. Herman, M. E. Churchill, S. J. Skerrett, and E. P. Greenberg.** 2009. Mutational analysis of *Burkholderia thailandensis* quorum sensing and self-aggregation. Journal of bacteriology **191:**5901-5909.

108. **Geng, H., and R. Belas.** 2010. Molecular mechanisms underlying roseobacter-phytoplankton symbioses. Curr. Opin. Biotechnol. **21:**332-338.

109. **Shen, H., Y. Niu, P. Xie, M. I. N. Tao, and X. I. Yang.** 2011. Morphological and physiological changes in *Microcystis aeruginosa* as a result of interactions with heterotrophic bacteria. Freshwater Biology **56:**1065-1080

110. **Handelsman, J.** 2004. Metagenomics: application of genomics to uncultured microorganisms. MMBR **68:**669-685.

111. **Zan, J., Y. Liu, C. Fuqua, and R. T. Hill.** 2014. Acyl-homoserine lactone quorum sensing in the roseobacter clade. Int. J. Mol. Sciences **15:**654-669.

112. **Strik, D. P. B. T. B., R. A. Timmers, M. Helder, K. J. J. Steinbusch, H. V. M. Hamelers, and C. J. N. Buisman.** 2011. Microbial solar cells: applying photosynthetic and electrochemically active organisms. Trends Biotechnol. **29:**41-49.

113. **Rosenbaum, M., Z. He, and L. T. Angenent.** 2010. Light energy to bioelectricity: photosynthetic microbial fuel cells. Curr. Opin. Biotech. **21:**259-264.

114. **Rabaey, K., and W. Verstraete.** 2005. Microbial fuel cells: novel biotechnology for energy generation. Trends Biotechnol **23:**291-298.

115. **Strik, D. P., H. Terlouw, H. V. Hamelers, and C. J. Buisman.** 2008. Renewable sustainable biocatalyzed electricity production in a photosynthetic algal microbial fuel cell (PAMFC). Appl .Microbiol. Biotechnol. **81:**659-668.

116. **De Schamphelaire, L., and W. Verstraete.** 2009. Revival of the biological sunlight-to-biogas energy conversion system. Biotechnol. Bioeng. **103:**296-304.

117. **Velasquez-Orta, S. B., T. P. Curtis, and B. E. Logan.** 2009. Energy from algae using microbial fuel cells. Biotechnol. Bioeng. **103:**1068-1076.

118. **De Schamphelaire, L., L. Van den Bossche, H. S. Dang, M. Hofte, N. Boon, K. Rabaey, and W. Verstraete.** 2008. Microbial fuel cells generating electricity from rhizodeposits of rice plants. Environ. Sci. Technol. **42:**3053-3058.

119. **Kaku, N., N. Yonezawa, Y. Kodama, and K. Watanabe.** 2008. Plant/microbe cooperation for electricity generation in a rice paddy field. Appl. Microbiol. Biotechnol. **79:**43-49.

120. **Timmers, R. A., D. P. Strik, H. V. Hamelers, and C. J. Buisman.** 2010. Long-term performance of a plant microbial fuel cell with *Spartina anglica.* Appl. Microbiol. Biotechnol. **86:**973-981.

121. **Helder, M., D. Strik, H. Hamelers, A. Kuhn, C. Blok, and C. Buisman.** 2010. Concurrent bio-electricity and biomass production in three Plant-Microbial Fuel Cells using *Spartina anglica, Arundinella anomala* and *Arundo donax.* Biores.Techn. **101:**3541-3547.

122. **Takanezawa, K., K. Nishio, S. Kato, K. Hashimoto, and K. Watanabe.** 2010. Factors affecting electric output from rice-paddy microbial fuel cells. Biosc. Biotech. Biochem. **74:**1271-1273.

123. **De Schamphelaire, L., A. Cabezas, M. Marzorati, M. W. Friedrich, N. Boon, and W. Verstraete.** 2010. Microbial community analysis of anodes from sediment microbial fuel cells powered by rhizodeposits of living rice plants. Appl. Env. Microbiol. **76:**2002-2008.

124. **Tanaka, K., R. Tamamushi, and T. Ogawa.** 2009. Bioelectrochemical fuel-cells operated by the cyanobacterium, *Anabaena variabilis*. J. Chem. Techn. Biotech. **35:**191-197.

125. **Yagishita, T., S. Sawayama, K. I. Tsukahara, and T. Ogi.** 1998. Performance of photosynthetic electrochemical cells using immobilized *Anabaena variabilis* M-3 in discharge/culture cycles. J. Ferment. Bioeng. **85:**546-549.

126. **Yagishita, T., S. Sawayama, K. Tsukahara, and T. Ogi.** 1997. Behavior of glucose degradation in *Synechocystis* sp. M-203 in bioelectrochemical fuel cells. Bioelectroch. Bioener. **43:**177-180.

127. **Pisciotta, J. M., Y. Zou, and I. V. Baskakov.** 2010. Light-dependent electrogenic activity of cyanobacteria. PloS One **5:**e10821.

128. **Ryu, W., S. J. Bai, J. S. Park, Z. Huang, J. Moseley, T. Fabian, R. J. Fasching, A. R. Grossman, and F. B. Prinz.** 2010. Direct extraction of photosynthetic electrons from single algal cells by nanoprobing system. Nano Letters **10:**1137-1143.

129. 2008. Reaction of aluminum with water to produce hydrogen. U.S. Department of Energy.

130. **Stanier, R. Y., R. Kunisawa, M. Mandel, and G. Cohen-Bazire.** 1971. Purification and properties of unicellular blue-green algae (order *Chroococcales*). Bact. Rev. **35:**171-205.

131. **Cusick, R. D., Y. Kim, and B. E. Logan.** 2012. Energy capture from thermolytic solutions in microbial reverse-electrodialysis cells. Science **335:**1474-1477.

132. **Suntivich, J., K. J. May, H. A. Gasteiger, J. B. Goodenough, and Y. Shao-Horn.** 2011. A perovskite oxide optimized for oxygen evolution catalysis from molecular orbital principles. Science **334:**1383-1385.